Journal of Sensors

Sensors and Embedded Systems in Agriculture and Food Analysis

Lead Guest Editor: Marco Grossi
Guest Editors: Annachiara Berardinelli, Edward Sazonov, Wesley Beccaro, and Martin E. Omaña

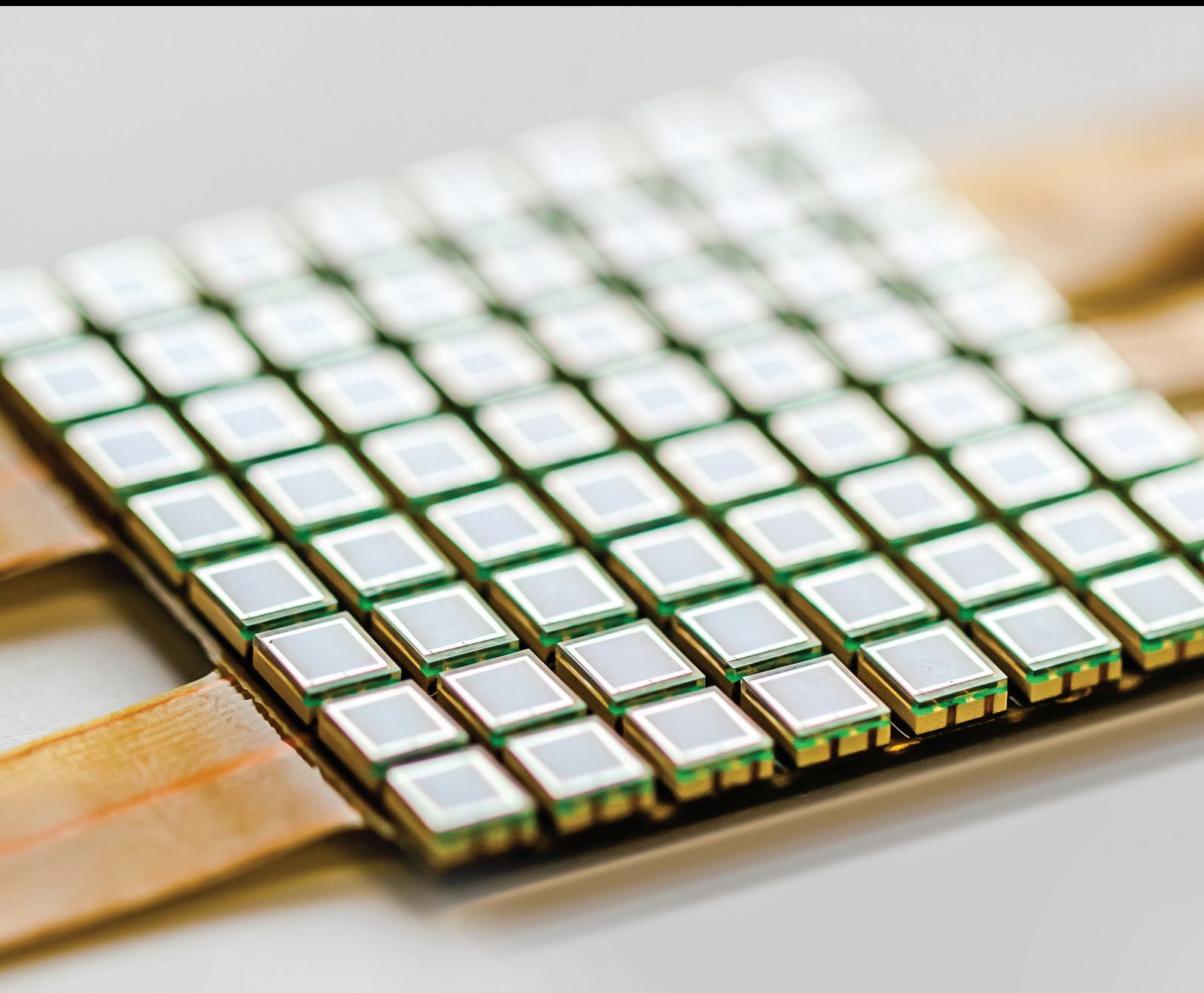

Sensors and Embedded Systems in Agriculture and Food Analysis

Journal of Sensors

Sensors and Embedded Systems in Agriculture and Food Analysis

Lead Guest Editor: Marco Grossi
Guest Editors: Annachiara Berardinelli, Edward Sazonov, Wesley Beccaro, and Martin E. Omaña

Editorial Board

Contents

Hindawi
Journal of Sensors
Volume 2019, Article ID 6808674, 2 pages
https://doi.org/10.1155/2019/6808674

Editorial

Sensors and Embedded Systems in Agriculture and Food Analysis

Marco Grossi,[1] **Annachiara Berardinelli**,[2] **Edward Sazonov**,[3] **Wesley Beccaro**,[4] **and Martin Omaña**[1]

[1]*Department of Electrical Energy and Information Engineering, University of Bologna, Bologna, Italy*
[2]*Department of Agricultural and Food Science, University of Bologna, Cesena, Italy*
[3]*Department of Electrical and Computer Engineering, University of Alabama, Alabama, USA*
[4]*Department of Electronic Systems Engineering, University of São Paulo, São Paulo, Brazil*

Correspondence should be addressed to Marco Grossi; marco.grossi8@unibo.it

Received 9 December 2018; Accepted 9 December 2018; Published 9 January 2019

The continuous advance in sensors and sensing systems has a strong impact in agriculture and food production.

Food is routinely screened to assess quality (such as physical appearance and organoleptic properties) and safety (absence of health threatening pathogens and chemical compounds). These tests are usually carried out in laboratory by skilled personnel, thus resulting in delayed response and high costs for the analysis. On the other hand, the availability of transduction techniques (such as electrical impedance spectroscopy, visible and near-infrared optical spectroscopy, fluorescence spectroscopy, and image processing) allows the design of low-cost embedded sensor systems for quick in-the-field analysis with benefits in terms of lower cost, shorter time response, and, in the end, more frequent screening and improved product quality.

Similarly, the introduction of sensor technologies in agriculture has led to the transition from standard farms, where activities are almost entirely carried out by humans, to "smart farms," where activities are automatized, critical parameters are timely monitored by networks of distributed sensors and cameras, information is shared using high-speed wireless communication technologies, and energy is scavenged from natural sources (solar, thermal, etc.). Moreover, the ever-increasing diffusion of modern mobile phones, merging strong computation capability with fast wireless communication, promotes even more the transition to the new "smart farms" in the paradigm of Internet of Things (IoT).

This special issue presents six papers that have been published after two rounds of rigorous peer review.

In the paper "Urban Lawn Monitoring in Smart City Environments," J. Marín et al. propose an Arduino-based system with a camera mounted on a drone that enables to monitor the state of the grass in urban lawns and consequently to optimize the irrigation regime. In the proposed strategy, the drone periodically flies over a garden and takes pictures of the grass. The pictures are then processed with an algorithm that classifies the grass into three categories, accordingly to its quality (thus to the need of irrigation). The authors apply their drone-based strategy to monitor gardens with different sizes to validate its cost and applicability, as well as to compare its pros and cons over alternative monitoring systems (mounted on mall autonomous vehicles). The experimental results demonstrate that for large gardens (bigger than $1000\,m^2$), the proposed strategy achieves a significantly lower monitoring time.

In the paper "The State-of-the-Art of Knowledge-Intensive Agriculture: A Review on Applied Sensing Systems and Data Analytics," B. Basnet and J. Bang reviewed existing sensors and data analytics techniques used in different areas of agriculture. The authors classified agriculture into five categories and reviewed the state-of-the-art technology in practice and ongoing research in each of these areas. The authors also discussed current and future challenges and provided their views on how such issues can be addressed.

In the paper "On-the-Go Grapevine Yield Estimation Using Image Analysis and Boolean Model," B. Millan et al. proposed a methodology for image-based automated estimation of vineyard yields. The paper suggests use of a Boolean model to tackle the problem of occlusions in the images and evaluates the model's performance on three different datasets. The number of berries in a cluster was estimated with a root mean square error (RMSE) of 20 and a coefficient of determination (R^2) of 0.80. The mass of berries on the images of the vines was estimated with 310 grams of mean error and $R^2 = 0.81$ (manually taken images) and 610 grams of mean error per segment (three vines) and $R^2 = 0.78$ from images taken by an automatic camera.

In the paper "The Development of an Intelligent Monitoring System for Agricultural Inputs Basing on DBN-SOFTMAX," L. Yang et al. proposed a system based on deep belief network (DBN) using a SOFTMAX classifier for the traceability of chemical fertilizers and pesticides in agricultural products. The system features sensor nodes performing measurement of pH, electrical conductivity and moisture, and a LoRa wireless communication module that transfers the measured data to a cloud server for further processing. Tests have been carried out on six agricultural inputs (three chemical fertilizers and three pesticides), and the results have shown how the proposed system provides an accuracy of 98.5%.

In the paper "Applicability of a 3D Laser Scanner for Characterizing the Spray Distribution Pattern of an Air-Assisted Sprayer," F. J. García-Ramos et al. presented an original work conducted by using a three-dimensional (3D) laser technology for the assessment of the performance of air-assisted spraying in fruit orchards. The authors developed a static test using an air-assisted sprayer equipped with two axial fans (front and back) with opposing directions of rotation. Two critical criteria were considered: the deposition of the product as a function of distance and the product distribution in the vicinity of the machine. The main results evidenced that measurements carried out by using the laser sensor allowed the quantification of the maximum distance of deposition of the product and the quantification of the amount of products applied in different areas in the vicinity of the sprayer.

In the paper "Monitoring and Control Systems in Agriculture Using Intelligent Sensor Techniques: A Review of the Aeroponic System," I. A. Lakhiar et al. presented a review on the use of wireless sensor network (WSN) in aeroponic cultivation. The authors discussed the advantages of aeroponics, a cultivation system where plant roots are hanged in the darkness in a growth chamber and provided with a nutrient mist in replacement of the soil, in terms of better control and possibility to investigate the effects of different nutrients on plant growth. A discussion on the problems faced by the application of aeroponics in terms of attention required by the grower to timely detect failures in the atomization nozzles and monitor critical parameters has been also presented. The authors discussed how the use of WSNs in aeroponics can effectively solve these drawbacks, thus helping the diffusion of the technique to farmers and scientists.

Conflicts of Interest

The guest editorial team as a whole declares that no conflict of interest or private agreement with companies exists.

Marco Grossi
Annachiara Berardinelli
Edward Sazonov
Wesley Beccaro
Martin Omaña

Hindawi
Journal of Sensors
Volume 2018, Article ID 8672769, 18 pages
https://doi.org/10.1155/2018/8672769

Review Article

Monitoring and Control Systems in Agriculture Using Intelligent Sensor Techniques: A Review of the Aeroponic System

Imran Ali Lakhiar,[1] **Gao Jianmin**,[1] **Tabinda Naz Syed**,[1] **Farman Ali Chandio**,[1] **Noman Ali Buttar**,[1] **and Waqar Ahmed Qureshi**[2]

[1]*Key Laboratory of Modern Agricultural Equipment and Technology, Ministry of Education, Institute of Agricultural Engineering, Jiangsu University, Zhenjiang, 212013 Jiangsu, China*
[2]*Research Centre of Fluid Machinery Engineering and Technology, Jiangsu University, Zhenjiang, 212013 Jiangsu, China*

Correspondence should be addressed to Gao Jianmin; gaojianminujs@163.com

Received 24 May 2018; Revised 1 October 2018; Accepted 15 October 2018; Published 19 December 2018

Guest Editor: Marco Grossi

In recent years, intelligent sensor techniques have achieved significant attention in agriculture. It is applied in agriculture to plan the several activities and missions properly by utilising limited resources with minor human interference. Currently, plant cultivation using new agriculture methods is very popular among the growers. However, the aeroponics is one of the methods of modern agriculture, which is commonly practiced around the world. In the system, plant cultivates under complete control conditions in the growth chamber by providing a small mist of the nutrient solution in replacement of the soil. The nutrient mist is ejected through atomization nozzles on a periodical basis. During the plant cultivation, several steps including temperature, humidity, light intensity, water nutrient solution level, pH and EC value, CO_2 concentration, atomization time, and atomization interval time require proper attention for flourishing plant growth. Therefore, the object of this review study was to provide significant knowledge about early fault detection and diagnosis in aeroponics using intelligent techniques (wireless sensors). So, the farmer could monitor several paraments without using laboratory instruments, and the farmer could control the entire system remotely. Moreover, the technique also provides a wide range of information which could be essential for plant researchers and provides a greater understanding of how the key parameters of aeroponics correlate with plant growth in the system. It offers full control of the system, not by constant manual attention from the operator but to a large extent by wireless sensors. Furthermore, the adoption of the intelligent techniques in the aeroponic system could reduce the concept of the usefulness of the system due to complicated manually monitoring and controlling process.

1. Introduction

Agriculture has an ancient history nearly dates back to thousands of years. Moreover, its advancement has been pushed by implementing the several new systems, practices, technologies, and approaches with the time. It employs over one-third of the global workforce [1]. The agriculture is the backbone of an economy for many countries and executes a significant contribution to the development of the economy for underdeveloped countries. Besides, it steers the process of economic prosperity in developed countries. Several research studies concluded that overall world agriculture uses approximately seventy percent per year available fresh water to irrigate only seventeen percent of the land. Another side, the total available irrigated land is gradually decreasing due to the rapidly increasing of food requirements and effects of global warming [2, 3]. In other words, agriculture is dealing with new main significant challenges. Foote [4] said FAO reported that world food production must be increased by seventy percent to provide sufficient food production for the fast-growing population and urbanisation. The expected world population growth for the half of the present century is daunting. However, depending on the estimate, it could be expected to rise above the nine billion people by midcentury. As many studies reported that the population is increasing very fast, the global population was one billion in 1800,

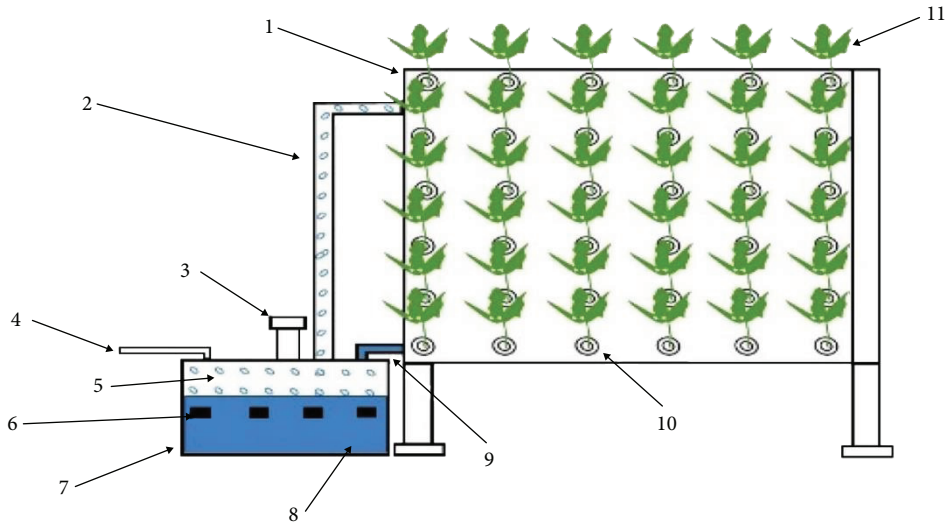

Figure 1: Basic diagram of the aeroponic plant cultivation system by Lakhiar et al. [15]. 1. Growth chamber. 2. Nutrient fog transmission pump. 3. Misting fan. 4. Power supply line. 5. Nutrient fog. 6. Ultrasonic atomizers. 7. Nutrient reservoir. 8. Nutrient solution. 9. Nutrient recycle line. 10. Plant holder. 11. Plant.

and it increased to seven billion people in 2012. However, studies report feared that at the end of the current century, it could be expected to reach eleven billion people and there could be many, many more mouths to feed soon. Thus, the rapid increase of the population, alongside the decrease in agriculture land, intensification of global climate changes, and exacerbation of water resources, declines labour force and energy crunches are posing tremendous challenges and hurdles to the agriculture sector [5, 6]. Furthermore, the developing and developed countries will deal with substantial water crises and issues due to rapid urbanisation and industrialisation. The available fresh water for irrigated agriculture land is supposed to decrease in future [7, 8]. Besides, the unpredictable climate changes include extreme weather conditions, intense storms, heat waves, and floods will have a substantial adverse impact on world agriculture sector. We need more production from agricultural systems to meet the growing food demands. Otherwise, we will suffer from food insecurity problems which will be the biggest threat. Moreover, Qiu and coworkers [9] revealed that the progress of the agriculture production is not only significant for to producing food to feed the population, but it is also essential for the industrial sector. Similarly, the agriculture is the main source to produce the raw material for many industrial sectors. Therefore, it must be understood that industrial and agricultural developments are not alternatives. However, both sectors are complementary to each other on the path to achieving the food security issues.

As the evolution of humankind from hunters and gatherers to agrarian societies, the efforts have mainly focused on improving the plant yield and productivity by either genetic changes, cultural or husbandry, management practices, or by developing and introducing plant protection measures. Accordingly, in the last and present century, peoples have started exploring the possibilities by adopting different modern techniques in agriculture. The adoption of the precision farming methods in agriculture is one of the excellent examples. The purpose is to try and mechanise them in agriculture to prevent the crop losses due to sudden climatic changes, soil-borne diseases, pest attaches, and so on. However, many research studies have been suggested and reported that problems and challenges of agriculture could overcome by adopting the precision farming methods. At present, several countries are increasing their farming productivities by implementing the precision farming methods.

Baudoin et al. [10] reported that the artificial plant growing method (e.g., greenhouse and factory farms) is one of the fundamental types of precision agriculture. Nowadays, the method is receiving importance and gaining the intention of the growers. The method can provide sufficient food supply throughout the year. In the system, the plant grows around the year by artificially adjusting and controlling the surrounding environmental conditions such as temperature, CO_2 (carbon dioxide), humidity, light intensity, airflow, and nutrients supply within the confined facilities [11, 12]. Besides, the system minimises environmental impact and maximises the crop yield with significant results as compared with traditional (open-field) cultivation system [13]. Savvas and team [14] informed that at present soilless plant cultivation is one of the most disruptive inventions ever presented in the field of artificial plant growing system. The soilless system refers to plant cultivation techniques without the use of soil by providing artificial solid material or water nutrient solution as a growing medium instead of soil. However, the water culture is related to the process of hydroponic and aeroponic plant cultivation (Figure 1). In both methods, the roots of the plant are continuously or intervalley nurtured with or within water nutrient solution by providing a specific control environment in artificial supporting structure [16, 17]. Both methods provide many benefits to the grower such as full control of nutrient concentration and supply and prevention of many soil-borne diseases and infections to plant, thus resulting in increased plant yield with significant

returns, high quality, and more efficient use of available natural resources [18, 19].

Several studies reported aeroponic and hydroponic systems as a modern and innovative plant cultivation techniques under the soilless system. By adopting these techniques, the growing food crises could be resolved [20, 21]. Moreover, the hydroponic system to grow initially leafy green vegetables was the first to emerge, which started taking commercial exploitation routes in industrialised countries in west and east but eventually was found to have particular defects and problems that forced people to discover and experiment with newer variations and techniques like the aeroponic system. According to the NASA report, the aeroponic system could reduce water, nutrient, and pesticide usage by 98, 60, and 100 percent, respectively, and increase the plant yield by 45 to 75 percent [22].

The primary motivation of this review article is to provide an idea about the use of intelligent sensor techniques in the aeroponic system. It could provide an opportunity for full automation, scalability, anytime-anyplace access monitoring, and fault diagnostics in the aeroponic system. Moreover, it would be helpful for the local farmer and grower to provide timely information about rising problems and influencing factors for successful plant growth in the aeroponic system. The farmers could start to understand their crops at a micro scale and able to communicate with plant through accessible technology. To the best of our knowledge, this is the first work to provide a brief review of the use of intelligent sensor techniques in the aeroponic system. However, the rest of the paper is organised as follows: Section 2 describes the current work in the aeroponic system with intelligent sensor techniques. In Sections 3, 4, and 5, we present the brief description about the aeroponic system, application, and working protocol of wireless sensor network in the aeroponic system. Sections 6, 7, 8, and 9 describe the advantages, future application, application of artificial intelligence in agriculture, and conclusion.

2. Related Work

Aeroponics is the new plant growing technique of modern agriculture. Until now, it is not entirely implicated among the farmers. Mostly, it is practiced by the researchers for performing the experimental studies. Their study reports concluded that it could be well accepted in agriculture as a modern-day plant cultivation activity where the modern farmer does not need soil to grow the plant. However, the aeroponic system has some substantial vulnerability like a failure of water supply pumps, nutrient distribution line and preparation, and atomization nozzle clogging, which require special knowledge and attention to avoid damage, rapid plant death, and failure of the system [23]. Furthermore, the integration of the intelligent agriculture techniques could be the best solution to avoid or deal with the above-mentioned issues without any technical expertise. Xiong and Qiao [24] reported that the integration of the intelligent agriculture systems could be an effective approach for solving complex problems of agriculture domains. Zhai et al. [25] reported that presently, several research studies had been conducted on the use of intelligent techniques in agriculture especially in the last two decades. Besides, several new techniques and application have been introduced and patented to improve the traditional agriculture practices. However, experts mainly focused and monitor the climatic condition, soil properties, water quality, plant development, livestock management, and fertilizer application, pesticide application, and illumination control through various intelligent techniques [26–32]. Meanwhile, it could be concluded that traditional agricultural logistics is improved and upgraded by introducing and implementing the several modern technologies and techniques in agriculture domains [33]. Basnet and Bang [34] reported that the collecting information through sensors and communication technology played a vital role in improving agricultural production. It has shifted agriculture from input-intensive to knowledge-intensive, and agriculture becomes more networked and decision-making. Both small- and large-scale farmer can benefit from introducing this technique into the agriculture value chain, having their productivity increased, quality improved, services extended, and costs reduced. It provides insights into various issues in the agriculture like weather prediction, crop and livestock disease, irrigation management, and supply and demand of agriculture inputs and outputs and helps in solving those problems. Rehman and Shaikh [35] concluded that at present, several information technologies including satellite navigation, grid and ubiquitous computing, and sensor network are exercised in agriculture. However, the application of the sensor network is supporting agriculture practices and activities in a very positive direction [36, 37]. Zhang and coworkers [38] used a sensor network to monitor air temperature, humidity, ambient light, and soil moisture and temperature. Also, the aeroponic system is the new application of the soilless agriculture. Besides, several studies had been successfully designed the aeroponic system by using various information technologies approaches such as Tik and coworkers [39] designed and implemented a wireless sensor network to monitor the aeroponic system. They used temperature, light intensity, pH, and EC monitoring sensors. Moreover, the study reported that the wireless sensor network offers a wide range of information which could be required for the horticulturist to provide a greater understanding of how these environmental and nutrient parameters are correlated with plant growth. The real-time information obtained from sensor nodes can be utilised to optimise strategies to control the temperatures and the other properties of the nutrient solution. A study by Pala et al. [40] proposed an approach to monitor automation and early fault detection tools in the aeroponic system through intelligent techniques. In the protocol, they designed a highly scalable aeroponic system and coded as aero-pot prototype. They developed software based on a genetic algorithm to optimise power consumption of the aeroponic system. Their study concluded that using this software user can define various properties and virtually configure the aeroponic system. The developed software can allow the user to add and remove the lights and pumps and define consumption of added devices with minimum grower effort. Laksono et al. [41] designed a wireless sensor and actuator network for the

controlling, monitoring, and conditioning of an aeroponic growth chamber. The designed wireless protocol was based on ZigBee technique. They also designed a data transmission system to transfer the data from the database server to administrator through text message. The proposed system was based on the sensors, actuators, communication system, and database server. The experiment results showed that the proposed wireless protocol based on ZigBee techniques was a useful tool of the wireless sensor network to monitor the aeroponic system. Jonas et al. [42] developed an automatic monitoring system to control the environmental and nutrient supply of the aeroponic system. The designed wireless protocol was based on Arduino development board. Their study concluded that the proposed system can control the nutrient atomization frequency based on the root chamber moisture content. However, the system can automatically transfer all the gathered information to a web server and also share on Twitter. Sani et al. [43] recommended a web-based control and monitoring system for the aeroponic system. Their system was composed of microcontrollers (using Arduino IDE program), actuators (two relays include atomization spray and fan on/off on specific time), the sensor (temperature and pH sensor), LDR (light intensity sensor), and communication modules (GSM/GPRS/3G modem). The present study concluded that our proposed design was able to monitor and measure the temperature, pH, light intensity, atomization time and interval time, and fan activation time and interval time in the aeroponic system. The proposed method was able to directly send the real-time information from the sensor to the server via the Internet using GSM. Anitha and Periasamy [44] designed wireless sensor technique to monitor the aeroponic system. The technique was based on the ZigBee prototype. The proposed network architecture was based on temperature, pressure, humidity, water level, and pH monitoring sensors. The sensors transmitted the gathered data to the GSM (Global System for Mobile) node or coordinator node, whereas the gateway device was used to transfer the data to the personal computer. However, a server was connected to the database where the maximum and minimum threshold values of pH, water level, and temperature were fixed. Furthermore, if the monitored value reaches above or below the threshold values stored in the database, thus, the system was able to start the alarm sound to aware the farmer. Another study in 2016 by Kernahan and Cupertino [45] invented a system to monitor and control the aeroponic system using wireless techniques. They concluded that a reliable aeroponic system provides a wireless connection between its subsystem for the exchange of data and commands. The various subsystems manage one or more plants growing atriums include nutrient atomization on hanged roots, maintenance, control of nutrient solution level, the addition of various nutrients, and control of the light quantity and cycle. A study by Montoya et al. [46] designed a wireless sensor system to monitor the aeroponic system. The system protocol was based on the Arduino development board. They used analog and digital sensors for monitoring temperature, nutrient atomization, EC, and pH fluctuations and level of nutrient solution in the nutrient reservoir. In order to acquire data and automation system, the two Arduinos were managed in a master-slave configuration and connected to each other through wireless by Wi-Fi. All the recorded data was autosaved in microSD memory and sent to a web page. Their study concluded that the proposed protocol could be used for automation and could monitor the aeroponic system. Kerns and Lee [47] firstly designed and introduced an aeroponic system using IoT (Internet of things) to automate the system. The proposed system is comprised of a mobile application, service platform, and IoT device with sensors (pH balance, temperature, and humidity). They used Raspberry Pi Zero device and designed a system to monitor and measure the selected parameters. The gathered data was autosaved into the database server by sending an SQL query. Their study concluded that the proposed system could help farmers to control and monitor the aeroponic system remotely. Furthermore, Karu [48] also designed and implemented a high-precision system for small-scale aeroponic plant cultivation. The system is allowed to precisely control the nutrient solutions, pH, and EC levels and gives data about humidity, temperature, pH, and EC concentration and amount of the nutrient solution in the reservoir. A recent study by Martin and Rafael [49] also proposed and suggested systems, methods, and devices for the aeroponic system. Mithunesh et al. [50] proposed an intelligent control system for an aeroponic system. The system protocol was based on an open-source development board called Raspberry Pi. Their study concluded that the developed system provides the simple management and high availability established by using both the local and global systems. Idris and Sani [51] designed monitoring and control system for the aeroponic system. They concluded that the developed system is able to monitor the aeroponic system working parameter such as temperature and humidity by sending the data in real time from sensor to the display system. Janarthanan et al. [52] concluded that the problems of the aeroponic system could be solved by the use of wireless sensor and actuator system. It allows the user to monitor and interact with the system through mobile app and a web interface. However, Liu and Zhang [53, 54] designed an aeroponic system for automatic control of water-fertilizer and temperature. They concluded that system supplies an experimental platform with features of simple structure and convenient control.

3. The Aeroponic System

The aeroponic system is one of the techniques of the soilless culture, where the plant grows in the air with the assistance of artificial support instead of soil or substrate culture. It is an air-water plant growing technique where lower portions such as the roots of the plant are hanged inside the growth chamber under complete darkness in controlled conditions. However, the upper portions of the plant such as leaves, fruits, and crown portion are extending outside the growth chamber. Usually, the artificial supporting structure (plastic or thermofoam) is provided to support and divide the plant into two parts (roots and leaves). In the system, plant roots are openly exposed in the air and directly irrigated with a small droplet size of the water nutrient at interval basis. The nutrient solution is supplied through different atomization nozzles with or

without high air pressure. Moreover, several studies considered aeroponics as a modern-day agricultural activity which is practiced in an enclosed growth chamber under entire controlled conditions, as it could eliminate the external environmental factors as compared with traditional agriculture activity. Hence, it is no longer dependent on large-scale land use, and it could be set up in any place, a building that has lifted global climate without considering the current climate such as rainy season and winter [23, 55–59]. Buer et al. [60] reported that atomization nozzle uses the tiny amount of the water nutrient solution and provides an excellent growth environment for the plant. Zobel and Lychalk [61] said it is a modern-day agricultural research tool which provides several agricultural research opportunities for a researcher with significant results by providing artificial growth conditions. However, Table 1 shows the essential monitoring and control parameters in the aeroponic system. Hessel et al. [62] and Clawson et al. [63] studies discovered that aeroponics contributes to the advances and developments in many areas of plant root studies. It provides an excellent chance for plant researchers to deeply study the behavior of plant root under different conditions and without any complications. Until now, many researchers had conducted plant root research and experimental studies root response to drought [64], effects of different oxygen concentrations on plant root development [65, 66], root microorganism [67–69], arbuscular mycorrhizal fungi production [70], and legume-rhizobia interaction [71]. Furthermore, studies also practiced the technique by growing vegetables, fruits, herbs, and medicinal root-based plant [72–74] such as tomato, potato, soybean, maize, lettuce, *Anthurium andreanum*, and *Acacia mangium* [15, 59, 75–79].

3.1. Present Status of the Aeroponic System. The aeroponic system is one of a holistic production management method in agriculture which promotes and improves agroecosystem, health, and biodiversity. The system has a paramount reputation in the horticulture department, because of its implications on the economic and technical aspects in the agriculture. Among all agriculture systems, only the aeroponic system is receiving the full attention of farmers, policymakers, entrepreneurs, and agricultural researchers. The grower could reduce the requirements of chemical inputs including fertilizers, herbicides, pesticides, and other agrochemicals. The grower could obtain higher cultivated plant yield and quality as compared with other growing methods. However, the aeroponic system is labour-intensive. It offers many opportunities for the farmers to increase rural employment. The farmer can grow a plant in their homes by providing artificial growth environment. Anitha and Periasamy [44] reported that nowadays many families are practicing the aeroponic system on their terrace. Besides, several countries of the world are using aeroponics for making an expansion in nourishment creation managing the monetary issues and making the nation naturally amicable to have their particular food supply. While some years ago, the use of the aeroponic system was limited almost around the world [84]. At present, the system is acquiring more attention from the farmers and several countries are being effectively adopting as an economical and environmentally friendly vegetable and fruit growing system. However, it is practiced in following countries: Abu Dhabi, Australia, Bhutan, Bolivia, Brazil, Bangladesh, Burkina Faso, China, Canada, Colombia, Ecuador, Egypt, Ethiopia, France, Germany, Ghana, Greece, Indonesia, Italy, India, Iran, Japan, Israel, Kenya, Korea, Malaysia, Mongolia, Malawi, New Zealand, Nigeria, Peru, Philippines, Poland, Russia, Rwanda, Saudi Arabia, South Africa, Spain, Singapore, South Korea, Slovakia, Sri Lanka, Taiwan, Thailand, Uzbekistan, and Vietnam. Besides, attempts are made to represent the system in other countries of the world [23].

3.2. Key Problems and Difficulties of the Aeroponic System. Aeroponic cultivation is performed in an outdoor and indoor installation and or in a greenhouse under controlled conditions. It may be carried out within a facility that includes the provision of light for plant growth, the centralised delivery of nutrient solution, and electrical power. The growing plants are set in a growth chamber and periodically soaked with nutrient solution small mist ejecting through atomization nozzle (Figure 2). In addition, the aeroponic system gives the chance to control the entire growth chamber environment precisely. The aeroponic system is the modern technique of the agriculture which is still under development. Until now, limited studies have been performed, and conducted studies concluded that the system has some problems and issues. Studies suggested that aeroponics is performed without soil or any solid media; thus, the main observed problems are water and nutrient buffer, any failure of the water pumps, nutrient solution distribution and preparation, atomization nozzle clogging, and so on, which lead to rapid death of the grown plant [40]. Kernahan and Cupertino [45] reported that the aeroponic system provides better control of the plant growth and nutritional availability and prevents the plant from various diseases and root rot. However, during plant growth from sowing to harvest time, the methods adopted in the aeroponic system require a little hand-operated contribution, interference regarding physical presence, and expertise in domain knowledge of plants, environment control, and operations to maintain and control the growth of the plant.

Moreover, there is a requirement to sustain and keep retain the nutrient solution parameters which include nutrient temperature, pH, and EC concentration in a narrow range of preferred values for optimal growth. If these parameters drift outside the desired range, it will create several problems for plant growth. In addition, some supplemental parameters can adjust to optimise the plant growth further. The additional parameters are atomization time, atomization interval time, air temperature, relative humidity, light intensity, and carbon dioxide (CO_2) concentration which make the system complicated and time-consuming with high human energy and with the higher level of expert training and skill for operating the system. However, the grower has the responsibility to control and monitor the fluctuations of the above parameters in the desired range to achieve the suitable growth conditions for the specific plants. A failure to accurately control and monitor the parameters could

Table 1: Basic monitoring and control parameters in the aeroponic system [23, 80–83].

No.	Parameters	Common value	Instruments
1	Nutrient atomization	Mist/spray/aerosol/droplet size at high pressure from 10 to 100, low pressure from 5 to 50, and ultrasonic foggers from 5 to 25 microns, respectively	Atomization nozzle (high and low pressure, atomization foggers)
2	Growing medium	Plant holder	Any artificial root supporting structure
3	Desirable pH of the nutrient solution	The pH value depends on the cultivar (onion 6.0–7.0, cucumber 5.8–6.0, carrot 5.8–6.4, spinach 5.5–6.6, lettuce 5.5–6.5, tomato 5.5–6.5, and potato 5.0–6.0)	pH measuring device
4	Desirable EC of the nutrient solution	The EC value depends on the cultivar (onion 1.4–1.8, cucumber 1.7–2.2, carrot 1.6–2.0, spinach 1.8–2.3, lettuce 0.8–1.2, tomato 2.0–5.0, and potato 2.0–2.5 $ds{\cdot}m^{-1}$)	EC measuring device
5	Humidity	Provide 100% available moisture	Humidity measuring device
6	Temperature	Optimum 15°C–25°C and should not increase to 30°C and less than 4°C	Temperature measuring device
7	The light inside the box	The light inside the growth box must be dark enough	Cover the growth chamber with locally available material
8	Atomization time	Depends on the cultivar growth stage	Manually operating the system with timer
9	Atomization interval time	Depends on the cultivar growth stage	Manually operating the system with timer

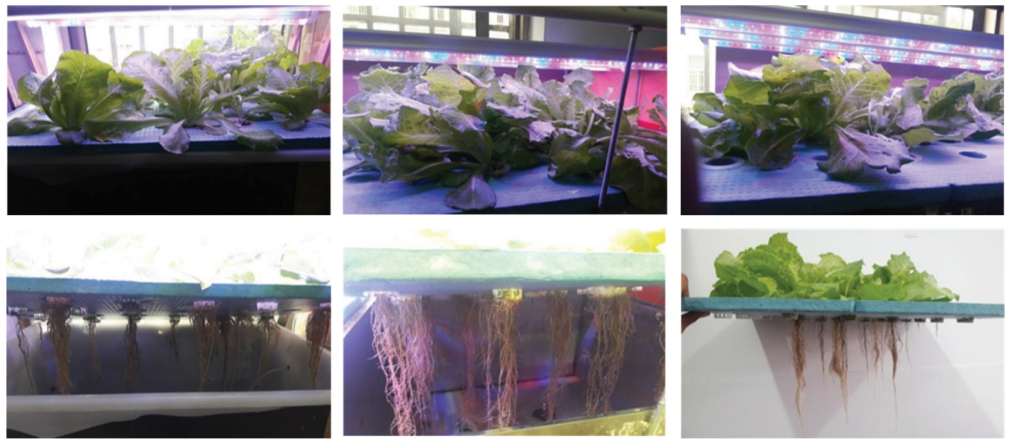

High-pressure atomization nozzle Low-pressure atomization nozzle Ultrasonic foggers

Figure 2: Aeroponically cultivated lettuce by Lakhiar et al. [23].

significantly affect the growth of the plant and cause financial loss. If any component failure occurs while the operator is not present on site, it may be detected too late to prevent harm, because systems generally include some automated means for periodically providing nutrient mist to the plant roots, refilling a nutrient reservoir, and managing light cycles and intensity. Therefore, the aeroponic cultivation considered hitherto to be somewhat unsuitable for the local grower and due to the above reasons and it is not common to find an installation. However, the main reason for the low acceptability of the aeroponic system is not a cost, but the main drawback is the amount of attention required of the grower with a high level of expertise and judgment. For the above-discussed reasons, more sophisticated and advanced monitoring techniques have implemented in the aeroponic system for early fault detection, real-time monitoring, and control and automation of the system. Hence, it would be advantageous to use artificial intelligent tools (Figure 3) in the aeroponic system to detect fault and diagnosis problems on time. Thus, it could help to avoid rapid damages to grown plants and help to fully automate the aeroponic system.

4. The Aeroponic System and Sensor Network

In recent years, early fault detection and diagnosis using an intelligent agricultural monitoring system is considered as the best tool to monitor plant without any complicated operations and laboratory analysis which required domain expertise and extensive time. The development of these convenient features has attracted much attention in the agriculture. The system is based on a wireless sensor network which comprises of a data server, a wireless convergence node, a plurality of wireless routers, and a plurality of wireless sensor nodes. However, the wireless sensor nodes are used as the

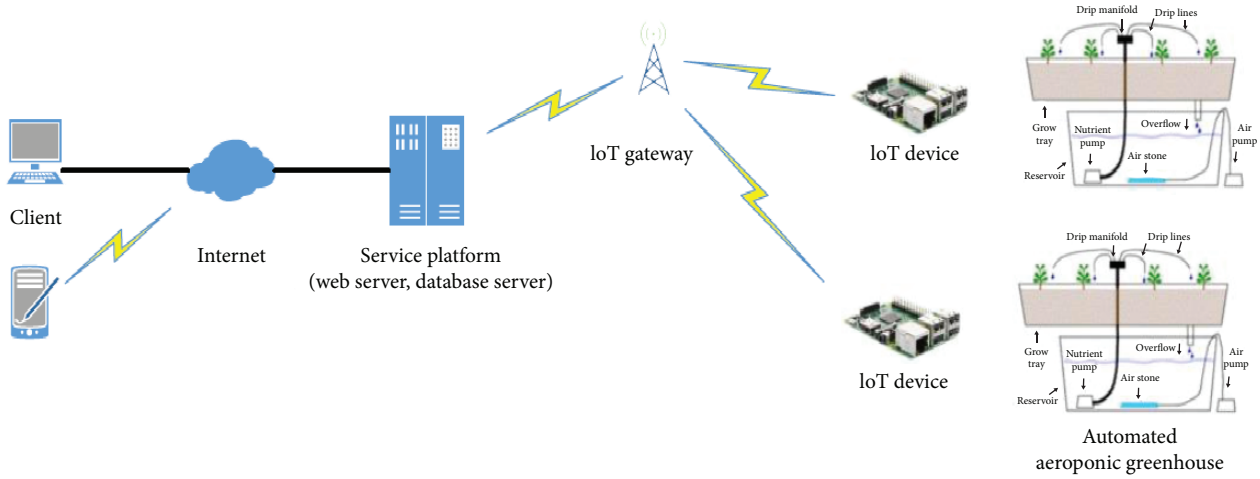

Figure 3: The aeroponic system using IoT technology by Kerns and Lee [47].

signal input of the intelligent agricultural monitoring system and are used to collect each selected parameter of farming operations to be monitored. Park et al. [85] stated that wireless sensor network-based systems could be a significant method to fully automate the agriculture system, because the sensors provide real-time significant information and believed to eliminate the considerable costs of just wiring. Another study by Kim [86] said that in agriculture, sensor network technique helps to improve existing systems installed in the greenhouse efficiently and smoothly by forwarding real-time collected information to the operator through the radio signals. The system optimises the transmission protocols more accurate and quick and maximises the application of energy to save the energy and reduce the consumption. Pala and team [40] suggested that the utilisation of artificial intelligence techniques in the aeroponic systems could lead not only to find early fault detection but also to fully automate the system without any or small interventions of human operators. The aeroponic system could gain more popularity among local farmers by deploying this technique in a system for monitoring and controlling purpose. However, it will conserve resources and minimise impacts on the environment. The farmers could start to understand their crops at a micro scale and able to communicate with plant through accessible technology. Therefore, in this article, we explored how wireless sensing technologies wove into the aeroponic system. Thus, the primary motivation of this review article was to provide an idea about different intelligent agriculture monitoring tools used for early fault detection and diagnosis for plant cultivation in the aeroponic system (Figure 4). Additionally, it would be helpful for the local farmer and grower to provide timely information about rising problems and influencing factors for successful plant growth in the aeroponic system. The adoption of the intelligent agriculture monitoring tools could reduce the concept of unsuitable for the amateur.

4.1. Number of Sensor Nodes and Input Parameters. At present, the utilisation of different sensor techniques is almost possible in every field of life due to the sharp progressions in the currently available technologies. Moreover, the sensor is a device that has capabilities to measure physical attributes and convert them into signals for the observer [87]. A WSN (wireless sensor network) traditionally consists of a few to dozens and in some cases thousands of the sensor nodes which are connected to one or more sensors [88]. Generally, it includes a BS (base station), which acts as a gateway between the WSN and the end users. Each sensor node is consisting of five main components, which are a microcontroller unit, a transceiver unit, a memory unit, a power unit, and a sensor unit [89]. Each one of these components is a determinant in designing a WSN for deployment. Furthermore, the microcontroller unit is in charge of the different tasks, data processing, and the control of the other components in the node [88]. Through the transceiver unit, a sensor mode performs its communication with other nodes and other parts of the WSN. It is the most dominant communication unit. The memory unit is another important part of the WSN system, which is used to store the observed data. The memory unit could be RAM, ROM, and their other memory types flash or even external storage devices such as USB. Lastly, the last one unit is the power unit. It is one of the critical components of the system which is for node energy supply. However, the power unit could be any source; it can store in batteries (most common) rechargeable or not on in capacitors. In addition, for extra power supply and recharging the power unit, the available natural resource could be used. The natural sources induce solar power energy in forms of photovoltaic panels and cells, wind power energy with turbines, kinetic energy from water, and so on. Last but not the least is the sensor unit, which includes several sensors for parameter measurements such as temperature, humidity, carbon dioxide, methane, and carbon monoxide [90]. However, in the aeroponic system, the total required number of sensors and actuators depends on the size and requirement of the operator.

4.2. Sensor Types and Monitoring Parameters. In this review study, we reviewed the previous work done on the aeroponic system using wireless sensor network technique. We found that the primary objective of a wireless sensor network

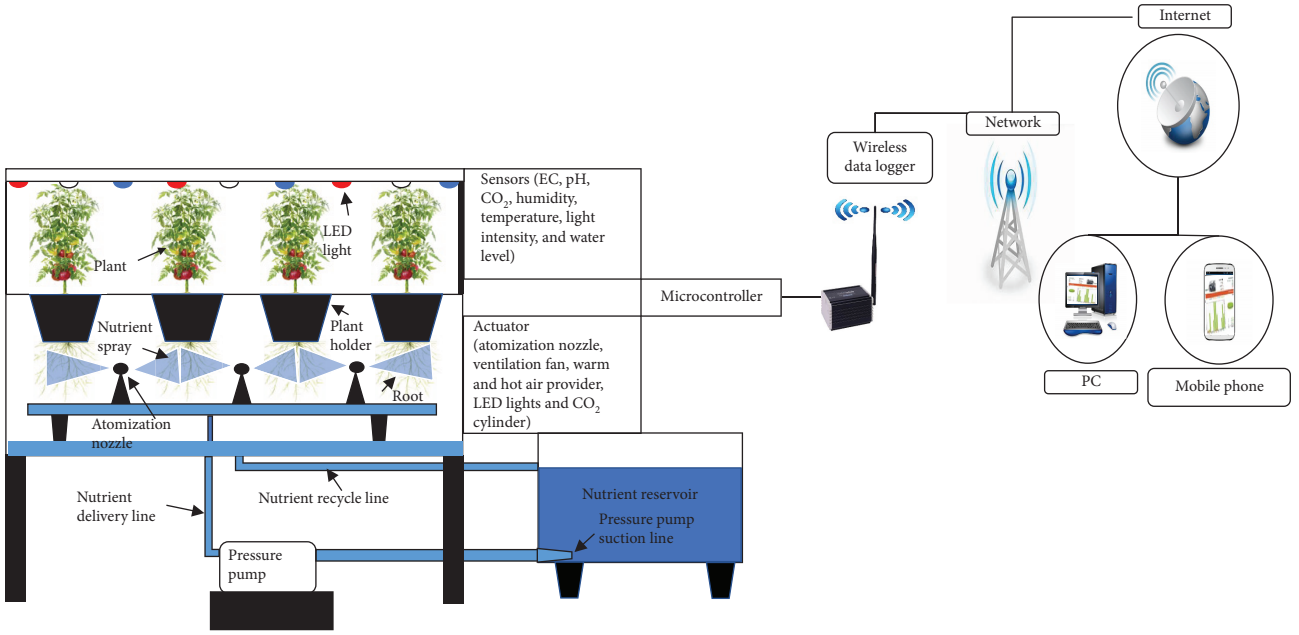

Figure 4: Aeroponic cultivation control system.

system for the aeroponic system is to control the growth chamber climatic condition as per the crop data sheet. However, the basic principle of the aeroponic system is to grow the plant by suspending in the closed, semiclosed, or dark environment in the air with artificial provided support. In the system, the plant stems, leaves, and any fruit grow in a vegetative zone above the suspension medium, and roots dangle below the suspension medium in an area commonly referred as a root zone [46]. Generally, closed cell foam is compressed around the lower stem and inserted into an opening in the aeroponic growth chamber, which decreases labour and expense. However, the trellising is used to suspend the weight of cultivated plant [44]. Ideally, the environment is kept free from pests and diseases so that the plants grow healthier and more quickly than other plants grown on techniques. Furthermore, the key to the success and high yields of the air gardening is a scientific grade monitoring of the conditions and accurate control of the growing environment. Each plant yields and needs a different environmental condition for growth. However, the plant growth is mainly influenced by the surrounding environmental and climatic variables and the amount of water and the fertilizers supplied by irrigation. There is a requirement to monitor and control liquid nutrient parameters in a narrow range of preferred values for optimal growth. The parameters include nutrient temperature, pH, and EC concentration. If the parameters drift outside the desired range, the plants can harm. Besides, there are some additional parameters which can be adjusted to further optimise growth, such as air temperature, relative humidity, light intensity, and carbon dioxide (CO_2) concentration. Idris and Sani [51] reported that the one solution to solve the problems of monitoring and controlling the growing conditions in the space environment is by applying some sensors. The sensor can detect and monitor a number of parameters such as temperature, humidity, light intensity, O_2 and CO_2 levels, direction, and wind speed. Aside from the sensors, there is also a requirement for the actuators to distribute nutrients and waters to plant roots or lower stems (Figure 5). The sensor collects the information of the various environmental conditions and forwards the signals to the actuator to take place and produce the outcome for the collected information to know the status of that parameter. The actuator can control the environment changes. The sensors store information that analyzes the environment and identifies the location, object, people, and their situations. The sensor provides multiple contributions in various domains that depend on a variety of attribute and variant in time [87, 91, 92].

4.2.1. Temperature Sensor. In the aeroponic system, the temperature is one of the critical factors significantly determining plant growth and development. A reduction in temperature below the optimal conditions often results in suboptimal plant growth. A different cultivar requires a different temperature level for the photosynthesis process and growth, which can advance the plant growth stage. It will eventually bring us substantial economic benefits. In the aeroponic system, the optimum growth chamber temperature should not be less and more than 4 and 30°C, respectively, for successful plant growth. The temperature fluctuations of aeroponic growth chamber can significantly affect the root growth, respiration, transpiration, flowering, and dormant period [93]. Therefore, the temperature sensors can be used to monitor the temperature fluctuations of the aeroponic system. At present, temperature sensors are used in many applications like environmental controls, food processing units, medical devices, and chemical handling. The temperature sensor is a device mainly composed of thermocouple or resistance temperature detector. The temperature sensor measures the real-time temperature reading through

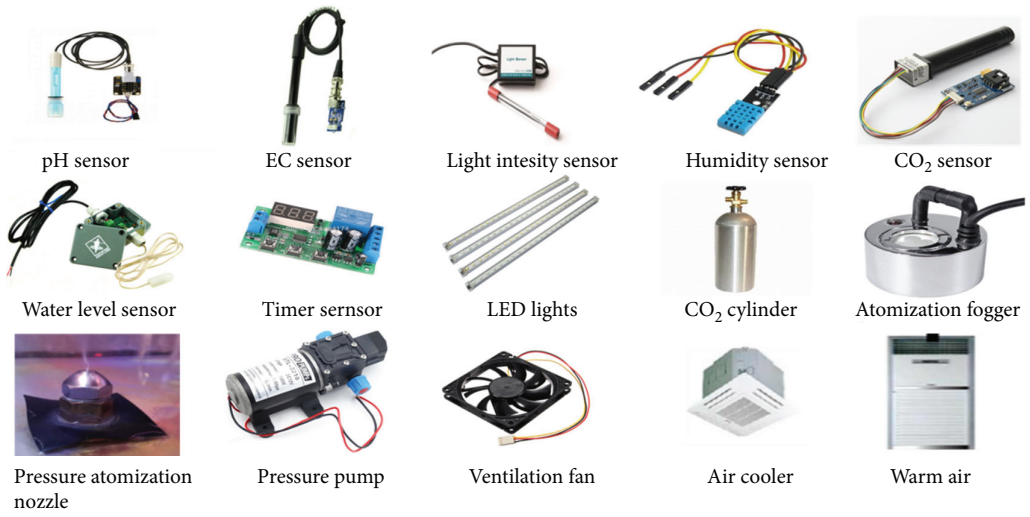

Figure 5: Sensors and actuators used in an aeroponic system.

an electrical signal. The sensors collect the data about temperature from a particular source and convert the data into an understandable form for a device or an observer. The temperature sensor accurately measures temperatures slower changing from critical applications such as facilities or rooms and sends them to the user's webpage.

4.2.2. Humidity Sensor. Aeroponics is the technique of cultivating plant by providing the water nutrient small spray in the air. Thus, the humidity is another important parameter of aeroponic growth chamber environments, and its control is recognised to be very important for significant plant growth. In the aeroponic system, the plant gets all available moisture in the growth chamber. Moreover, if the growth chamber has too high or less moisture content, both conditions will create many problems for the plant. Accordingly, an accurate and precise means of testing moisture content in the growth chamber will help farmers to monitor their crops and provide a suitable growth environment for the plant. Wang et al. [94] reported that a humidity sensor is a device that detects and measures water vapour present in the air within a room or enclosure. At present, humidity sensors are widely used in medicine, agriculture, and environmental monitoring. However, the most commonly used units for humidity measurement are relative humidity [95]. The development of humidity sensors has shown remarkable progress because of using various types of sensing materials in recent years. The sensing materials used in humidity sensors can classify into ceramics, polymers, and composites [96]. The humidity sensor could be placed in the growth chamber to maintain the moisture level. If the moisture level becomes less than the plant requirement, the sensors will forward the signals to atomization nozzles to perform their work.

4.2.3. Light Intensity Sensor. As we know, all vegetable plants and flowers require large amounts of sunlight, and each plant group reacts differently and has the different physiology to deal with light intensity. Some plant performs well in low light intensity and some in high light intensity. However, the aeroponic system implements in indoor conditions, so it is necessary for the farmer to provide sufficient light quantity of at least 8 to 10 hours for a day to grow the healthy plant. The artificial lighting is a better option to present enough intensity to produce a healthy plant [97, 98]. In the conventional aeroponic system, the control of the light quantity present in the growth chamber is mostly done by farmer through observing the plant condition. However, it is a time-consuming and challenging task for the farmer to provide the required light concentration accurately. It could be a better option to use intelligent agriculture techniques to monitor the light intensity in the aeroponic system. The intelligent agriculture techniques mean using the sensor system to control the light intensity. The light sensor is an electronic device which is used to detect the presence or nonpresence of light and darkness. There are several types of light sensors including photoresistors, photodiodes, and phototransistors. These light sensors distinguish the substance of light in a growth chamber and increase or decrease the brightness of light to a more comfortable level. Light sensors can be used to automatically control the lights such as on/off. By adopting the sensor network in aeroponics, the farmer could be able to monitor light intensity without any human interference. Because the sensors will perform all work such as if the light intensity in the growth chamber will be less than the required light quantity for plant growth, the sensor will automatically forward the signal to the LED light to turn on until the light quantity reaches to the desired level.

4.2.4. CO_2 Sensor. The appropriate oxygen concentration in the root environment is crucial to keep the root metabolism in nutrition solution. The available oxygen concentration for the root environment is a hugely significant factor since low concentrations affect the root respiration, nutrient absorption, and, consequently, the plant growth [66]. Thus, the CO_2 sensor could be used to monitor the carbon dioxide fluctuations in the aeroponic growth chamber. A carbon dioxide sensor is an instrument which is used for the measurement of carbon dioxide gas concentration. Bihlmayr

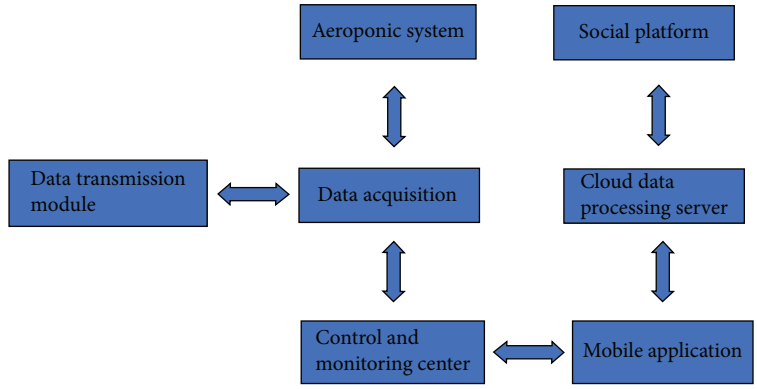

Figure 6: Schematic protocol of wireless network in the aeroponic system.

[99] reported that CO_2 sensors are used to measure indoor air quality in a building to perform demand-based ventilation. However, the CO_2 sensor data measuring range is in between 500 and 5000 parts per million. There are two main types of the CO_2 sensors which include nondispersive infrared carbon dioxide sensors (NICDS) and chemical carbon dioxide sensors (CCDS), whereas the NICDS detected CO_2 in a gaseous environment by its characteristic absorption and composed of an infrared detector, an interference filter, a light tube, and an infrared source. However, the CCDS of sensitive layers are based on polymer or heteropolysiloxane with low-energy consumption [100].

4.2.5. Water Level Sensor. The aeroponics is the method of the plant cultivation by providing a small mist of the nutrient solution in the growth chamber. Thus, there is no any use of soil; just water is required to cultivate the plant throughout the germination to harvest time. Therefore, the water nutrient solution reservoir is one of the major components of the aeroponic system which should be monitored throughout the growth period. In the conventional aeroponic system, the farmer checks the water nutrient level in the nutrient solution reservoir, and if he founds water level less than the desired level, he maintained accordingly. However, by adopting the precision agriculture techniques, the farmer will be able to monitor and control water nutrient level through the intelligent methods such as wireless sensors. The water nutrient level sensors detect the liquid level in the reservoirs and facilitate operator in collecting water nutrient level data in real time. The sensors will alert the operator about any potential property damage that results from any leaks and also allowing to know when a container is nearing empty.

4.2.6. EC and pH Sensor. In the aeroponic system, the plant productivity is closely related to nutrient uptake and the EC and pH regulation of the nutrient solution. The EC and pH concentration of the nutrient solution affects the availability of the nutrients to plants [101]. The pH and EC concentrations are controlled to prevent barrier growth. Their measurement is essential because the solubility of minerals in acidic, alkaline, and ion concentration of all the species in solutions is different and the solution concentration changes with solubility [102, 103]. The unmonitored EC and pH concentration of the nutrient solution will quickly lead to a situation where plants cannot absorb the essential nutrients, if not corrected this will eventually lead to harmful plant growth and poor productivity. Thus, the EC and pH concentration of the nutrient solution is a critical parameter to be measured and controlled throughout the plant growth. Moreover, in the conventional aeroponic system, the EC and pH value of the nutrient solution is mostly monitored manually by performing laboratory analysis or using advanced equipment which is a time-consuming process. For instance, when the EC of the nutrient solution decreased or increased, the control of nutrient solution concentration is mostly achieved by adding more high concentration nutrient solution or the fresh water, respectively, to the nutrient solution to maintain the EC level to the prescribed target range. Similarly, for pH, an acid solution and an alkali solution are used to control the pH fluctuation of the nutrient solution within a specified target range [101]. However, these conventional methods are time-consuming and challenging task for the farmer to maintain the EC and pH value at the desired range accurately. In addition, the EC and pH sensor could be used to deal with the above challenges.

5. Sensor Working Protocol in the Aeroponic System

Today, the world demands automatic tools to do most of the work for them without bothering its user for doing some task. So, the concept is all about a very high level of automation system which will be independent of its users to a very great extent, reduce human efforts, and save all kinds of resource utilisation, as monitoring and controlling will be done by computers leaving very few easily manageable tasks for humans, and it will interest more people to join this field [104–106]. Moreover, the monitoring and control system for the aeroponic system mainly consists of following sections which include the aeroponic system, data acquisition, controlling the equipment, data transmission module, cloud data processing server, social communication platform, and mobile application. A typical architecture of sensor nodes for controlling and monitoring the aeroponic system is shown in Figure 6. Furthermore, in architecture, the data acquisition section refers to some sensor nodes used in the

system to establish a data acquisition module. The data acquisition module is placed in the aeroponic system or near the growth chamber to collect the real-time information from selected parameters (temperature, light intensity, humidity, nutrient solution level, atomization quantity, and photos of the growing plants) and transmit the gathered data to the control and management centre. However, the control and management section refers to the central processing unit (CPU) of the system. The CPU of the system consists of some primary functions such as Arduino and WRTnod protocols, whose work is to store, manage gathered data from collection nodes, process, and then accurately and automatically send to the web server in real time [104–109]. Thus, the system can help the farmer and grower to monitor and control the smart aeroponic system remotely using the mobile app. In other words, the plant will be able to talk with the farmer through a mobile app that whether the selected parameters are working well or not.

6. Advantages of Sensor Techniques in the Aeroponic System

The continuously increasing food demands require rapid improvement and development in the food production system. However, to enhance the quality and productivity of the cultivated crop, peoples are moving towards the modern plant cultivation technologies in agriculture. Thus, the aeroponics is one of the rising plant growing technologies in agriculture as a modern-day cultivation technique, where the plant is cultivated in an air environment, and no any soil support is provided. In the aeroponic system, a number of the parameters are required to control for successful plant growth because there is no any growing medium provided to the plant. For example, if the plant has some sudden stress and the farmer is not present at the site that means the plant will die. Therefore, the proper management of the crop is essential. In the conventional aeroponic system, grower uses his knowledge, skills, and judgment to adjust and maintain the parameters such as EC and pH meter, minimum and maximum temperature, light intensity, and humidity level through several instruments and checks the readings which are labour-intensive and time-consuming task. To deal with the above problems, the aeroponic system can be developed with a wireless sensor and actuator network for monitoring the key parameters at lower labour cost, time, and without any technical knowledge. The wireless sensor and actuator network offer several advantages including faster response to confrontational climatic conditions and better quality control of the crop that produces at a lower labour cost. This advancement in the aeroponic system through wireless sensor network for monitoring growth chamber environment is beneficial. However, the monitoring system also offers a range of information which could be required by plant scientists or grower to provide a greater understanding of how these environmental and nutrient parameters correlate with plant growth. It is now recognised that plant grower can perfectly and easily acquire the skills needed to operate an aeroponic system. It provides the full control of the system, not by constant manual attention from the operator but to a large extent by wireless sensors.

7. Future Application

Artificial intelligence agriculture techniques are considered as a high potential, improving technique for decision-making in agriculture. Nowadays, it is quickly getting peoples' intention, more and more visible in our society and dynamically turning our social awareness and lifestyle. The techniques provide several opportunities to monitor the plant growth and development from pre- to postharvest. Aeroponics is the new plant cultivation technology of agriculture which is still under development. However, we reviewed the literature and found that only limited study had been conducted on the implementation of the intelligent agricultural techniques in the aeroponic system. Moreover, until now, most of the studies had been designed the aeroponic system using a wireless sensor network using ZigBee and Arduino system with Bluetooth, global system of mobile and Wi-Fi, and communication modules. During a literature survey, we noted that no any single study had implemented the idea of the cloud computing and big data techniques in aeroponics to collect real-time information via the Internet. The techniques provide many advantages to the user such as reduction of the initial cost, allocation of the resources on demand, and maintenance and upgrade performed in the back-end, easy, and rapid development. The techniques present a chance to the operator to stay connected with the system using mobile accessories like a smartphone, tablet, and PCs at any location via the Internet which is not restricted by conditions, locations, and time. Furthermore, the system would be designed using additional artificial intelligence techniques such as image processing, automatic seedling transplanters, and harvesting and packing robots. The purpose of image processing and analysis is to measure and identify the physiology, growth, development, nutrient deficiencies, diseases, and other phenotypic properties of the plants through automated and nondestructive analysis.

8. Application of Artificial Intelligence Techniques in Agriculture

Agriculture is the primitive and ancient application that humans started first after born on earth. It has an extensive history between numerous industries and very intimately linked to the human development on earth. Moreover, in the past, the agriculture sector was labour-intensive, but the next-generation farmers, researchers, and associated organisations proposed and applied new farming methods, technologies, skills, and knowledge in agriculture as a modern era to reduce labour-intensive task. Presently, the technology is considered as a key tool to overcome many challenges and eases the way how people live. In the past, the many problems of agriculture, especially in irrigation water management, crop yield production, environment predication, and decision-making, were decided by many factors. In addition, the fertilization often decided by the mathematical equations, formulas, or the experiences of the experts. The cultivation is

represented by descriptive and causal knowledge, and diagnosis of pests and diseases is represented by uncertain knowledge. Thus, this knowledge and experience are illogically incomplete and imprecise, and the traditional procedures can not handle them. However, artificial intelligence has its superiority. It could be an effective approach for solving complex problems to the levels of experts using imitate experts [110]. The term artificial intelligence (AI) was developed in 1956, as "the science and engineering of making intelligent machines" [111]. It is a abroad discipline, which was developed for the interaction of several types of fields such as computer science, information theory, cybernetics, linguistics, neurophysiology, and psychology [112]. The main purpose of the creation of the intelligence techniques is to find the solutions for complex problems and to work, react, and respond like humans. It performed work better than a well-qualified person and brought positive economic and environmental results [112, 113]. Artificial intelligence (AI) tools have helped to predict the behavior of nonlinear systems and to control variables to improve the operating conditions of a system's environment [114–117]. A recently published report highlighted that artificial intelligence is emerging as part of the solutions towards improved agricultural productivity. The global artificial intelligence in agriculture is expected to grow at a significant level. It is employed to improve the efficiency of daily tasks in agriculture such as the adoption of robots and drones, crop health monitoring protocols, automated irrigation system, and driverless tractors [118]. At present, several research studies have been performed by implementing the artificial intelligent techniques in agriculture. Popa [119] revealed that some of the developed applications for agriculture are expert systems and software, sensors for collecting and transmitting data, and robotic and automation which are adapted from different industries into agriculture, whereas the expert systems and software is the planning process such as strategic or operational; it has benefited substantially, due to the expansion of personal computer and Internet use. The systems are generated through the structured knowledge base and reasoning mechanisms acquired from a human expert but with an enhanced computational power and speed [120]. These systems can demarcate management zones taking in consideration with relevant factors and able to recommend suitable crop rotations, optimal plant density, water requirements, appropriate fertilizer use, diagnosing pests and diseases for crops, and suggesting preventive or curative measures [121]. Huang et al. [122] discussed soft computing and applications in agriculture. The study reported that soft computing is the combination of the computing technologies, such as an artificial neural networks (ANNs), fuzzy logic (FL), and genetic algorithms (GAs). These techniques are opposed to the hard computing method which states to a huge set of stochastic and statistical methods. The hard computing provides inaccurate solutions and results of very complex problems through modelling and analysis with a tolerance of imprecision, uncertainty, partial truth, and an approximation. However, the soft computing techniques are used to achieve tractability and robustness. It provides a low-cost solution with a tolerance of imprecision, uncertainty, partial truth, and approximation [123–127]. Sui and Thomasson [128] developed a BP-trained feedforward ANNs to predict nitrogen status in cotton plants based on a data from a ground-based sensing system. Tumbo and team [129] used an on-the-go system for sensing chlorophyll status in corn using BP-trained feedforward ANNs and fiber optic spectrometry to acquire spectral response pattern data in corn fields. Tang et al. [130] developed a texture-based weed classification method consisting of a low-level Gabor wavelet-based feature extraction algorithm and a high-level ANN-based pattern recognition algorithm. El-Faki and group [131] established and tested ANN-based weed detection algorithms capable of detecting the leading weed species competing with wheat and soybean crops. A study by Krishnaswamy and Krishnan [132] predicted the nozzle wear rates for four fan nozzles using regression and ANN methods. Pearson and Wicklow [133] developed a neural network to identify fungal species that infect single kernels using principal components of the reflectance spectra as input features. Smith et al. [134] developed year-round air temperature prediction models for prediction horizons from 1 to 12 h using feedforward-style ANNs. Zadeh [123] introduced the concept of fuzzy sets as a mean for describing complex systems without the requirements for precision. Fuzzy logic may also be useful for descriptive systems, those that fall somewhere between hard systems and soft systems, such as biology and agriculture [135]. Studies reported that in agriculture, fuzzy logic is used for multicriteria analysis of the image, image classification, vegetation mapping, assessment of soil suitability, and planning forest harvesting [136–143]. Al-Faraj and coworkers [144] established a rule-based FL crop water stress index (CWSI) using growth chamber data and tested this method on tall fescue canopies grown in a greenhouse. Thomson et al. [145] and Thomson and Ross [146] developed a coupled sensor- and model-based irrigation scheduling method. Yang et al. [147, 148] informed on the development of an image capture/processing system to detect weeds and a fuzzy logic decision-making system to determine where and how much herbicide to apply in an agricultural field. Gil and team [149] applied multiple linear regression and FL inference models to evaluate the effects of micrometeorological conditions on pesticide application for two spray qualities (fine and very fine). Qiu et al. [150] established a fuzzy irrigation decision-making system using virtual instrumentation platform of sensors, test instruments, data logger, and LabVIEW. Generally, published studies use on/off controllers where the inherent complexity of irrigation process made it difficult to achieve optimal results [151]. Ali et al. [152] developed temperature and humidity controller inside the greenhouse using fuzzy logic. However, several studies have been conducted to develop many control strategies to optimise the greenhouse environment using artificial intelligence techniques such as neural network, fuzzy logic controller, adaptive predictive control, PID, and nonlinear adaptive PID control [153–159]. Zhu et al. [160] used the remote wireless system for water quality online monitoring in intensive aquaculture using artificial neural networks. The results demonstrate that online monitoring for water quality information could be

accurately acquired and predicted by using the remote wireless system. Mahajan et al. [161] reported that agriculture is noteworthy that computer vision applications have grown due to reduced equipment costs, increased computational power, and increasing interest in nondestructive food assessment methods. The use of these techniques presents advantages when compared with traditional methods based on manual work; however, there are still some challenges to be overcome. Moreover, the principle of artificial intelligence in agriculture is one where a machine can perceive its environment, and through a certain capacity of flexible rationality, can act to address a specified goal related to that environment.

9. Conclusion

The objective of our study was to present the information about the use of automated monitoring and controlling technique in the aeroponic system. The aeroponic system is the new plant cultivation method of the modern agriculture. Its existence can allow producing food whole year without any interval. The system could create an excellent set which encourages the sustainable city life for those peoples who want to live in urban area. Moreover, during plant growth from sowing to harvest time, the methods adopted in the aeroponic system require a little hand-operated contribution, interference regarding physical presence, and expertise in domain knowledge of plants, environment control, and operations to maintain and control the growth of the plant. Therefore, the system is considered hitherto to be somewhat unsuitable for the grower, and due to the above reasons, it is not common to find an installation. We reviewed the literature and found that implementation of advanced monitoring technology tools in aeroponics could provide an opportunity for the farmer to monitor and control several paraments without using laboratory instruments, and the farmer can control the entire system remotely. Thus, it could reduce the concept of the usefulness of the system due to the complicated manual monitoring and controlling process. The technology offers incredible opportunities for the aeroponic system to increase the capability, reliability, and availability among the farmers and growers. We believe that our review article will contribute to the adoption of the advanced monitoring technology in the aeroponic system. However, the technique provides a range of information which could be required by plant scientists to provide a greater understanding of how these environmental and nutrient parameters correlate with plant growth.

Conflicts of Interest

The authors declare that they have no conflicts of interest.

Acknowledgments

We acknowledged that this work was financially supported by the Jiangsu Agriculture Science and Technology Innovation Fund (CX (18) 3048), the National Natural Science Foundation of China Program (no. 51275214), and the project funded by the Priority Academic Program Development of Jiangsu Higher Education Institutions (no. 37(2014)).

References

[1] J. James and M. P. Maheshwar, "Plant growth monitoring system, with dynamic user-interface," in *2016 IEEE Region 10 Humanitarian Technology Conference (R10-HTC)*, pp. 1–5, Agra, India, December 2016.

[2] D. Pimentel, B. Berger, D. Filiberto et al., "Water resources: agricultural and environmental issues," *Bioscience*, vol. 54, no. 10, pp. 909–918, 2004.

[3] M. Taher Kahil, J. Albiac, A. Dinar et al., "Improving the performance of water policies: evidence from drought in Spain," *Water*, vol. 8, no. 2, p. 34, 2016.

[4] W. Foote, *To Feed the World in 2050, We Need to View Small-Scale Farming as a Business*, Skoll World Forum, Oxford, UK, 2015.

[5] V. Doknić, *Internet of Things Greenhouse Monitoring and Automation System. Internet of Things: Smart Devices, Processes, Services*, 2014, http://193.40.244.77/idu0330/wpcontent/uploads/2015/09/140605_Internet-of-Things_Vesna-Doknic.pdf.

[6] D. K. Großkinsky, J. Svensgaard, S. Christensen, and T. Roitsch, "Plant phenomics and the need for physiological phenotyping across scales to narrow the genotype-to-phenotype knowledge gap," *Journal of Experimental Botany*, vol. 66, no. 18, pp. 5429–5440, 2015.

[7] E. Playán and L. Mateos, "Modernization and optimization of irrigation systems to increase water productivity," *Agricultural Water Management*, vol. 80, no. 1-3, pp. 100–116, 2006.

[8] L. Levidow, D. Zaccaria, R. Maia, E. Vivas, M. Todorovic, and A. Scardigno, "Improving water-efficient irrigation: prospects and difficulties of innovative practices," *Agricultural Water Management*, vol. 146, pp. 84–94, 2014.

[9] R. Qiu, S. Wei, M. Zhang et al., "Sensors for measuring plant phenotyping: a review," *International Journal of Agricultural and Biological Engineering*, vol. 11, no. 2, pp. 1–17, 2018.

[10] W. Baudoin, R. Nono-Womdim, N. Lutaladio et al., *Good Agricultural Practices for Greenhouse Vegetable Crops: Principles for Mediterranean Climate Areas (No. 217)*, Food and Agriculture Organization of The United Nations, Rome, 2013.

[11] M. Lee and H. Yoe, "Analysis of environmental stress factors using an artificial growth system and plant fitness optimization," *BioMed Research International*, vol. 2015, Article ID 292543, 6 pages, 2015.

[12] S. M. Moon, S. Y. Kwon, and J. H. Lim, "Minimization of temperature ranges between the top and bottom of an air flow controlling device through hybrid control in a plant factory," *The Scientific World Journal*, vol. 2014, Article ID 801590, 7 pages, 2014.

[13] C. Stanghellini, "Horticultural production in greenhouses: efficient use of water," *Acta Horticulturae*, vol. 1034, pp. 25–32, 2014.

[14] D. Savvas, G. Gianquinto, Y. Tuzel, and N. Gruda, "Soilless culture," in *Good Agricultural Practices for Greenhouse Vegetable Crops: Principles for Mediterranean Climate Areas (No. 217)*, W. Baudoin, R. Nono-Womdim, N. Lutaladio, A. Hodder, N. Castilla, C. Leonardi, S. Pascale, and M. Qaryouti,

Eds., pp. 303–354, Food and Agriculture Organization of The United Nations, Rome, 2013.

[15] I. A. Lakhiar, X. Liu, G. Wang, and J. Gao, "Experimental study of ultrasonic atomizer effects on values of EC and pH of nutrient solution," *International Journal of Agricultural and Biological Engineering*, vol. 11, no. 5, pp. 59–64, 2018.

[16] J. P. Beibel, *Hydroponics -The Science of Growing Crops without Soil*, Department of Agriculture. Tallahassee. Bulletin, 1960.

[17] J. L. Reyes, R. Montoya, C. Ledesma, and R. Ramírez, "Development of an aeroponic system for vegetable production," *Acta Horticulturae*, vol. 947, pp. 153–156, 2012.

[18] M. Raviv and L. Lieth, "Significance of soilless culture in agriculture," in *Soilless Culture: Theory and Practice*, M. Raviv and J. H. Lieth, Eds., pp. 117–156, Elsevier, Amsterdam, 2007.

[19] V. Valenzano, A. Parente, F. Serio, and P. Santamaria, "Effect of growing system and cultivar on yield and water-use efficiency of greenhouse-grown tomato," *The Journal of Horticultural Science and Biotechnology*, vol. 83, no. 1, pp. 71–75, 2008.

[20] L. Maharana and D. N. Koul, "The emergence of hydroponics," *Yojana*, vol. 55, pp. 39-40, 2011.

[21] International Center of Applied Aeroponics (ICAA), *Press Release: Golden Potato*, Hanoi, Vietnam, 2014, http://www.icaeroponics.com/press-release.html.

[22] NASA Spinoff, *Innovative Partnership Program*, Publications and Graphics Department NASA Center for Aerospace Information (CASI), 2006.

[23] I. A. Lakhiar, J. Gao, T. N. Syed, F. A. Chandio, and N. A. Buttar, "Modern plant cultivation technologies in agriculture under controlled environment: a review on aeroponics," *Journal of Plant Interactions*, vol. 13, no. 1, pp. 338–352, 2018.

[24] F. Xiong and K. Qiao, "Intelligent systems and its application in agriculture," *IFAC Proceedings Volumes*, vol. 32, no. 2, pp. 5597–5602, 1999.

[25] Z. Zhai, J.-F. Martínez Ortega, N. Lucas Martínez, and J. Rodríguez-Molina, "A mission planning approach for precision farming systems based on multi-objective optimization," *Sensors*, vol. 18, no. 6, p. 1795, 2018.

[26] S. O. Petersen, C. C. Hoffmann, C. M. Schafer et al., "Annual emissions of CH_4 and N_2O, and ecosystem respiration, from eight organic soils in Western Denmark managed by agriculture," *Biogeosciences*, vol. 9, no. 1, pp. 403–422, 2012.

[27] G. Mohammed, F. Trolard, M. Gillon, A. L. Cognard-Plancq, A. Chanzy, and G. Bourrie, "Combination of a crop model and a geochemical model as a new approach to evaluate the sustainability of an intensive agriculture system," *Science of The Total Environment*, vol. 595, pp. 119–131, 2017.

[28] J. Gago, C. Douthe, R. E. Coopman et al., "UAVs challenge to assess water stress for sustainable agriculture," *Agricultural Water Management*, vol. 153, pp. 9–19, 2015.

[29] D. H. Park and J. W. Park, "Wireless sensor network-based greenhouse environment monitoring and automatic control system for dew condensation prevention," *Sensors*, vol. 11, no. 4, pp. 3640–3651, 2011.

[30] A. Barriuso, G. Villarrubia González, J. de Paz, Á. Lozano, and J. Bajo, "Combination of multi-agent systems and wireless sensor networks for the monitoring of cattle," *Sensors*, vol. 18, no. 2, p. 108, 2018.

[31] M. Perez-Ruiz, P. Gonzalez-de-Santos, A. Ribeiro et al., "Highlights and preliminary results for autonomous crop protection," *Computers and Electronics in Agriculture*, vol. 110, pp. 150–161, 2015.

[32] A. Maher, E. Kamel, F. Enrico, I. Atif, and M. Abdelkader, "An intelligent system for the climate control and energy savings in agricultural greenhouses," *Energy Efficiency*, vol. 9, no. 6, pp. 1241–1255, 2016.

[33] A. R. De la Concepcion, R. Stefanelli, and D. Trinchero, "A wireless sensor network platform optimized for assisted sustainable agriculture," in *IEEE Global Humanitarian Technology Conference (GHTC 2014)*, pp. 159–165, San Jose, CA, USA, October 2014.

[34] B. Basnet and J. Bang, "The state-of-the-art of knowledge-intensive agriculture: a review on applied sensing systems and data analytics," *Journal of Sensors*, vol. 2018, Article ID 3528296, 13 pages, 2018.

[35] Aqeel-ur-Rehman and Z. A. Shaikh, "Smart agriculture," in *Application of Modern High-Performance Networks*, pp. 120–129, Bentham Science Publishers Ltd, 2009.

[36] N. Wang, N. Zhang, and M. Wang, "Wireless sensors in agriculture and food industry—recent development and future perspective," *Computers and Electronics in Agriculture*, vol. 50, no. 1, pp. 1–14, 2006.

[37] L. Ruiz-Garcia, L. Lunadei, P. Barreiro, and I. Robla, "A review of wireless sensor technologies and applications in agriculture and food industry: state of the art and current trends," *Sensors*, vol. 9, no. 6, pp. 4728–4750, 2009.

[38] W. Zhang, G. Kantor, and S. Singh, "Integrated wireless sensor/actuator networks in an agricultural application," in *Proceedings of the 2nd international conference on Embedded networked sensor systems - SenSys '04*, p. 317, Baltimore, MD, USA, November 2004.

[39] L. B. Tik, C. T. Khuan, and S. Palaniappan, "Monitoring of an aeroponic greenhouse with a sensor network," *IJCSNS International Journal of Computer Science and Network Security*, vol. 9, no. 3, pp. 240–246, 2009.

[40] M. Pala, L. Mizenko, M. Mach, and T. Reed, "Aeroponic greenhouse as an autonomous system using intelligent space for agriculture robotics," in *Robot Intelligence Technology and Applications 2. Advances in Intelligent Systems and Computing, vol 274*, J. H. Kim, E. Matson, H. Myung, P. Xu, and F. Karray, Eds., pp. 83–93, Springer, Cham, 2014.

[41] P. Laksono, I. Idris, M. I. Sani, and D. N. Putra, "Lab prototype of wireless monitoring and control for seed potatoes growing chamber," *Proceedings of the Asia-Pacific Advanced Network*, vol. 37, pp. 20–29, 2014.

[42] P. Jonas, A. Maskara, A. Salguero, and A. Truong, "Garduino: a cyber-physical aeroponics system," 2015, http://arxiv.org/abs/1011.1669v3, http://ecal.berkeley.edu/files/ce186/projects/truonganders{_}4941954{_}63829747{_}Garduino-1.pdf.

[43] M. I. Sani, S. Siregar, A. P. Kurniawan, R. Jauhari, and C. N. Mandalahi, "Web-based monitoring and control system for aeroponics growing chamber," in *2016 International Conference on Control, Electronics, Renewable Energy and Communications (ICCEREC)*, pp. 162–168, Bandung, Indonesia, September 2016.

[44] P. Anitha and P. S. Periasamy, "Energy efficient green house monitoring in the aeroponics system using Zigbee networks," *Asian Journal of Research in Social Sciences and Humanities*, vol. 6, no. 6, pp. 2243–2250, 2016.

[45] K. Kernahan and C. A. Cupertino, "Aeroponics growth system wireless control system and method of using," US Patent 20160021836A1, 2016.

[46] A. P. Montoya, F. A. Obando, J. G. Morales, and G. Vargas, "Automatic aeroponic irrigation system based on Arduino's platform," *Journal of Physics: Conference Series*, vol. 850, article 012003, 2017.

[47] S. C. Kerns and J. L. Lee, "Automated aeroponics system using IoT for smart farming," in *8th International Scientific Forum, ISF 2017*, UNCP, USA, September 2017.

[48] T. Karu, "High precision farming system based on aeroponics," Master's Thesis. Tallinn University of Technology, Faculty of Information Technology, 2017.

[49] J. A. Martin and S. Rafael, "Systems, methods and devices for aeroponics plant growth," US Patent US20180007845A1, 2018.

[50] P. Mithunesh, K. Gupta, S. Ghule, and P. S. Hule, "Aeroponic based controlled environment based farming system," *IOSR Journal of Computer Engineering (IOSR-JCE)*, vol. 17, no. 6, pp. 55–58, 2015.

[51] I. Idris and M. I. Sani, "Monitoring and control of aeroponic growing system for potato production," in *2012 IEEE Conference on Control, Systems & Industrial Informatics*, Bandung, Indonesia, September 2012.

[52] K. Janarthanan, K. Theviyanthan, F. M. Najath, and I. A. Ahamed, "Cyberponics – a fully automated greenhouse systemBachelors Thesis. Project ID: CTP/2017/01.

[53] J. Liu and Y. W. Zhang, "An automatic aeroponics growth system for bamboo seedling and root observation," *Applied Mechanics and Materials*, vol. 307, pp. 97–102, 2013.

[54] J. Liu and Y. W. Zhang, "An automatic aeroponics growth system based on ultrasonic atomization," *Applied Mechanics and Materials*, vol. 288, pp. 161–166, 2013.

[55] J. Osvald, N. Petrovic, and J. Demsar, "Sugar and organic acid content of tomato fruits (Lycopersicon lycopersicum mill.) grown on aeroponics at different plant density," *Acta Alimentaria*, vol. 30, no. 1, pp. 53–61, 2001.

[56] I. Nir, "Growing plants in aeroponics growth system," *Acta Horticulturae*, vol. 126, pp. 435–448, 1982.

[57] F. Zsoldos, A. Vashegyi, and L. Erdei, "Lack of active K+ uptake in aeroponically grown wheat seedlings," *Physiologia Plantarum*, vol. 71, no. 3, pp. 359–364, 1987.

[58] P. Barak, J. D. Smith, A. R. Krueger, and L. A. Peterson, "Measurement of short-term nutrient uptake rates in cranberry by aeroponics," *Plant Cell and Environment*, vol. 19, no. 2, pp. 237–242, 1996.

[59] M. W. Mbiyu, J. Muthoni, J. Kabira et al., "Use of aeroponics technique for potato (Solanum tuberosum) minitubers production in Kenya," *Journal of Horticulture and Forestry*, vol. 4, no. 11, pp. 172–177, 2012.

[60] C. S. Buer, M. J. Correll, T. C. Smith et al., "Development of a nontoxic acoustic window nutrient-mist bioreactor and relevant growth data," *In Vitro Cellular & Developmental Biology - Plant*, vol. 32, no. 4, pp. 299–304, 1996.

[61] R. W. Zobel and R. F. Lychalk, "Aeroponic growth system with nutrient fog stabilization," US Patent US5937575A, 1999.

[62] M. I. Hessel, G. E. Richert, and J. G. E. Nevill, "Airflow-contained aeroponic nutrient delivery for a microgravity plant growth unit," *Biotronics*, vol. 21, pp. 33–38, 1993.

[63] J. M. Clawson, A. Hoehn, L. S. Stodieck, and P. Todd, *NASA-Review of Aeroponics, Aeroponics for Spaceflight Plant Growth*, Society of Automotive Engineers, Inc, 2000, http://aeroponicsdiy.com/nasa-review-of-aeroponics/.

[64] K. T. Hubick, D. R. Drakeford, and D. M. Reid, "A comparison of two techniques for growing minimally water-stressed plants," *Canadian Journal of Botany*, vol. 60, no. 3, pp. 219–223, 1982.

[65] D. V. Shtrausberg and E. G. Rakitina, "On the aeration and gas regime of roots in aeroponics and water culture," *Agrokhitniia*, vol. 4, pp. 101–110, 1970.

[66] H. Soffer and D. W. Burger, "Effects of dissolved oxygen concentration in aero-hydroponics on the formation and growth of adventitious roots," *Journal of the American Society for Horticultural Science*, vol. 113, pp. 218–221, 1988.

[67] L. L. Hung and D. M. Sylvia, "Production of vesicular-arbuscular mycorrhizal fungus inoculum in aeroponic culture," *Applied and Environmental Microbiology*, vol. 54, pp. 353–357, 1988.

[68] D. M. Sylvia and A. G. Jarstfer, "Sheared—root inocula of vesicular— arbuscular mycorrhizal fungi," *Applied and Environmental Microbiology*, vol. 58, no. 1, pp. 229–232, 1992.

[69] R. E. Wagner and H. T. Wilkinson, "An aeroponics system for investigating disease development on soybean taproots infected with *Phytophthora sojae*," *Plant Disease*, vol. 76, no. 6, pp. 610–614, 1992.

[70] D. M. Sylvia and D. H. Hubbel, "Growth and sporulation of vesicular-arbuscular mycorrhizal fungi in aeroponic and membrane systems," *Symbiosis*, vol. 1, pp. 259–267, 1986.

[71] R. W. Zobel, P. del Tredici, and J. G. Torrey, "Method for growing plants aeroponically," *Plant Physiology*, vol. 57, no. 3, pp. 344–346, 1976.

[72] C. B. Christie and M. A. Nichols, "Aeroponics – a production system and research tool. South pacific soilless culture conference," *Acta Horticulturae*, vol. 648, pp. 185–190, 2004.

[73] A. L. Hayden, "Aeroponic and hydroponic systems for medicinal herb, rhizome and root crops," *HortScience*, vol. 41, no. 3, pp. 536–538, 2006.

[74] S. Chandra, S. Khan, B. Avula et al., "Assessment of total phenolic and flavonoid content, antioxidant properties, and yield of aeroponically and conventionally grown leafy vegetables and fruit crops: a comparative study," *Evidence-Based Complementary and Alternative Medicine*, vol. 2014, Article ID 253875, 9 pages, 2014.

[75] L. J. du Toit, H. W. Kirby, and W. L. Pedersen, "Evaluation of an aeroponics system to screen maize genotypes for resistance to fusarium graminearum seedling blight," *Plant Disease*, vol. 81, no. 2, pp. 175–179, 1997.

[76] D. S. Mueller, S. Li, G. L. Hartman, and W. L. Pedersen, "Use of aeroponic chambers and grafting to study partial resistance to Fusarium solani f. sp. glycines in soybean," *Plant Disease*, vol. 86, no. 11, pp. 1223–1226, 2002.

[77] N. Kacjan-Maršić, and J. Osvald, "Nitrate content in lettuce (*Lactuca sativa* L.) grown on aeroponics with different quantities of nitrogen in the nutrient solution," *Acta Agronomica Hungarica*, vol. 50, no. 4, pp. 389–397, 2002.

[78] G. Fascella and G. V. Zizzo, "Preliminary results of aeroponic cultivation of *Anthurium andreanum* for cut flower production. VIII international symposium on protected cultivation in mild winter climates: advances in soil and soilless

cultivation under protected environment," *Acta Horticulturae*, no. 747, pp. 233–240, 2007.

[79] F. Martin-Laurent, F. Y. Tham, S. K. Lee, J. He, and H. G. Diem, "Field assessment of aeroponically grown and nodulated Acacia mangium," *Australian Journal of Botany*, vol. 48, no. 1, pp. 109–114, 2000.

[80] T. Buckseth, A. K. Sharma, K. K. Pandey, B. P. Singh, and R. Muthuraj, "Methods of pre-basic seed potato production with special reference to aeroponics—a review," *Scientia Horticulturae*, vol. 204, pp. 79–87, 2016.

[81] A. H. Calori, T. L. Factor, J. C. Feltran, E. Y. Watanabe, C. C. Moraes, and L. F. V. Purquerio, "Electrical conductivity of the nutrient solution and plant density in aeroponic production of seed potato under tropical conditions (winter/spring)," *Bragantia*, vol. 76, no. 1, pp. 23–32, 2017.

[82] S. Abdullateef, M. H. Bohme, and I. Pinker, "Potato minituber production at different plant densities using an aeroponic system," *Acta Horticulturae*, vol. 927, pp. 429–436, 2012.

[83] I. Farran and A. M. Mingo-Castel, "Potato minituber production using aeroponics: effect of plant density and harvesting intervals," *American Journal of Potato Research*, vol. 83, no. 1, pp. 47–53, 2006.

[84] H. S. Kim, E. M. Lee, M. A. Lee et al., "Production of high-quality potato plantlets by autotrophic culture for aeroponic systems," *Journal of the Korean Society for Horticultural Science*, vol. 123, pp. 330–333, 1999.

[85] D. H. Park, B. J. Kang, K. R. Cho et al., "A study on greenhouse automatic control system based on wireless sensor network," *Wireless Personal Communications*, vol. 56, no. 1, pp. 117–130, 2011.

[86] Y.-S. Kim, "Expert development for automatic control of greenhouse environment," *Journal of Korean Flower Research Society*, vol. 12, no. 4, pp. 341–345, 2004.

[87] Aqeel-ur-Rehman, A. Z. Abbasi, N. Islam, and Z. A. Shaikh, "A review of wireless sensors and networks' applications in agriculture," *Computer Standards & Interfaces*, vol. 36, no. 2, pp. 263–270, 2014.

[88] A. Arora, R. Ramnath, E. Ertin et al., "ExScal: elements of an extreme scale wireless sensor network," in *11th IEEE International Conference on Embedded and Real-Time Computing Systems and Applications (RTCSA'05)*, pp. 102–108, Hong Kong, China, August 2005.

[89] R. Aquino-Santos, A. Gonzalez-Potes, A. Edwards-Block, and R. A. Virgen-Ortiz, "Developing a new wireless sensor network platform and its application in precision agriculture," *Sensors*, vol. 11, no. 1, pp. 1192–1211, 2011.

[90] S. Yoo, J. Kim, T. Kim, S. Ahn, J. Sung, and D. Kim, "A^2S: automated agriculture systems based on WSN," in *2007 IEEE International Symposium on Consumer Electronics*, pp. 1–5, Irving, TX, USA, June 2007.

[91] G. Abowd, A. K. Dey, P. Brown, N. Davies, M. Smith, and P. Steggles, *Towards a Better Understanding of Context and Context-Awareness, The Workshop on The What, Who, Where, When, and How of Context-Awareness as Part of the 2000 Conference on Human Factors in Computing Systems (CHI 2000)*, Springer, The Netherlands, 1999.

[92] B. N. Schilit and M. M. Theimer, "Disseminating active map information to mobile hosts," *IEEE Network*, vol. 8, no. 5, pp. 22–32, 1994.

[93] V. Otazú, *Manual on Quality Seed Potato Production Using Aeroponics*, vol. 44, International Potato Center (CIP), Lima, Peru, 2010, http://cippotato.org.research/publication/manaul-on-quality-seed-potato-production-using-aeroponics.

[94] C. Wang, A. Zhang, and H. R. Karimi, "Development of La^{3+} doped CeO_2 thick film humidity sensors," *Abstract and Applied Analysis*, vol. 2014, Article ID 297632, 6 pages, 2014.

[95] Z. Chen and C. Lu, "Humidity sensors: a review of materials and mechanisms," *Sensor Letters*, vol. 3, no. 4, pp. 274–295, 2005.

[96] S. D. Zor and H. Cankurtaran, "Impedimetric humidity sensor based on nanohybrid composite of conducting poly (diphenylamine sulfonic acid)," *Journal of Sensors*, vol. 2016, Article ID 5479092, 9 pages, 2016.

[97] I. Ioslovich and P. O. Gutman, "Optimal control of crop spacing in a plant factory," *Automatica*, vol. 36, no. 11, pp. 1665–1668, 2000.

[98] K. Kato, R. Yoshida, A. Kikuzaki et al., "Molecular breeding of tomato lines for mass production of miraculin in a plant factory," *Journal of Agricultural and Food Chemistry*, vol. 58, no. 17, pp. 9505–9510, 2010.

[99] W. Bihlmayr, *Application Note 313. Subject to Modifications*, pp. 2–14, 2011, http://www.enocean.com.

[100] K. Kalwinder, *Carbon Dioxide Sensor. AZO Sensor. Article ID=234*, 2013, http://www.azosensors.com/article.aspx?ArticleID=234.

[101] T. Asao, *Hydroponics - A Standard Methodology for Plant Biological Researches*, Intech, Rijeka, Croatia, 1st edition, 2012.

[102] D. Borgognone, G. Colla, Y. Rouphael, M. Cardarelli, E. Rea, and D. Schwarz, "Effect of nitrogen form and nutrient solution pH on growth and mineral composition of self-grafted and grafted tomatoes," *Scientia Horticulturae*, vol. 149, pp. 61–69, 2013.

[103] S. P. Friedman, "Soil properties influencing apparent electrical conductivity: a review," *Computers and Electronics in Agriculture*, vol. 46, no. 1-3, pp. 45–70, 2005.

[104] L. Yang, V. Sarath Babu, J. Zou, X. C. Cai, T. Wu, and L. Lin, "The development of an intelligent monitoring system for agricultural inputs basing on DBN-SOFTMAX," *Journal of Sensors*, vol. 2018, Article ID 6025381, 11 pages, 2018.

[105] T. L. Dinh, W. Hu, P. Sikka, P. Corke, L. Overs, and S. Brosnan, "Design and deployment of a remote robust sensor network: experiences from an outdoor water quality monitoring network," in *32nd IEEE Conference on Local Computer Networks*, pp. 799–806, Dublin, Ireland, October 2007.

[106] P. Marino, F. P. Fontan, M. A. Dominiguez, and S. Otero, "Environmental monitoring based on emerging wireless technologies," in *Fourth International Conference on Networking and Services (icns 2008)*, pp. 30–34, Gosier, Guadeloupe, March 2008.

[107] I. F. Akyildiz, W. Su, Y. Sankarasubramaniam, and E. Cayirci, "Wireless sensor networks: a survey," *Computer Networks*, vol. 38, no. 4, pp. 393–422, 2002.

[108] M. A. Hebel, "Meeting wide-area agricultural data acquisition and control challenges through ZigBee wireless network technology," in *4th World Congress Conference on Computers in Agriculture and Natural Resources*, Orlando, FL, USA, July 2006.

[109] P. K. Haneveld, *Evading Murphy: A Sensor Network Deployment in Precision Agriculture*, Delft, Netherlands,

2007http://www.st.ewi.tudelft.nl/koen/papers/LOFAR-agro-take2.pdf.

[110] Y.-D. Lee, "Implementation of greenhouse environment monitoring system based on wireless sensor networks," *Journal of the Korea Institute of Information and Communication Engineering*, vol. 17, no. 11, pp. 2686–2692, 2013.

[111] S. L. Andresen, "John McCarthy: father of AI," *IEEE Intelligent Systems Magazine*, vol. 17, no. 5, pp. 84-85, 2002.

[112] P. Lu, S. Chen, and Y. Zheng, "Artificial intelligence in civil engineering," *Mathematical Problems in Engineering*, vol. 2012, Article ID 145974, 22 pages, 2012.

[113] K. de Koning, "Automatic milking–common practice on dairy farms," in *Proceedings of the First North American Conference on Precision Dairy Management and the Second North American Conference on Robotic Milking*, pp. 52–67, Toronto, Canada, 2010.

[114] S. H. Chen, A. J. Jakeman, and J. P. Norton, "Artificial intelligence techniques: an introduction to their use for modelling environmental systems," *Mathematics and Computers in Simulation*, vol. 78, no. 2-3, pp. 379–400, 2008.

[115] W. Batayneh, O. Al-Araidah, and K. Bataineh, "Fuzzy logic approach to provide safe and comfortable indoor environment," *International Journal of Engineering, Science and Technology*, vol. 2, no. 7, pp. 65–72, 2010.

[116] T. K. Das and Y. Das, "Design of a room temperature and humidity controller using fuzzy logic," *American Journal of Engineering Research*, vol. 2, no. 11, pp. 86–97, 2013.

[117] P. G. Lee, "Process control and artificial intelligence software for aquaculture," *Aquacultural Engineering*, vol. 23, no. 1-3, pp. 13–36, 2000.

[118] "Energias market research. Global artificial intelligence (AI) in agriculture market," March 2018, https://www.energiasmarketresearch.com/global-artificial-intelligence-ai-agriculture-market/.

[119] C. Popa, "Adaption of artificial intelligence in agriculture," *Bulletin UASVM Agriculture*, vol. 68, no. 1, pp. 284–293, 2011.

[120] A. Rafea, *Expert System Applications: Agriculture*, Central Laboratory for Expert Systems, Giza Egypt, 2009.

[121] K. S. Wai, A. L. B. A. Rahman, M. F. Zaiyadi, and A. A. Aziz, *Expert System in Real World Applications*, pp. 1–4, 2005, http://citeseerx.ist.psu.edu/viewdoc/download?doi=10.1.1.117.9964&rep=rep1&type=pdf.

[122] Y. Huang, Y. Lan, S. J. Thomson, A. Fang, W. C. Hoffmann, and R. E. Lacey, "Development of soft computing and applications in agricultural and biological engineering," *Computers and Electronics in Agriculture*, vol. 71, no. 2, pp. 107–127, 2010.

[123] L. A. Zadeh, "Fuzzy sets," *Information and Control*, vol. 8, no. 3, pp. 338–353, 1965.

[124] L. A. Zadeh, "Outline of a new approach to the analysis of complex systems and decision processes," *IEEE Transactions on Systems, Man, and Cybernetics*, vol. SMC-3, no. 1, pp. 28–44, 1973.

[125] L. A. Zadeh, "Possibility theory and soft data analysis," in *Mathematical Frontiers of the Social and Policy Sciences*, L. Cobb and R. M. Thrall, Eds., pp. 69–129, Westview Press, Boulder, CO, USA, 1981.

[126] D. E. Rumelhart and J. L. McClelland, *Parallel Distributed Processing: Explorations in the Microstructures of Cognition, vol. I*, MIT Press, Cambridge, MA, USA, 1986.

[127] D. E. Goldberg, *Genetic Algorithms in Search, Optimization, and Machine Learning*, Addison Wesley, Reading, MA, USA, 1989.

[128] R. Sui and J. A. Thomasson, "Ground-based sensing system for cotton nitrogen status determination," *Transactions of the ASABE*, vol. 49, no. 6, pp. 1983–1991, 2006.

[129] S. D. Tumbo, D. G. Wagner, and P. H. Heinemann, "On-the-go sensing of chlorophyll status in corn," *Transactions of the ASAE*, vol. 45, no. 4, pp. 1207–1215, 2002.

[130] L. Tang, L. Tian, and B. L. Steward, "Classification of broadleaf and grass weeds using Gabor wavelets and an artificial neural network," *Transactions of the ASAE*, vol. 46, no. 4, pp. 1247–1254, 2003.

[131] M. S. El-Faki, N. Zhang, and D. E. Peterson, "Weed detection using color machine vision," *Transactions of the ASAE*, vol. 43, no. 6, pp. 1969–1978, 2000.

[132] M. Krishnaswamy and P. Krishnan, "Nozzle wear rate prediction using regression and neural network," *Biosystems Engineering*, vol. 82, no. 1, pp. 49–56, 2002.

[133] T. C. Pearson and D. T. Wicklow, "Detection of corn kernels infected by fungi," *Transactions of the ASABE*, vol. 49, no. 4, pp. 1235–1245, 2006.

[134] B. A. Smith, G. Hoogenboom, and R. W. McClendon, "Artificial neural networks for automated year-round temperature prediction," *Computers and Electronics in Agriculture*, vol. 68, no. 1, pp. 52–61, 2009.

[135] B. Center and B. P. Verma, "Fuzzy logic for biological and agricultural systems," *Artificial Intelligence Review*, vol. 12, pp. 213–225, 1998.

[136] G. C. Vieira, A. R. de Mendonca, G. F. da Silva, S. S. Zanetti, M. M. da Silva, and A. R. dos Santos, "Prognoses of diameter and height of trees of eucalyptus using artificial intelligence," *Science of the Total Environment*, vol. 619-620, pp. 1473–1481, 2018.

[137] N. T. R. Ahamed, K. G. Rao, and J. S. R. Murthy, "GIS-based fuzzy membership model for crop-land suitability analysis," *Agricultural Systems*, vol. 63, no. 2, pp. 75–95, 2000.

[138] M. Boyland, J. Nelson, F. L. Bunnell, and R. G. D'Eon, "An application of fuzzy set theory for seral-class constraints in forest planning models," *Forest Ecology and Management*, vol. 223, no. 1-3, pp. 395–402, 2006.

[139] P. F. Fisher, "Remote sensing of land cover classes as type 2 fuzzy sets," *Remote Sensing of Environment*, vol. 114, no. 2, pp. 309–321, 2010.

[140] H. Jiang and J. R. Eastiman, "Application of fuzzy measures in multi-criteria evaluation in GIS," *International Journal of Geographical Information Science*, vol. 14, no. 2, pp. 173–184, 2000.

[141] B. N. Joss, R. J. Hall, D. M. Sidders, and T. J. Keddy, "Fuzzy-logic modeling of land suitability for hybrid poplar across the Prairie Provinces of Canada," *Environmental Monitoring and Assessment*, vol. 141, no. 1-3, pp. 79–96, 2008.

[142] J. Oldeland, W. Dorigo, L. Lieckfeld, A. Lucieer, and N. Jürgens, "Combining vegetation indices, constrained ordination and fuzzy classification for mapping semi-natural vegetation units from hyperspectral imagery," *Remote Sensing of Environment*, vol. 114, no. 6, pp. 1155–1166, 2010.

[143] T. Phillips, S. Leyk, H. Rajaram et al., "Modeling moulin distribution on Sermeq Avannarleq glacier using ASTER and WorldView imagery and fuzzy set theory," *Remote Sensing of Environment*, vol. 115, no. 9, pp. 2292–2301, 2011.

[144] A. Al-Faraj, G. E. Meyer, and G. L. Horst, "A crop water stress index for tall fescue (*Festuca arundinacea* Schreb.) irrigation decision-making—a fuzzy logic method," *Computers and Electronics in Agriculture*, vol. 32, no. 2, pp. 69–84, 2001.

[145] S. J. Thomson, R. M. Peart, and J. W. Mishoe, "Parameter adjustment to a crop model using a sensor-based decision support system," *Transactions of the ASAE*, vol. 36, no. 1, pp. 205–213, 1993.

[146] S. J. Thomson and B. B. Ross, "Model-based irrigation management using a dynamic parameter adjustment method," *Computers and Electronics in Agriculture*, vol. 14, no. 4, pp. 269–290, 1996.

[147] C. C. Yang, S. O. Prasher, J. A. Landry, J. Perret, and H. S. Ramaswamy, "Recognition of weeds with image processing and their use with fuzzy logic for precision farming," *Canadian Agricultural Engineering*, vol. 42, no. 4, pp. 195–200, 2000.

[148] C.-C. Yang, S. O. Prasher, J.-A. Landry, and H. S. Ramaswamy, "Development of an image processing system and a fuzzy algorithm for site-specific herbicide applications," *Precision Agriculture*, vol. 4, no. 1, pp. 5–18, 2003.

[149] Y. Gil, C. Sinfort, S. Guillaume, Y. Brunet, and B. Palagos, "Influence of micrometeorological factors on pesticide loss to the air during vine spraying: data analysis with statistical and fuzzy inference models," *Biosystems Engineering*, vol. 100, no. 2, pp. 184–197, 2008.

[150] Z. Qiu, X. Tong, J. Shen, and Y. Bao, "Irrigation decision-making system based on the fuzzy-control theory and virtual instrument," *Nongye Gongcheng Xuebao/Transactions of the Chinese Society of Agricultural Engineering*, vol. 23, no. 8, pp. 165–169, 2007.

[151] F. Touati, M. Al-Hitmi, K. Benhmed, and R. Tabish, "A fuzzy logic based irrigation system enhanced with wireless data logging applied to the state of Qatar," *Computers and Electronics in Agriculture*, vol. 98, pp. 233–241, 2013.

[152] R. B. Ali, E. Aridhi, M. Abbes, and A. Mami, "Fuzzy logic controller of temperature and humidity inside an agricultural greenhouse," in *2016 7th International Renewable Energy Congress (IREC)*, Hammamet, Tunisia, March 2016.

[153] F. Fourati, "Multiple neural control of a greenhouse," *Neurocomputing*, vol. 139, pp. 138–144, 2014.

[154] M. Taki, Y. Ajabshirchi, S. Faramarz Ranjbar, A. Rohani, and M. Matloobi, "Heat transfer and MLP neural network models to predict inside environment variables and energy lost in a semi-solar greenhouse," *Energy and Buildings*, vol. 110, pp. 314–329, 2016.

[155] F. Lafont and J.-F. Balmat, "Optimized fuzzy control of a greenhouse," *Fuzzy Sets and Systems*, vol. 128, no. 1, pp. 47–59, 2002.

[156] P. Salgado and J. B. Cunha, "Greenhouse climate hierarchical fuzzy modelling," *Control Engineering Practice*, vol. 13, no. 5, pp. 613–628, 2005.

[157] M. Azaza, K. Echaieb, F. Tadeo, E. Fabrizio, A. Iqbal, and A. Mami, "Fuzzy decoupling control of greenhouse climate," *Arabian Journal for Science and Engineering*, vol. 40, no. 9, pp. 2805–2812, 2015.

[158] A. Chouchaine, E. Feki, and A. Mami, "Stabilization using a discrete fuzzy PDC control with PID controllers and pole placement: application to an experimental greenhouse," *Journal of Control Science and Engineering*, vol. 2011, Article ID 537491, 9 pages, 2011.

[159] S. Zeng, H. Hu, L. Xu, and G. Li, "Nonlinear adaptive PID control for greenhouse environment based on RBF network," *Sensors*, vol. 12, no. 5, pp. 5328–5348, 2012.

[160] X. Zhu, D. Li, D. He, J. Wang, D. Ma, and F. Li, "A remote wireless system for water quality online monitoring in intensive fish culture," *Computers and Electronics in Agriculture*, vol. 71, pp. S3–S9, 2010.

[161] S. Mahajan, A. Das, and H. K. Sardana, "Image acquisition techniques for assessment of legume quality," *Trends in Food Science and Technology*, vol. 42, no. 2, pp. 116–133, 2015.

Hindawi
Journal of Sensors
Volume 2018, Article ID 9634752, 14 pages
https://doi.org/10.1155/2018/9634752

Research Article

On-the-Go Grapevine Yield Estimation Using Image Analysis and Boolean Model

Borja Millan,[1,2] **Santiago Velasco-Forero**,[2] **Arturo Aquino**,[1] **and Javier Tardaguila**[1]

[1]*Instituto de Ciencias de la Vid y del Vino (University of La Rioja, CSIC, Gobierno de La Rioja), Finca La Grajera, 26007 Logroño, La Rioja, Spain*
[2]*MINES ParisTech, PSL Research University, CMM-Center of Mathematical Morphology, 77300 Fontainebleau, France*

Correspondence should be addressed to Javier Tardaguila; javier.tardaguila@unirioja.es

Received 31 March 2018; Revised 3 September 2018; Accepted 9 October 2018; Published 16 December 2018

Guest Editor: Edward Sazonov

This paper describes a new methodology for noninvasive, objective, and automated assessment of yield in vineyards using image analysis and Boolean model. Image analysis, as an inexpensive and noninvasive procedure, has been studied for this purpose, but the effect of occlusions from the cluster or other organs of the vine has an impact that diminishes the quality of the results. To reduce the influence of the occlusions in the estimation, the number of berries was assessed using the Boolean model. To evaluate the methodology, three different datasets were studied: cluster images, manually acquired vine images, and vine images captured on-the-go using a quad. The proposed algorithm estimated the number of berries in cluster images with a root mean square error (RMSE) of 20 and a coefficient of determination (R^2) of 0.80. Vine images manually taken were evaluated, providing 310 grams of mean error and $R^2 = 0.81$. Finally, images captured using a quad equipped with artificial light and automatic camera triggering were also analysed. The estimation obtained applying the Boolean model had 610 grams of mean error per segment (three vines) and $R^2 = 0.78$. The reliability against occlusions and segmentation errors of the Boolean model makes it ideal for vineyard yield estimation. Its application greatly improved the results when compared to a simpler estimator based on the relationship between cluster area and weight.

1. Introduction

Sustainable viticulture requires continuous monitoring of the vineyard to assist the decision-making procedure and to optimize cultural practices like pruning, irrigation, and disease management. The use of noninvasive proximal sensors reduces the time and labour resources, favouring objective data acquisition. Image analysis techniques allow for fast and reliable measurements, and recent studies have aimed its use in viticulture. Application examples include canopy status assessment [1, 2] and, more recently, pruning mass determination [3]. As a noninvasive, reliable, and low-cost technology, image analysis is also a candidate for its integration in fully automated systems for vineyard monitoring [4]. These tools are key devices for the future viticulture, as they will reduce management costs and will allow the application of more sustainable practices.

Grapevine yield estimation is encouraged by its economical relevance [5–7] and can help to optimize plant growth and to improve fruit quality [8]. Early yield estimation can be generated from the flower number per inflorescence assessed using computer vision [9]. Estimations representing final yield variability can be acquired nearby to harvest time using cluster images [10]. To improve the image quality and ease the segmentation process, some authors captured the images under controlled conditions, in the laboratory or using a specially developed chamber [11, 12]. Due to the destructive, slow, and labour-demanding nature of this process, it is hard to scale it to increase the sample points. Another approach would be the manual acquisition of images on the field [13–15], but although this method

requires less workforce, a more automatized procedure is desirable for an industrial application. Finally, modified agricultural vehicles can be used to automate the image capture of large datasets [16, 17]. This approach has to face the limitation introduced by the lack of supervision during the capture, which greatly affects image quality. The segmentation process of images acquired on the field is challenging, because of the uncontrolled scenario characteristics and the unevenness in the berry surface caused by the pruina [11]. Also, it must be noted that not all the berries in a cluster are visible due to occlusions from other berries or vegetal material from the vine. A method that has resistance to these problems (occlusions and segmentation errors) will greatly improve the prediction reliability.

The Boolean model and random set theory was developed by Matheron [18] and Serra [19]. From an image-processing viewpoint, the practical advantage of this model relies in its capability to estimate the number of particles present in an image, even when errors in the segmentation or occlusions are present. It has been mainly used for modelling material structure characteristics [18–20], for estimating the spatial distribution of bacterial colonies in cheese [21] or the number of cells in a cluster [22]. However, to the best of our knowledge, it has not been used in agriculture for berry and yield estimation.

This study aims at grapevine yield assessment using image analysis and the Boolean model. This solution was tested under three different scenarios: cluster images, manually acquired vine images and on-the-go captured vine images using a quad at a speed comparable to other agricultural equipment used in vineyard management.

2. Materials and Methods

2.1. Image Acquisition. The experiments were conducted in September 2014 and 2015 in a commercial vineyard located in Falces (latitude 42°27′45.96″, longitude 1°48′13.42″, and altitude 325 m; Navarra, Spain). The vines were growing in a vertical shoot-positioning system, with north-south row orientation at 2 × 1 m disposition. Five different grapevine (*Vitis vinifera* L.) varieties were used. The choice of a multivarietal experiment was made to increase the variability in yield components (number of berries per cluster, mean berry weight, and mean cluster weight). The six first basal leaves of the selected vines were manually removed after berry set.

Three different sets of images were captured:

(i) Manually Acquired Cluster Images. A set of 45 cluster images from four different grapevine varieties (Cabernet Sauvignon, Garnacha, Syrah, and Tempranillo) was captured in the field on the 4th of September 2014 and harvested the next day. The images were taken using a Nikon D5300 digital reflex camera (Nikon Corp., Tokyo, Japan) equipped with a Sigma 50 mm F2.8 macro (Sigma Corp., Kanagawa, Japan). RGB images were captured with uncontrolled illumination using an orange cardboard as background and saved at a resolution of 24 Mpx (6000 × 4000 pixels), 8 bits per channel.

(ii) Manually Acquired Vine Images. A set of 45 images from four different grapevine varieties (Cabernet Sauvignon, Garnacha, Syrah, and Touriga Nacional) were taken in the field at the same date as the cluster images. RGB images were captured using a Nikon D5300 digital reflex camera equipped with a Nikon AF-S DX 10 NIKKOR 18–55 mm f/3.5–5.6G VR lens. The acquisition was realized under uncontrolled illumination using a white panel as background and a tripod to maintain a capturing distance around 120 cm. The images were saved at a resolution of 24 Mpx (6000 × 4000 pixels), 8 bits per channel.

(iii) On-the-Go Acquired Vine Images. 64 images from three different grapevine varieties (Cabernet Sauvignon, Syrah, and Tempranillo) were captured at night time on the 9th of September of 2015 using a quad (Trail Boss 330, Polaris Industries, Minnesota, USA) at a speed around 7 km/h. Clusters were harvested and weighted the next day. The vehicle was equipped with a Sony alpha 7-II digital mirrorless camera (Sony Corp., Tokyo, Japan). The camera had a Vario-Tessar FE 24–70 mm lens. RGB images were saved at a resolution of 24 Mpx (6000 × 3376 pixels), 8 bits per channel, and manually combined to obtain 28 sections composed of three vines. A 900 LED Bestlight panel and two Travor spash IS-L8 LED lights were used for scene illumination. The quad was fitted with an adjustable mechanical structure that allowed for different height and depth fixation to adapt to the vine configuration (Figure 1(a)). The structure also provided protection against branch impact and allowed the attachment of the illumination equipment. The camera was triggered by a custom-built controller using an Arduino MEGA (Arduino LLC, Italy). The controller generated the shooting signal based on the information received from an inductive sensor attached to the rear axle. This sensor produced 3 pulses per rear-axle revolution, thus allowing the camera to obtain images with an approximate 40% of superposition rate.

2.2. Boolean Model for Berry Number Estimation. Boolean random closed sets [18] have been widely used for particle number estimation in images [23]. The main strength of this model is its robustness against partly covered objects and errors in segmentation.

The model can be applied if the structure is Boolean [19] but is not limited to this case due to the central limit theorem [22]. To estimate the number of objects in a region Z, the following formulation can be used:

$$\text{Number of objects} = -\frac{a_z}{a'} \log q, \tag{1}$$

where a_z is the area under study (ROI), a' is the mean area of the object, and q is the ROI porosity:

$$q = \frac{\#\text{pixels of the ROI} - \#\text{pixels of the segmented area}}{\#\text{pixels of the ROI}}. \tag{2}$$

(a)

(b)

Figure 1: On-the-go capturing system: (a) modified quad with automatic camera triggering, LED illumination, and structure for easy position adjustment; (b) example of an on-the-go captured vine image.

The Boolean model can be directly used for berry number estimation, but the ROI must be defined so that the concentration of particles is similar on it. In the case of vine images, particle (berries) concentration is limited to portions in the image (clusters), so a ROI not corresponding to all the image areas must be selected for proper porosity calculation. The ROI was automatically obtained by applying a morphological opening [24] (morphological erosion followed by dilation) for all the segmented clusters using a circular kernel of the same radius of the mean berry size.

To evaluate the prediction capabilities of the Boolean model, four tests were conducted (each one composed of 100 simulations). The tests were performed by using MATLAB (R2010b, MathWorks, Natick, MA, USA) to generate synthetic images containing randomly placed particles. First, the test compared the error of the Boolean model for 50 randomly positioned particles of a radius equal to 5 in an image composed of 100×100 pixels. Next, random variation on the radius of each particle (up to 30%) was used to generate a new set of simulations. The same tests were also

performed for 500 particles in an identical area for fixed and variable radii.

For comparison purposes, a naïve estimator was also defined as follows:

$$\text{Number of objects} = \frac{\#\text{pixels segmented as cluster}}{\#\text{pixels corresponding to mean object area}}. \quad (3)$$

This estimator only takes into account the relationship between the total area of the particles (cluster/s) and the mean particle area (berry). This formulation is similar to other approaches used in the bibliography [13, 14].

2.3. Image Analysis Algorithm for Berry Number Estimation. The three previously described sets of images (manually acquired cluster images, vine images acquired manually, and vine images captured on-the-go) were analysed using similar approaches: first the clusters were segmented, then the Boolean model was applied to estimate berry number.

The Boolean model used for berry number estimation only requires as inputs an average radius of the particle (berry) and the area of the segmented regions or, more specifically for this application, the segmented cluster (the procedure is described in Section 2.4). To determine the mean berry radius, different approaches were used depending on the type of the images to be analysed:

(i) Cluster Images. The berry radius was manually extracted (an operator selected two points at the equatorial line of a berry). This process was repeated for every image because of the measurement variation depending on the distance between the camera and the cluster.

(ii) Vine Images. An average radius was set (manually extracted in one image as in the cluster dataset) and applied to all images from the same grapevine variety.

The algorithm for image analysis was implemented in MATLAB and process batches of images in a fully automated way. The cluster segmentation procedure was based on a Mahalanobis distance classifier and is defined in the following section. For the on-the-go images, misclassification between the pixels corresponding to clusters and the metal wires used for the vine support were observed. An additional filtering step is described in Section 2.5 and the benchmarking and validation process of the classification in Section 2.6.

2.4. Cluster Segmentation. In our approach, cluster segmentation was the first step that must be implemented to obtain the yield estimation. Every pixel in the image was characterized as a six-dimension vector denoted by $\overrightarrow{u}$, using two different colour models: red-green-blue (RGB) and the hue-saturation-value (HSV) representation. HSV and RGB are different colour spaces, with RGB being closer to physical image acquisition and HSV having the advantage of separating the colour and illumination information (*croma* and *luma*, respectively), thus making colour information invariant to nonuniform illumination. We note that the hue component in HSV colour space is an angular variable with values between 0° to 360°. In this case, the "beginning" coincides with the "end," i.e., 0° has the same meaning as 360°, and methods to measure distances between any two points should take careful note of that. Taking advantage of the blue colour (with the hue value centred at 240°) is the dominant coloration for the clusters; the H component of the vector definition of the pixel was calculated using a modification of the standard definition of the HSV to RGB conversion, assigning the blue colour to the centre of the interval (128).

Colour-based segmentation was performed using the Mahalanobis distance [25] on each pixel. The Mahalanobis distance between two vectors $(\overrightarrow{u}, \overrightarrow{v})$ with the same distribution and covariance matrix Σ is defined as

$$d_m(\overrightarrow{u}, \overrightarrow{v}) = \sqrt{(\overrightarrow{u} - \overrightarrow{v})^T \Sigma^{-1} (\overrightarrow{u} - \overrightarrow{v})}. \quad (4)$$

In this application, $\overrightarrow{u}$ is an image pixel, $\overrightarrow{v}$ represents the reference pixels (seeds) for each class to be identified, and the covariance matrix (Σ) is calculated as follows:

$$\Sigma = \begin{bmatrix} \sigma_{RR} & \sigma_{RG} & \sigma_{RB} & \sigma_{RH} & \sigma_{RS} & \sigma_{RV} \\ \sigma_{GR} & \sigma_{GG} & \sigma_{GB} & \sigma_{GH} & \sigma_{GS} & \sigma_{GV} \\ \sigma_{BR} & \sigma_{BG} & \sigma_{BB} & \sigma_{BH} & \sigma_{BS} & \sigma_{BV} \\ \sigma_{HR} & \sigma_{HG} & \sigma_{HB} & \sigma_{HH} & \sigma_{HS} & \sigma_{HV} \\ \sigma_{SR} & \sigma_{SG} & \sigma_{SB} & \sigma_{SH} & \sigma_{SS} & \sigma_{SV} \\ \sigma_{VR} & \sigma_{VG} & \sigma_{VB} & \sigma_{VH} & \sigma_{VS} & \sigma_{VV} \end{bmatrix}, \quad (5)$$

and the covariance matrix elements can be calculated as

$$\sigma_{RG} = \sigma_{GR} = \frac{1}{n-1} \sum_{i=0}^{n} (Ri - \bar{R})(Gi - \bar{G}), \quad (6)$$

where $Ri, Gi \ldots Si, Vi$ are the values of the ith match, and $\bar{R}, \bar{G} \ldots \bar{S}, \bar{V}$ are the mean values in the image to be processed.

The seeds used as reference for each set were manually selected from a different image for each variety (as there exists differences in the cluster colorations between them). The number of classes depends on the type of images: three for cluster images (grape, rachis, and background) and six for vine images, including manual and on-the-go (leaf, background, trunk, shoot, cable, and cluster) corresponding to the different elements present in the scene.

The Mahalanobis distance considers not only the distance to the centroid of the sample pixels but also the fact that the variances in each direction are different, as well as the covariance between variables [13]. The use of Mahalanobis distance in colour images standardizes the influence of the distribution of each feature, taking into account the correlation between each pair of terms [26].

After the distance was calculated for each pixel, it was converted to an occurrence probability to obtain a membership probability map (MPM) [27] using the Boltzmann

distribution [28]. The Boltzmann distribution is a probability distribution that gives the probability for a system to be in a certain state as a function of that state's energy and temperature. For this application, the Mahalanobis distance is used as the energy of the system. The formula that describes the probability for a given pixel in the coordinates (x, y) for a class i is

$$\text{MPMcolour}_{x,y,i} = \frac{e^{(-d_i(x,y)/\text{kT})}}{\sum_{j=1}^{M} e^{\left(-d_j(x,y)/\text{kT}\right)}}, \tag{7}$$

where $d_k(x, y)$ corresponds to the Mahalanobis distance of the pixel located at the (x, y) coordinates and its reference value for the class i. kT is a constant that in the original formulation of the Boltzmann distribution corresponds to the multiplication of the Boltzmann constant and the thermodynamic temperature; for this application, it was set to 10. The denominator guarantees that all the probabilities are normalized, and the sum of the M class probabilities is equal to 1 for every pixel of the MPM.

Cluster segmentation in both the cluster and manually acquired vine images was performed using the maximum pertinence to cluster class from MPMcolour. Additional MPMs were used for on-the-go acquired vine images as described in the following section.

2.5. Additional Filters for Cluster Segmentation for On-the-Go Captured Images. The MPMcolour information can be combined with other MPMs generated using morphological data to aid in the segmentation process. Hence, three additional MPMs were defined to improve the cluster segmentation for the on-the-go images:

(i) Cluster Proximity MPM (MPMcluster_proximity). As a preprocess, a pyramidal decomposition with step values similar to berry size (5 by 5 pixels) was conducted on the pixels that had the maximum likelihood of being part of the cluster class (from MPMcolour). Next, a Gaussian filter with a standard deviation set to 3 times the average grape radius was used to expand the cluster pertinence probabilities. By doing this, pixels in the neighbourhood of the previously filtered cluster candidates increase their possibility of pertinence to the cluster class. Also, isolated pixels that were not close to clusters will decrease its cluster class membership probabilities.

(ii) Shape-Angle MPM (MPMcable). Due to the misclassifications between the cluster and cable class, and taking advantage of the well-defined shape characteristics of the cable, a filter was defined. As a first step, all the connected components (CCs) corresponding to the cable and cluster class (from MPMcolour) were extracted, and all the CCs whose areas were lower than the size of the mean berry were eliminated, which is to say

$$\text{Area}(\text{CC}_i) > r_{\text{berry}}^2 * \pi, \tag{8}$$

where $\text{Area}(\text{CC}_i)$ corresponds to the number of pixels of the ith CC and r_{berry} is the mean berry radius.

Then, the length and orientation of the major and minor axes for every remaining CC were determined. The shape relation was calculated as the division of the major by the minor axis length:

$$\text{Shape relation} = \frac{\text{major axis length}}{\text{minor axis length}}. \tag{9}$$

Combining these two descriptors, a new MPM was generated as follows:

$$\text{MPMcable} = (1 - \text{Shape relation}) * \left(1 - \text{abs}\left(\frac{\text{Major axis orientation}}{90}\right)\right). \tag{10}$$

(iii) Linear Occurrence Zone (MPMlinear_occurrence_zone). As the cables along the vines were usually placed at fixed heights, there were horizontal sections in the images where the probability of a pixel to belong to the cable class was higher. To determine these zones independently from the camera or cable position in the image, an automatic detector was built. The CCs most likely to correspond to the cable class were used. For this purpose, all the CCs with an orientation around ±30° and with a shape relation lower than 0.5 were chosen to generate a binary image (Cable_b). From this, an accumulator for each row based on the sum of the number of pixels selected as the cable class was generated using the following expression:

$$\text{Accumulator}_y = \sum_{x=1}^{\text{number of columns}} \text{Cable}_b(x, y), \tag{11}$$

being

$$\text{Cable}_b(x, y) = \begin{cases} 1 \text{ if } I(x, y) \in \text{Filtered CCcable} \\ 0 \text{ otherwise} \end{cases} \tag{12}$$

for every column x and row y in the image I.

This accumulator holds the number of pixels of the filtered cable candidates for each row; as an example, the accumulator of Figure 2(a) is shown in Figure 2(b). The next step is to apply a Gaussian filtering, thus allowing for some flexibility in the angle of the cables and not limiting it to the horizontal case. The result of the smoothing is presented in Figure 2(c). The final MPM of the linear occurrence zone is obtained by expanding the smoothed accumulator to all the rows of the image. Figure 2(d) shows the MPM (in grayscale) along with the filtered CCs that were overprinted in red colour for illustration purposes.

The final MPM used to classify the pixels as clusters for the on-the-go images was obtained by the element-wise multiplication of the four previously calculated MPMs: MPMcolour, MPMcluster_proximity, MPMcable, and MP

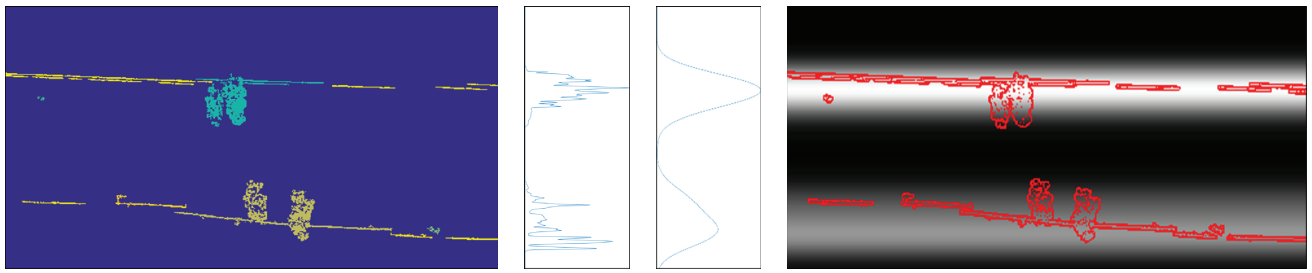

Figure 2: Steps for the generation of the MPMlinear_occurrence_zone aimed for reduction of misclassification between the cluster and cable class during segmentation: (a) objects segmented as cable candidates from automatically taken images using a quad; (b) accumulator of the number of pixels of cable candidates for each row; (c) smoothed accumulator; (d) membership probability map (MPM) for cable occurrence based on the position of the cable (in grayscale) with the original candidates over imposed in red.

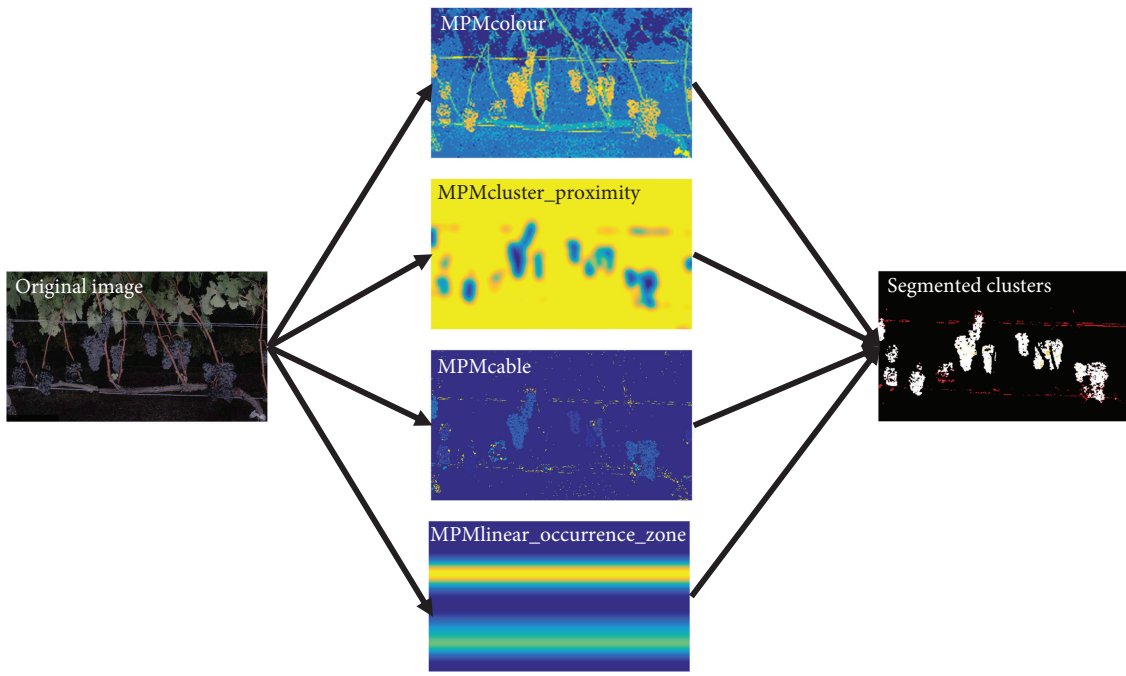

Figure 3: Cluster segmentation process for on-the-go captured image. The original image is used to obtain four MPMs (membership probability maps): MPMcolour, MPMcluster_proximity, MPMcable, and MPMlinear_occurrence_zone. These MPMs were combined to classify the pixels corresponding to clusters for the on-the-go captured images.

Mlinear_occurrence_zone. The process is represented in Figure 3.

2.6. Validation. To evaluate the developed algorithms, yield estimation has to be compared with real data. Also, due to the especial characteristics of the on-the-go images, the segmentation was ranked before and after the filtering MPMs were applied.

The ground truth for every data set was obtained as follows:

(i) Manually Acquired Cluster Images. All the photographed clusters were picked and introduced into pretagged plastic bags to allow their conservation during their transport to the laboratory. Then, they were destemmed, and the berries were detached, counted, and weighted. The number of berries per cluster and their weight was used to obtain the average berry weight.

(ii) Manually Acquired Vine Images. After the image capturing process, all the vines were harvested, and the clusters were weighted together to obtain the final yield per vine.

(iii) On-the-Go Acquired Vine Images. After image acquisition, the sections composed of three vines were harvested and the clusters weighted together to obtain the final yield per section.

To evaluate the segmentation process of the on-the-go images and the improvements of the multi-MPM filtering, it is necessary to obtain a ground truth. An application

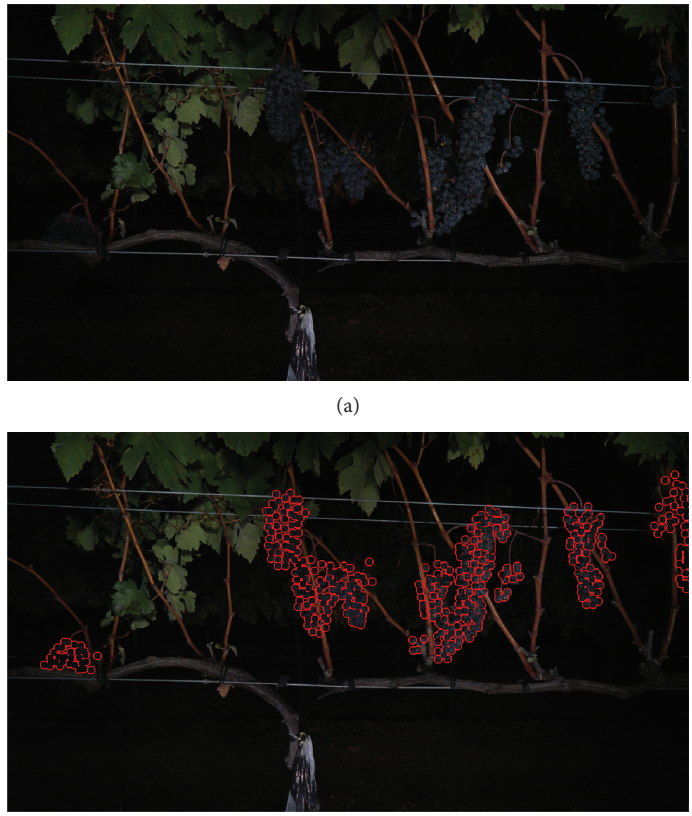

(a)

(b)

Figure 4: Ground truth generation for segmentation performance benchmarking: (a) example image of a vine captured on-the-go of cv. Tempranillo; (b) ground truth mask of the clusters. The berries were manually selected using a custom-built application.

allowing to manually select the berry centres was built to generate a mask representing the area occupied by the clusters in the image. An example of an on-the-go automatically captured photograph is shown in Figure 4(a), and the manually selected pixel classification for benchmarking this image is shown in Figure 4(b).

The mask generated using this application was used to obtain the following metrics:

(i) True Positive (TP). A pixel classified as corresponding to a cluster that actually matches a cluster pixel in the manually selected mask.

(ii) False Positive (FP). A pixel classified as corresponding to a cluster that does not match a cluster pixel in the manually selected mask.

(iii) False Negative (FN). A pixel that was automatically classified as not corresponding to a cluster but actually corresponding to a cluster in the mask.

Finally, the Recall and Precision metrics were used for evaluating the quality of each analysed image as follows:

$$\text{Recall} = \frac{\text{TP}}{\text{TP} + \text{FN}}, \tag{13}$$

where Recall provides the percentage of actual cluster pixels detected;

$$\text{Precision} = \frac{\text{TP}}{\text{TP} + \text{FP}}, \tag{14}$$

where Precision indicates the percentage of pixels correctly assessed.

3. Results and Discussion

3.1. Evaluation of the Occlusion Robustness of the Boolean Model. As described in Section 2.2, four tests were performed to evaluate the occlusion robustness of the Boolean model and to compare its results to those generated by the naïve estimator. Figures 5(a) and 5(b) show the simulations corresponding to 50 particles of fixed and variable radii, respectively. As can be checked in Table 1, the error rates for both estimators were low and similar but with slight improvement for the case of the naïve estimator. For the third and fourth experiments, the number of particles was 10-fold higher, making particle occlusion more likely to occur under these conditions (Figures 5(c) and 5(d)). The Boolean model estimates the number of particles with an error rate similar to the low occlusion case. On the contrary, the error yielded by the naïve estimator rose to 25% for fixed and variable

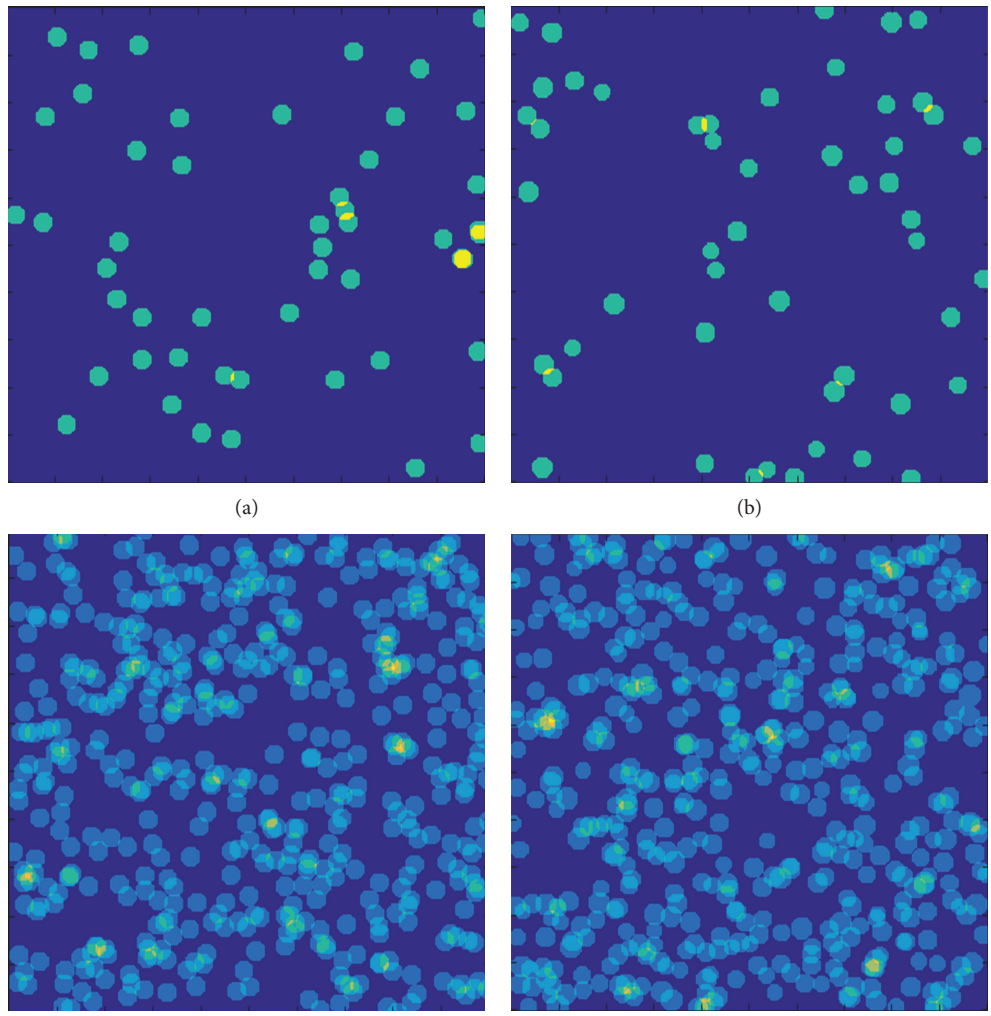

Figure 5: Simulation example of a random distribution of particles in a 100×100 pixel area: (a) 50 particles of radius = 5, (b) 50 particles with a random variation in the radius up to 30%, (c) 500 particles with radius = 5, and (d) 500 particles with a random variation in the radius of the particle up to 30%.

Table 1: Results for the estimation error of the number of particles for randomly generated simulations of 50 and 500 particles, with and without variation in radius, for the naïve estimator and the Boolean model.

	50 particles		500 particles	
	Rad = 5	Rad = 5 ± 15%	Rad = 5	Rad = 5 ± 15%
Naïve estimator*	1.7%	2.3%	24.9%	25.1%
Boolean model*	2.4%	2.7%	2.1%	2.1%

The presented error rates were standardized to the total particle number. *Results after 100 iterations.

radii. These findings are coincident to the ones obtained by Angulo [22] for the number of cell cluster estimation in fluorescence marked cell images, where the number of nuclei obtained by the Boolean model is more robust than a simple ratio of surfaces (equivalent to the naïve estimator). Some approaches had been studied for evaluating berry occlusions within a cluster. Nuske et al. [16] tested the relationship between total berry count, visible berry count, and 3D models from 2D images, but the results showed no improvement on partially occluded berry assessment. As showed in the simulations, the use of the Boolean model would improve the berry number estimation robustness.

3.2. Evaluation of the Berry Number per Cluster Estimation. An example image of a cluster, corresponding to the Cabernet Sauvignon variety, is shown in Figure 6(a). The uncontrolled conditions during the capturing process explains the excess of illumination in the berries that are placed at the right side of the image, which received direct sun illumination, in contrast to the rest of the cluster that had indirect lighting. Due to the image characteristics, segmentation errors occurred affecting the area finally segmented (Figure 6(b)). Results obtained after applying the estimation models (Boolean and naïve) are shown in

(a)

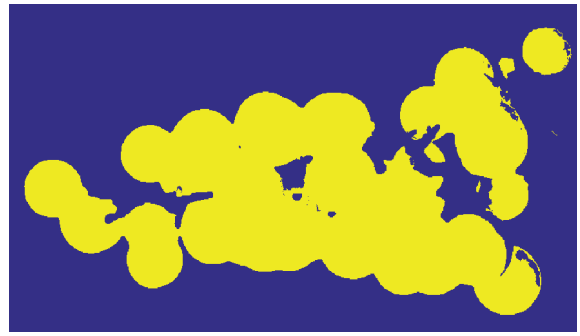

(b)

Figure 6: Segmentation of manually taken cluster images: (a) Example image of a cluster of cv. Cabernet Sauvignon captured under field conditions with an orange cardboard as background; (b) segmented image of the cluster using the Mahalanobis distance on six dimensions (i.e., using RGB and HSV representations).

Table 2: Results obtained for the estimation of the berry number per cluster using the naïve estimator and the Boolean model in manually acquired cluster images of four different grapevine varieties.

Grapevine variety	Manual counting		Naïve estimator			Boolean model		
	Mean berry number	Number of clusters	Mean berry number	RMSE	R^2	Mean berry number	RMSE	R^2
Cabernet Sauvignon	68.4	15	26.7	48.8	0.34^{*}	79.1	14.8	0.86^{***}
Grenache	53.8	12	18.2	37.5	0.72^{***}	44.1	23.3	0.54^{**}
Syrah	79.0	11	32.3	50.7	0.72^{***}	92.5	21.2	0.69^{**}
Tempranillo	141.4	7	43.9	107.6	0.81^{**}	136.6	22.0	0.66^{*}
Total	85.7	45	30.3	60.0	0.71^{***}	88.1	20.1	0.80^{***}

Manual counting refers to the berry number obtained by manually destemming the cluster in the laboratory. The naïve and Boolean estimation was generated based on the analysis of the cluster images manually taken under field conditions. Asterisks represent statistical significance: $^{*}P \leq 0.05$; $^{**}P \leq 0.01$; $^{***}P \leq 0.001$.

Table 2 and in Figure 7. Table 2 describes the results obtained per variety using the two models: the naïve estimator and the Boolean model, including the ground truth generated by manually destemming the clusters. Figure 7 compares the results analysing all the images together ($n = 45$), including the 4 varieties, using the naïve estimator and the Boolean model. The naïve estimator failed to provide a good prediction, with a global RMSE = 60 (Table 2) vs RMSE = 20.1 obtained using the Boolean model. It can be understood by observing Figure 7, as the naïve estimation slope was not close to 1 and its prediction interval of 95% (represented in dotted lines) does not surround the 1 : 1 line, greatly affecting to the estimation precision. This contrasted with the results obtained from the Boolean model, whose slope was 0.93, and the prediction lines are almost in parallel with the 1 : 1 line, demonstrating its prediction capabilities.

Table 2 shows that the results obtained using the naïve estimator were very variable upon the grapevine variety. This was caused by the occlusions (more likely to occur in more compact varieties) and errors in the segmentation. On the other hand, the results obtained with the Boolean model were more homogenous, minimizing differences between varieties and improving the results when all of them were examined together. This homogeneity suggests that this method is more generalizable, although more extensive studies must be conducted to prove this premise.

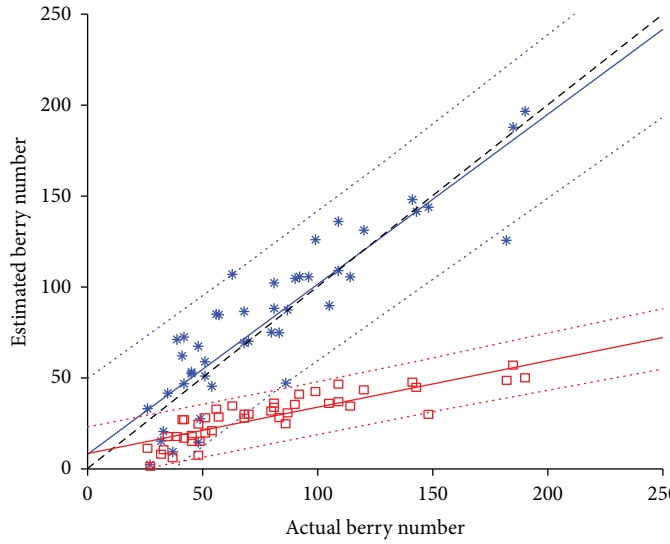

Figure 7: Berry number per cluster estimation using manually captured images ($n = 45$) and a naïve estimator represented in red squares ($y = 0.25x + 8.4$) and a Boolean model represented in blue stars ($y = 0.93x + 8.1$). The dashed line corresponds to 1 : 1, and dotted lines relate to 95% prediction intervals.

Table 3: Comparison of the measured coefficient of determination (R^2) for the estimation of berry number per cluster using image analysis for different varieties in other published studies (under different capturing conditions) and in this work using the Boolean model.

	Tempranillo	Grenache	Syrah	Cabernet Sauvignon	Cabernet Sauvignon and Syrah	Capturing conditions
Diago et al. [11]	0.84	0.69	—	0.62	—	Laboratory
Herrero-Huerta et al. [15]	0.78	—	—	—	—	Field
Liu et al. [12]	—	—	—	—	0.85	Laboratory
The present work	0.66	0.54	0.69	0.86	0.79	Field

The results obtained are comparable to others in the bibliography. The outcomes obtained by Diago et al. [11] are similar (Table 3), but it must be noted that their methodology is not applicable under field conditions. The procedure requires collecting the clusters and taking the images in a chamber with controlled lighting and background. Apart from that, the algorithm is more complex, requiring the segmentation of the image, edge detection, circle detection, and filtering. On the other hand, the presented method only requires the segmentation and mean berry radius for the berry number estimation. Herrero-Huerta et al. [15] developed a system for berry number assessment from images taken in the field. This procedure relies on a 3D structure reconstruction from at least 5 images with high overlapping (80–90%). Their findings (Table 3) are very similar to the ones detailed in this publication but without the need of multiple image acquisitions per cluster. Finally, Liu et al. [12] proposed a similar methodology using 3D models extracted from images captured in a laboratory under controlled conditions. They presented their results combining Cabernet Sauvignon and Syrah clusters; these figures are also included in Table 3. Results are similar to those obtained by the Boolean model but without the constraint of taking the images in the laboratory. It must be noted that the experiments conducted under laboratory conditions are destructive and labour demanding, and thus, it is not easy to expand the sampling rate for an industrial application.

3.3. Evaluation of the Yield Estimation from Manually Captured Vine Images. An example image of a vine of cv. Cabernet Sauvignon can be observed in Figure 8(a). The image segmentation was carried out using the described Mahalanobis classifier (Section 2.4), and the result of the segmentation can be observed in Figure 8(b). Even when the overall classification quality was good, some errors were observed, especially with parts of the trunk being classified as clusters. This greatly affected the performance of the naïve estimator (Table 4), providing a RMSE of 777.2 g when all the varieties were studied together ($n = 45$). On the contrary, the Boolean model offered more robustness against errors in the segmentation and occlusions. Indeed, the RMSE for yield estimation was 310.2 g when all the varieties were studied as a whole, and also, performance for each grapevine variety was higher for the Boolean model than for the naïve estimator. R^2 values showed less difference between the two models. However, looking at Figure 9, it is clear that the naïve model did not offer a correct estimation (the slope is far from 1 and the prediction interval does not surround the 1 : 1 line), even when providing appropriate R^2 values.

(a) (b)

Figure 8: Cluster segmentation on manually captured vine images: (a) image of a vine cv. Cabernet Sauvignon captured under uncontrolled illumination conditions with a digital camera fixed on a tripod and using a white panel as background; (b) segmentation result using the Mahalanobis distance classifier on six dimensions (i.e., using RGB and HSV representations).

Table 4: Results obtained for the yield estimation per vine based on manually captured grapevine images using the naïve estimator and the Boolean model.

Grapevine variety	Manual harvest		Naïve estimator			Boolean model		
	Mean yield (g)	Number of vines	Mean yield (g)	R^2	*RMSE* (g)	Mean yield (g)	R^2	*RMSE* (g)
Cabernet Sauvignon	1311	12	736	0.82^{***}	661.0	1386	0.85^{***}	214.2
Grenache	1750	12	938	0.87^{***}	993.9	1816	0.89^{***}	320.6
Syrah	1231	11	509	0.93^{***}	673.8	966	0.88^{***}	263.7
Touriga Nacional	1249	10	622	0.55^{*}	713.7	1202	0.45^{*}	421.9
Total	1431	45	728	0.82^{***}	777.2	1389	0.81^{***}	310.2

Manual harvest refers to the weight of all the clusters corresponding to each vine. Asterisks represent statistical significance: $^{*}P \leq 0.05$; $^{**}P \leq 0.01$; $^{***}P \leq 0.001$.

Dunn and Martin [14] analysed the prediction potential of the segmentation of Cabernet Sauvignon grapevines. They obtained a $R^2 = 0.85$ for the relation of normalized cluster area on a section of 1 m by 1 m. It should be pointed out that their measured R^2 did not correspond to the validation of a model, but it was calculated on the calibration set. Nevertheless, this value is similar to those obtained for the validation of the models presented in this study without the need of a hanging frame that was used to extract the ROI. Diago et al. [13] used the number of pixels segmented as the cluster class to generate a linear model for yield estimation. The prediction produced $R^2 = 0.73$ and RMSE = 749 g. This approach is similar to the use of the naïve model, and the obtained results are equivalent to the ones produced by this estimator but sensibly surpassed by the performance of the Boolean model ($R^2 = 0.81$ and RMSE = 310 g).

3.4. Evaluation of the Yield Estimation from On-the-Go Captured Vine Images. The images were captured using the modified quad shown in Figure 1(a). The setup allowed for image capture at a speed of 7 km/h, being similar to the operation speed of other agricultural vehicles. The continuous movement of the vehicle, the vibrations induced by the rough terrain, and the explosion motor did not produce motion blur in the images due to camera automatic stabilization and precise camera parametrization (Figure 1(b)). Errors were encountered in the classification process, with cross interference between the cluster and the cable class (representing the metal wire used for trellising the vines to a vertical shoot positioning system). To evaluate the convenience of the multi-MPM-filtering approach (described in Section 2.5), the segmentation was quantified using manually classified images as ground truth. The differences in the results when multiple MPMs were applied are not remarkable in terms of Recall but are notable for the Precision (Table 5). This demonstrated that false positives were correctly eliminated during the filtering, with little loss of true positives. The relative low values of Recall (Table 5) can be explained by the difficulty in pixel discrimination because of the lack of uniformity in the illumination. Figure 4(b) shows the regions manually segmented as clusters. As can be confirmed, these regions were hardly distinguishable even by manual evaluation. An illumination improvement might enhance the segmentation process and thus Recall.

The problems during the segmentation clearly affected the performance of the naïve estimator (Table 6), whose RMSE = 2472 g, when all the varieties were studied together ($n = 28$), resulted in a lack of its practical application, even

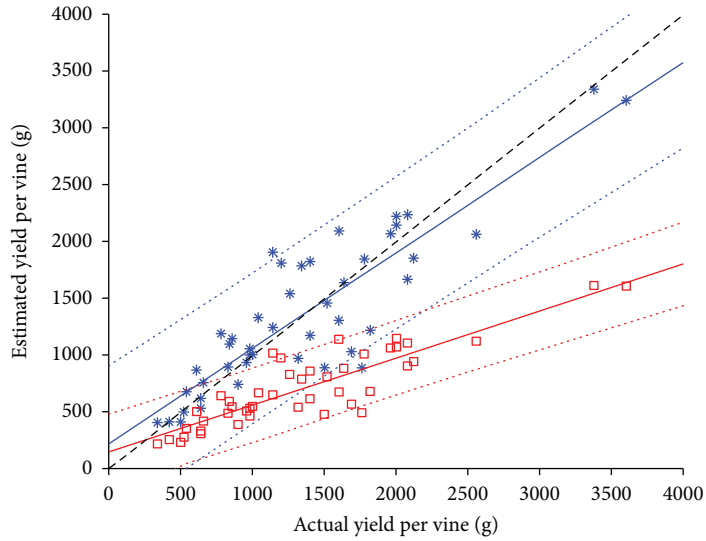

Figure 9: Yield per vine estimation using manually captured images ($n = 45$) and a naïve estimator represented in red squares ($y = 0.42x + 133.0$) and a Boolean model represented in blue stars ($y = 0.86x + 195.2$). The dashed line corresponds to 1 : 1, and dotted lines relate to 95% prediction intervals.

Table 5: Benchmark of the segmentation of clusters in images taken automatically on-the-go with and without applying filtering (cluster proximity, shape-angle, and linear occurrence zone).

Grapevine variety	Without filtering		With filtering	
	Recall	Precision	Recall	Precision
Cabernet Sauvignon	0.54	0.73	0.56	0.82
Syrah	0.64	0.68	0.57	0.80
Tempranillo	0.58	0.69	0.55	0.73
Total	0.58	0.71	0.56	0.79

The performance of the segmentation was tested against manually segmented images.

when the coefficient of determination was acceptable ($R^2 = 0.71$). This represents the same scenario as in the cluster and manually taken images: the naïve estimator did not compensate for the occlusions and errors in the segmentation, and the prediction interval does not surround the 1 : 1 line in all the intervals (Figure 10). On the other hand, the Boolean model was capable of correctly estimating the yield, offering RMSE = 610.1 g. It must be noted that the estimation refers to segments composed by three vines, so this value represents an improvement if it is compared to the manually captured images that yielded a RMSE = 374.2 g for one isolated vine.

Similar to this work, Font et al. [17] used a quad equipped with cameras and artificial illumination to capture 25 cluster images (not the entire grapevine) at night time. Then, they estimated cluster weight from its segmented area. The prediction had 16% of error when all the varieties were analysed together. In comparison, the results obtained for the Boolean model had 15.6% of error using images framing three vines instead of cluster images (the mean cluster number per section was 47). In another recent article, Nuske et al. [16] also used a quad with artificial lighting for image capturing of grapevines. The collected images were analysed to identify visible berries to estimate yield. This setup allowed assessing yield with a $R^2 = 0.73$ for the best datasheet, being comparable to the results given by the naïve estimator ($R^2 = 0.71$), which also bases its estimation on the visible berries. They also tried to boost the yield estimation thru an evaluation of the self-occlusion of berries using 3D models of berries (ellipsoid 3D model) and clusters (convex hull 3D model). The results showed that the proposed correction models did not improve the overall estimation. In contrast to this, the Boolean estimator, which also compensates for partially occluded berries, generated better results ($R^2 = 0.78$).

4. Conclusions

This work presented a new method for accurate, nondestructive, and in-field grapevine yield estimation by using computer vision. Yield information is very valuable for viticulturists and grape growers, allowing them to take decisions prior to harvest based on objective measurements. A novel use of Boolean models has been assessed over three different data sets: images of isolated clusters, manually captured images of grapevines, and on-the-go captured images of grapevines using a modified quad at night time.

The use of Boolean models allowed to overcome two of the major difficulties in visual yield estimation: this technique is robust against segmentation errors and partial occlusions, situations that are usual in the case of images taken under field conditions. It provided more precision, using not only a model that is simpler than other previous proposals but also less complex image analysis techniques. The capacity to estimate the visible berry number and the

Table 6: Results obtained for the estimation of the yield per segment (composed of three vines) based on images captured with an "on-the-go" platform.

Grapevine variety	Manual harvest		Naïve estimator			Boolean model		
	Mean yield (g)	Number of segments	Mean yield (g)	R^2	RMSE (g)	Mean yield (g)	R^2	RMSE (g)
Cabernet Sauvignon	3406	8	1321	0.64^{*}	1863.7	3235	0.50^{*}	574.5
Syrah	3322	10	1598	0.87^{***}	2031.9	3115	0.86^{***}	390.6
Tempranillo	5031	10	2175	0.59^{**}	3194.1	4660	0.60^{**}	790.8
Total	3920	28	1698	0.71^{***}	2472.0	3670	0.78^{***}	610.1

These measurements were obtained when using a naïve estimator and the Boolean model on images segmented using a Mahalanobis distance classifier and a three-step filtering process. Asterisks represent statistical significance: $^{*}P \leq 0.05$; $^{**}P \leq 0.01$; $^{***}P \leq 0.001$.

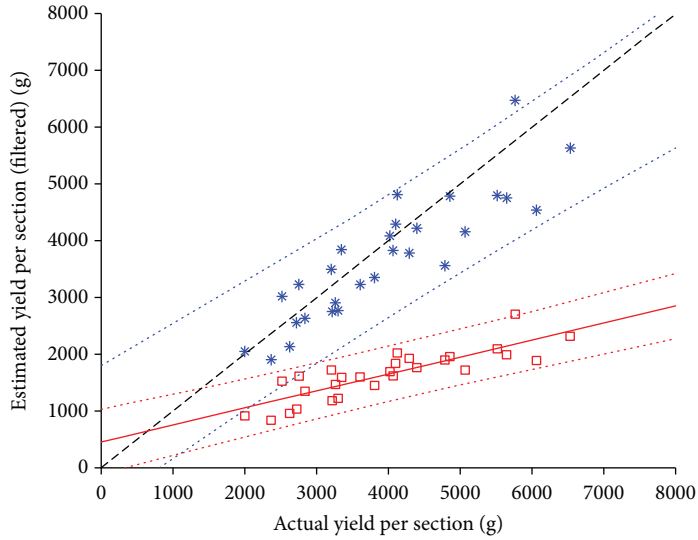

Figure 10: Yield per section (composed by 3 vines) using images (64 images combined to generate 28 segments) captured on-the-go and a naïve estimator represented in red squares ($y = 0.30x + 460.6$) and a Boolean model represented in blue stars ($y = 0.80x + 552.7$). A multistep filtering process was applied to improve the cluster segmentation (described in Section 2.5). The dashed line corresponds to 1 : 1, and dotted lines relate to 95% prediction intervals.

partially hidden ones was confirmed by the comparison between the results obtained with the Boolean model and the naïve estimator.

The simplicity and precision of the Boolean model formulation makes it ideal for its application on grapevine yield estimation, allowing its implementation in a fully automated system. The images were captured around 7 km/h, comparable to other agricultural equipment used in vineyard management, establishing this procedure close to industrial application. This methodology can also be used to generate maps that represent the spatial variability of the vineyards, allowing for grapevine zoning, segmented harvest, and thus an increase in quality.

Data Availability

The images and on-the-field recorded data used to support the findings of this study have not been made available because our institution is currently defining a protocol for data sharing.

Conflicts of Interest

The authors declare that there is no conflict of interest regarding the publication of this paper.

Acknowledgments

We would like to thank Vitis Navarra for their help with the field measurements. We also thank Dr. Jesús Angulo for his comments and suggestions. Borja Millan would like to thank the Center of Mathematical Morphology for the support, guidance, and laboratory facilities during his 6-month research stay conducting to this publication. Borja Millán was funded by the FPI grant [536/2014] by the University of La Rioja.

References

[1] M. P. Diago, M. Krasnow, M. Bubola, B. Millan, and J. Tardaguila, "Assessment of vineyard canopy porosity using machine vision," *American Journal of Enology and Viticulture*, vol. 67, no. 2, pp. 229–238, 2016.

[2] M. Gatti, P. Dosso, M. Maurino et al., "MECS-VINE®: a new proximal sensor for segmented mapping of vigor and yield parameters on vineyard rows," *Sensors*, vol. 16, no. 12, p. 2009, 2016.

[3] A. Kicherer, M. Klodt, S. Sharifzadeh, D. Cremers, R. Töpfer, and K. Herzog, "Automatic image-based determination of pruning mass as a determinant for yield potential in grapevine management and breeding," *Australian Journal of Grape and Wine Research*, vol. 23, no. 1, pp. 120–124, 2017.

[4] A. Kicherer, K. Herzog, M. Pflanz et al., "An automated field phenotyping pipeline for application in grapevine research," *Sensors*, vol. 15, no. 3, pp. 4823–4836, 2015.

[5] J. A. Wolpert and E. P. Vilas, "Estimating vineyard yields: introduction to a simple, two-step method," *American Journal of Enology and Viticulture*, vol. 43, no. 4, pp. 384–388, 1992.

[6] S. R. Martin, G. M. Dunn, T. Hoogenraad, M. P. Krstic, P. R. Clingeleffer, and W. J. Ashcroft, "Crop forecasting in cool climate vineyards," in *Proceedings for the 5th International Symposium on Cool Climate Viticulture and Enology*, Melbourne, Australia, 2002.

[7] G. Dunn, *Yield Forecasting*, Grape and Wine Research and Development Corporation, 2010.

[8] G. M. Dunn and S. R. Martin, "The current status of crop forecasting in the Australian wine industry," in *Proceedings of the ASVO Seminar Series: Grapegrowing at the Edge*, pp. 4–8, Tanunda, Barossa Valley, South Australia, 2003.

[9] B. Millan, A. Aquino, M. P. Diago, and J. Tardaguila, "Image analysis-based modelling for flower number estimation in grapevine," *Journal of the Science of Food and Agriculture*, vol. 97, no. 3, pp. 784–792, 2017.

[10] S. Nuske, S. Achar, T. Bates, S. Narasimhan, and S. Singh, "Yield estimation in vineyards by visual grape detection," in *2011 IEEE/RSJ International Conference on Intelligent Robots and Systems*, pp. 2352–2358, San Francisco, CA, USA, September 2011.

[11] M. P. Diago, J. Tardaguila, N. Aleixos et al., "Assessment of cluster yield components by image analysis," *Journal of the Science of Food and Agriculture*, vol. 95, no. 6, pp. 1274–1282, 2015.

[12] S. Liu, M. Whitty, and S. Cossell, "A lightweight method for grape berry counting based on automated 3D bunch reconstruction from a single image," in *ICRA, International Conference on Robotics and Automation (IEEE), Workshop on Robotics in Agriculture*, p. 4, Seattle, WA, USA, 2015.

[13] M. P. Diago, C. Correa, B. Millán, P. Barreiro, C. Valero, and J. Tardaguila, "Grapevine yield and leaf area estimation using supervised classification methodology on RGB images taken under field conditions," *Sensors*, vol. 12, no. 12, pp. 16988–17006, 2012.

[14] G. M. Dunn and S. R. Martin, "Yield prediction from digital image analysis: a technique with potential for vineyard assessments prior to harvest," *Australian Journal of Grape and Wine Research*, vol. 10, no. 3, pp. 196–198, 2004.

[15] M. Herrero-Huerta, D. González-Aguilera, P. Rodriguez-Gonzalvez, and D. Hernández-López, "Vineyard yield estimation by automatic 3D bunch modelling in field conditions," *Computers and Electronics in Agriculture*, vol. 110, pp. 17–26, 2015.

[16] S. Nuske, K. Wilshusen, S. Achar, L. Yoder, S. Narasimhan, and S. Singh, "Automated visual yield estimation in vineyards," *Journal of Field Robotics*, vol. 31, no. 5, pp. 837–860, 2014.

[17] D. Font, M. Tresanchez, D. Martínez, J. Moreno, E. Clotet, and J. Palacín, "Vineyard yield estimation based on the analysis of high resolution images obtained with artificial illumination at night," *Sensors*, vol. 15, no. 4, pp. 8284–8301, 2015.

[18] G. Matheron, *Random Sets and Integral Geometry*, Wiley, New York, NY, USA, 1975.

[19] J. Serra, "The Boolean model and random sets," *Computer Graphics and Image Processing*, vol. 12, no. 2, pp. 99–126, 1980.

[20] D. Jeulin, "Random texture models for material structures," *Statistics and Computing*, vol. 10, no. 2, pp. 121–132, 2000.

[21] S. Jeanson, J. Chadœuf, M. N. Madec et al., "Spatial distribution of bacterial colonies in a model cheese," *Applied and Environmental Microbiology*, vol. 77, no. 4, pp. 1493–1500, 2011.

[22] J. Angulo, "Nucleus modelling and segmentation in cell clusters," in *Progress in Industrial Mathematics at ECMI 2008. Mathematics in Industry, Vol 15*, A. Fitt, J. Norbury, H. Ockendon, and E. Wilson, Eds., pp. 217–222, Springer, Berlin, Heidelberg, 1st edition, 2010.

[23] J. P. Serra, *Image Analysis and Mathematical Morphology*, Academic Press, Orlando, FL, USA, 1982.

[24] P. Soille, *Morphological Image Analysis: Principles and Applications*, Springer-Verlag, Berlin, Heidelberg, 2nd edition, 2004.

[25] G. J. McLachlan, "Mahalanobis distance," *Resonance*, vol. 4, no. 6, pp. 20–26, 1999.

[26] H. M. Al-Otum, "Morphological operators for color image processing based on Mahalanobis distance measure," *Optical Engineering*, vol. 42, no. 9, p. 2595, 2003.

[27] J. Angulo and S. Velasco-forero, "Semi-supervised hyperspectral image segmentation using regionalized stochastic watershed," in *Proceedings Volume 7695, Algorithms and Technologies for Multispectral, Hyperspectral, and Ultraspectral Imagery XVI; 76951F*, Orlando, FL, USA, May 2010.

[28] D. A. McQuarrie, *Statistical Mechanics*, University Science Books, 1976.

Hindawi
Journal of Sensors
Volume 2018, Article ID 6025381, 11 pages
https://doi.org/10.1155/2018/6025381

Research Article

The Development of an Intelligent Monitoring System for Agricultural Inputs Basing on DBN-SOFTMAX

Ling Yang,[1] V. Sarath Babu,[2] Juan Zou,[1] Xu Can Cai,[1] Ting Wu,[1] and Li Lin[2]

[1]*School of Information Science and Technology, Zhongkai University of Agriculture and Engineering, Guangzhou 510225, China*
[2]*Guangdong Provincial Water Environment and Aquatic Products Security Engineering Technology Research Center, Guangzhou Key Laboratory of Aquatic Animal Diseases and Waterfowl Breeding, Guangdong Provincial Key Laboratory of Waterfowl Healthy Breeding, College of Animal Sciences and Technology, Zhongkai University of Agriculture and Engineering, Guangzhou, Guangdong 510225, China*

Correspondence should be addressed to Ting Wu; 405684932@qq.com and Li Lin; linli@zhku.edu.cn

Received 7 May 2018; Revised 13 August 2018; Accepted 30 August 2018; Published 28 October 2018

Academic Editor: Marco Grossi

To solve the problem of unreliability of traceability information in the traceability system, we developed an intelligent monitoring system to realize the real-time online acquisition of physicochemical parameters of the agricultural inputs and to predict the varieties of input products accurately. Firstly, self-developed monitoring equipment was used to realize real-time acquisition, format conversion and pretreatment of the physicochemical parameters of inputs, and real-time communication with the cloud platform server. In this process, LoRa technology was adopted to solve the wireless communication problems between long-distance, low-power, and multinode environments. Secondly, a deep belief network (DBN) model was used to learn unsupervised physicochemical parameters of input products and extract the input features. Finally, these input features were utilized on the softmax classifier to establish the classification model, which could accurately predict the varieties of agricultural inputs. The results showed that when six kinds of pesticides, chemical fertilizers, and other agricultural inputs were predicted through the system, the prediction accuracy could reach 98.5%. Therefore, the system can be used to monitor the varieties of agrarian inputs effectively and use in real-time to ensure the authenticity and accuracy of the traceability information.

1. Introduction

The traceability system of agricultural products is a powerful tool for solving the food safety issues [1]. The information on the farm inputs, such as pesticides and fertilizers used for cultivation, is one of the most concerned problems of the consumers. Currently, some companies have established their own traceability system of agricultural products [2]. However, it is reasonable that the consumers do not trust the appreciable information recorded by the producers themselves because of the lack of supervision. Therefore, the establishment of a traceability system, which can record the information timely, accurately, and ultimately is an urgent need.

There have been many reports about the rapid techniques for detection of agricultural inputs. To name a few, Deng et al. established a liquid chromatography-tandem mass spectrometry (LC-MS) method for the simultaneous determination of benzoylurea pesticide residues in vegetables [3]. Zheng et al. found LC-MS method for the detection of pesticide residues in milk [4]. Selisker et al. used a competitive enzyme-linked immunosorbent assay (ELISA) to detect paraquat [5]. Alcocer et al. have developed a polyclonal antibody for detection of organophosphorus pesticides [6]. Kumaran and Tran-Minh used cholinesterase electrode to detect pesticides [7]. Chough et al. used a carbon electrode to identify the organophosphorus insecticide [8]. Seemingly, many of the rapid detection techniques for agricultural inputs have been established. However, most of the current monitoring of agricultural input information is still a kind of residue detection of the postproduction stage, and it is still difficult to monitor the data via real-time online. Furthermore, the current established traceability system records the

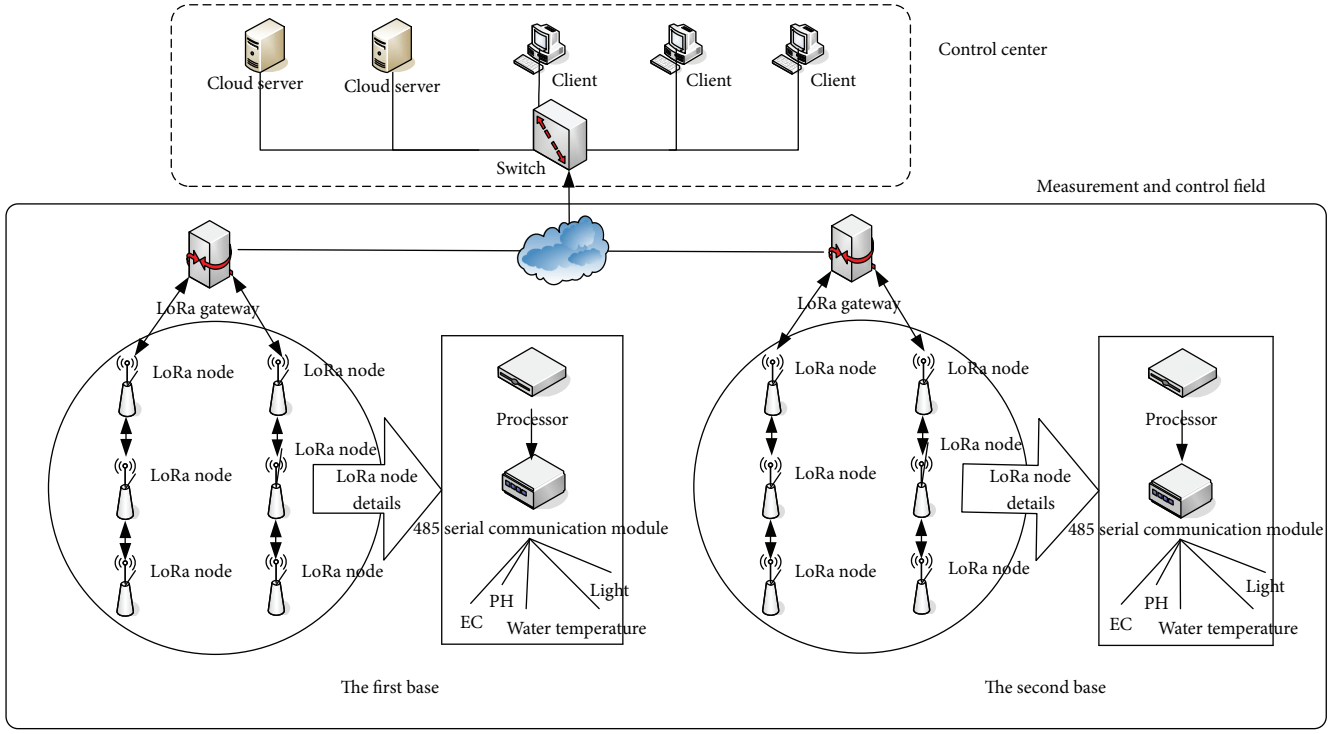

Figure 1: The overall system architecture.

traceability information, which is mainly entered manually; therefore, the information is not timely and accurate.

It is desirable to seek an alternative method to overcome these drawbacks. In this report, based on sensors and DBN-SOFTMAX algorithm, we developed an intelligent monitoring system for the agricultural inputs. Different from chemical-based agrarian inputs detection methods described above. This paper proposed using the sensors arranged in the soil to realize the monitoring and prediction of farming inputs. In general, sensors were employed in agriculture to achieve environmental monitoring such as moisture and temperature [9, 10] or to attain precise agricultural control [11]. In this paper, the sensors placed in the soil were used to collect the physicochemical characteristics of the inputs such as pH and EC value, and then the artificial intelligence algorithm was used to analyze the above sensor data and finally realized the intelligent monitoring and prediction of agricultural inputs.

2. Monitoring System Design

2.1. Working Principles and Overall Architecture. The overall structure of the intelligence-monitoring platform for agricultural inputs is shown in Figure 1.

The monitoring equipment collects data every 15 seconds to obtain the physicochemical parameters of agricultural inputs, such as pH value, electronic conductivity (EC), and temperature, in real time. After data preprocessing, analog-to-digital conversion, and RS485 [12] format conversion, LoRa (long range) module transmits the data to the LoRa gateway [13] and converts them into the RJ45 format. Subsequently, the data will be received and stored in the cloud server, and data cleaning and reduction process are performed to obtain useful data for further modeling and classification. During the modeling process, the input data is continuously increased to the training samples, and the model is updated once a week to obtain more accurate prediction results.

2.2. Hardware Design. The monitoring system mainly consists of sensor module, low-power digital processor, multichannel AD/DA conversion module, RS485 serial communication module, LoRa wireless communication module, and solar power module. The sensor module includes a pH sensor, an EC sensor, and a temperature sensor. The RS485 serial port communication module provides multisensor data fusion service. It uses polling mode to collect different sensor data of the same monitoring point through the RS485 interface to complete multisensor data fusion. LoRa wireless communication module developed by LoRa spread spectrum chip SX1278; its transmission distance and penetration ability are more than one time higher than those of traditional FSK [14]. In LoRa wireless communication, the capability of error correction is stronger since the algorithm of cyclic interleaving error correction coding is expected to be adopted. The maximum continuous error correction is 64 bits, which can reduce the retransmission of a large number of erroneous data packets, to improve the anti-interference performance and transmission distance. The hardware structure of the monitoring system is shown in Figure 2.

2.3. Software Design

2.3.1. The LoRa Node Software Design. There are three kinds of nodes in LoRA, namely, sensor, routing, and aggregation

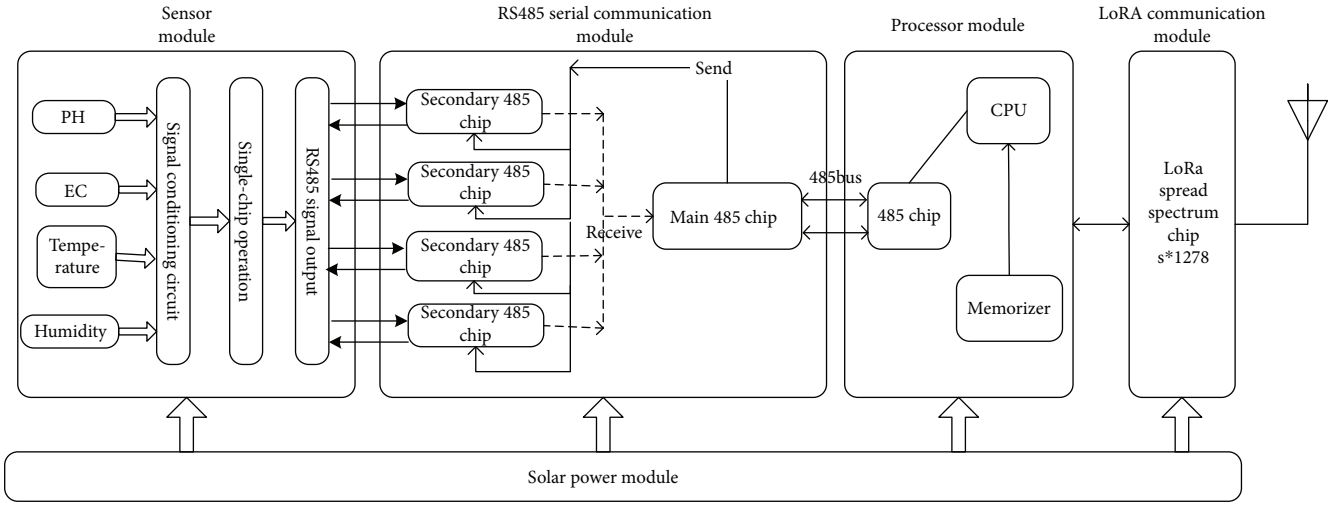

Figure 2: The hardware structure of monitor terminal.

nodes. The routing node is responsible for forwarding data. The aggregation node does not collect data, but as a control center, it sends synchronization information to the monitoring network and the received data to the local monitoring and remote monitoring centers. The corresponding node software is designed to perform the functions of each node. In this paper, the sensor node was used as an example to introduce the software design method. The C language was used to develop software, and the flow chart of the program is shown in Figure 3:

The entire programming process uses the modular design, mainly including equipment initialization, data acquisition and processing, serial communication, and wireless communication. PC monitoring controls acquisition cycle and acquisition command and controlling center software. If the node software receives the acquisition command sent by the PC monitoring center program, it immediately responds and transmits the collected data to the corresponding sensor according to different Modbus protocol commands.

2.3.2. The Monitoring Center Software Design. The software workflow diagram is shown in Figure 4. The monitoring center software uses C# to develop and communicate with the LoRa gateway module through TCP/IP network programming and obtains monitoring data transmitted by the LoRa gateway to the Internet network. The monitoring software mainly includes parameters setting, real-time monitoring, data processing, and other functions. Parameter setting function is to set the acquisition cycle, acquisition Modbus command, and other parameter settings. The real-time monitoring function is to collect sensor data in real time. A data processing function included calling DBN-SOFTMAX prediction model code, analyzing the received data, matching the established model, and predicting the varieties of inputs.

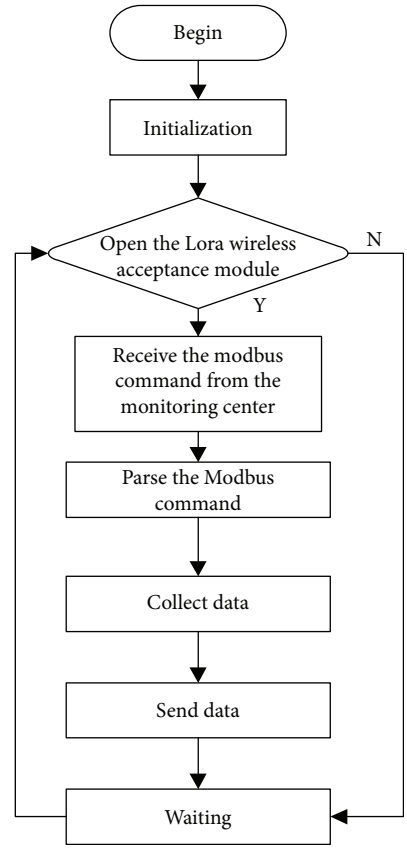

Figure 3: The node program flow.

3. DBN-SOFTMAX Algorithm and Modeling

3.1. The DBN-Based Feature Extraction Method. Restricted Boltzmann Machine (RBM) [15], which was part of DBN [16, 17], could extract features that are more abstract and significantly improve the ability of neural network generalization [18]. Each RBM was a two-layer model that contained only one hidden layer, and each RBM training output was used as the input for the next RBM.

3.1.1. Restricted Boltzmann Machine (RBM). If $\theta = \{W_{ij}, a_i, b_j\}$, where W_{ij} represented the connection weight between the visible unit i and the hidden element j. m, n was the

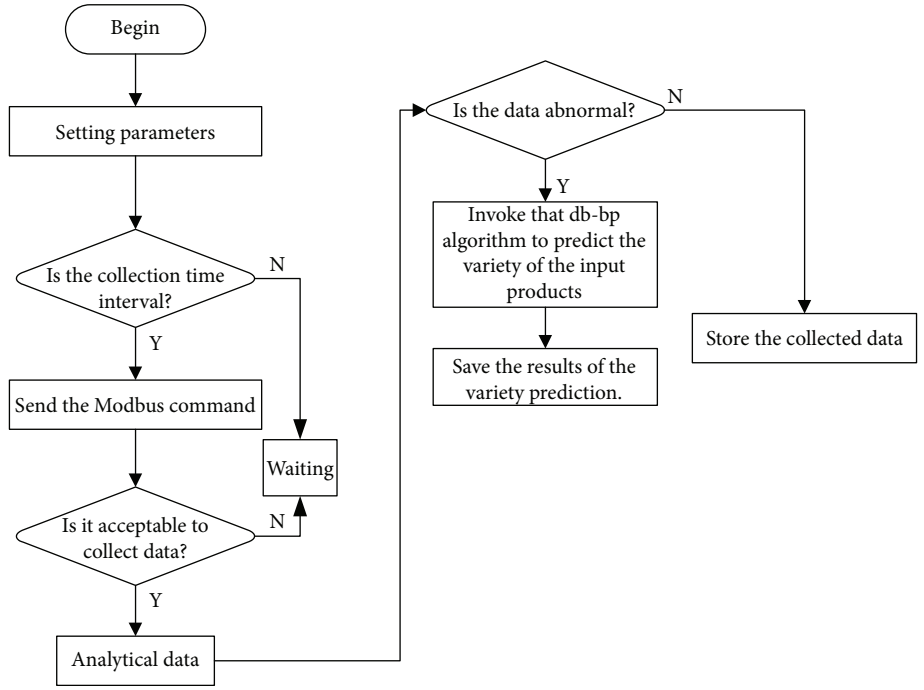

Figure 4: The software workflow.

number of hidden cells and visible cells, respectively. Both the visible and hidden units were binary variables. That is, $\forall i, j, v_i \in \{0,1\}, h_j \in \{0,1\}$, a_i was the offset of the visible element i, b_j was the offset of the visible element j, T was the number of samples, h was a hidden layer unit, and v was a visible layer unit.

RBM was an undirected graph model [19, 20] which was used to solve the value of the parameter θ, to fit the given training data, and the extracted feature (Figure 5).

RBM task was used to fit the input training data, figured out the optimal parameter θ, and completed the feature extraction. The parameter θ could be learned in the training set to maximize the logarithmic likelihood function. The formula was as follows:

$$\theta^* = \arg\max \mathscr{L}(\theta) = \arg\max \sum_{t=1}^{T} \log P\left(V^{(t)} \mid \theta\right), \quad (1)$$

where

$$\begin{aligned}\mathscr{L}(\theta) &= \sum_{t=1}^{T} \log P\left(V^{(t)} \mid \theta\right) = \sum_{t=1}^{T} \log \sum_{h} P\left(V^{(t)}, h \mid \theta\right) \\ &= \sum_{t=1}^{T} \left(\log \sum_{h} \exp\left[-E\left(V^{(t)}, h \mid \theta\right)\right] \right. \\ &\quad \left. - \log \sum_{v} \sum_{h} \exp[-E(v, h \mid \theta)] \right).\end{aligned} \quad (2)$$

The key to solving the optimal parameter θ^* was to obtain the partial derivative of $\log P(V^{(t)} \mid \theta)$ for W_{ij}, a_i, b_j, and other parameters. Assuming that θ' was a parameter value of θ, the logarithmic likelihood function concerning θ' was

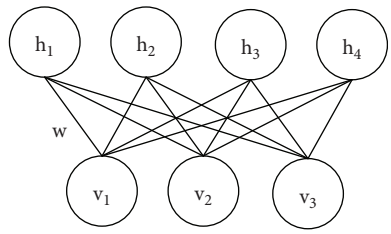

Figure 5: The RBM model.

$$\begin{aligned}\frac{\partial \mathscr{L}}{\partial \theta'} &= \sum_{t=1}^{T} \frac{\partial}{\partial \theta'} \left(\log \sum_{h} \exp\left[-E\left(V^{(t)}, h \mid \theta\right)\right] \right. \\ &\quad \left. - \log \sum_{v} \sum_{h} \exp[-E(v, h \mid \theta)] \right) \\ &= \sum_{t=1}^{T} \left(\sum_{h} \frac{\exp\left[-E\left(V^{(t)}, h \mid \theta\right)\right]}{\sum_h \exp\left[-E\left(V^{(t)}, h \mid \theta\right)\right]} \times \frac{\partial\left(-E\left(V^{(t)}, h \mid \theta\right)\right)}{\partial \theta} \right. \\ &\quad \left. - \sum_{v} \sum_{h} \frac{\exp\left[-E(v, h \mid \theta)\right]}{\sum_v \sum_h \exp[-E(v, h \mid \theta)]} \times \frac{\partial(-E(v, h \mid \theta))}{\partial \theta} \right) \\ &= \sum_{t=1}^{T} \left(\left\langle \frac{\partial\left(-E\left(V^{(t)}, h \mid \theta\right)\right)}{\partial \theta} \right\rangle_{P\left(h \mid V^{(t)}, \theta\right)} \right. \\ &\quad \left. - \left\langle \frac{\partial(-E(v, h \mid \theta))}{\partial \theta} \right\rangle_{P(v, h \mid \theta)} \right).\end{aligned} \quad (3)$$

Since the number of samples T was known, the partial derivative of the logarithmic likelihood function for the connection weight W_{ij}, the offset a_i of the visible layer element, and the offset b_j of the hidden layer unit could be expressed by $P(h \mid V^{(t)}, \theta)$ and $P(v, h \mid \theta)$. $P(h \mid V^{(t)}, \theta)$ was a hidden probability distribution of training sample $V^{(t)}$; $P(v, h \mid \theta)$ was a joint probability function for a given state (v, h); the function was

$$P(v, h \mid \theta) = \frac{e^{-E(v,h|\theta)}}{Z(\theta)}, \tag{4}$$

where $E(v, h \mid \theta)$ was the energy function of RBM and $Z(\theta)$ was the normalization factor.

$$\begin{aligned} E(v, h \mid \theta) &= -\sum_{i=1}^{n} a_i v_i - \sum_{j=1}^{m} b_j h_j - \sum_{i=1}^{n}\sum_{j=1}^{m} v_i W_{ij} h_j, \\ Z(\theta) &= \sum_{v,h} e^{-\mathrm{E}(v,h|\theta)}. \end{aligned} \tag{5}$$

3.1.2. CD Algorithm. It has been shown that the normalization factor $Z(\theta)$ was difficult to be solved [21]. Therefore, the joint probability function $P(v, h \mid \theta)$ was also difficult to calculate. To solve this problem, the fast learning algorithm based on contrast divergence was used to training data, and the steps were as follows:

(1) $P(v, h \mid \theta)$ was given by the formula $P(v, h \mid \theta) = e^{-E(v,h|\theta)}/Z(\theta)$, $P(v \mid \theta) = 1/Z(\theta)\sum_h e^{-E(v,h|\theta)}$

(2) The RBM network structure was connected between layers, no connection within the layer and the structure of symmetry, i.e., when the state of the visible cell was fixed, an activating probability of the jth hidden element was

$$P\left(h_j = 1 \mid v, \theta\right) = \sigma\left(b_j + \sum_i v_i W_{ij}\right). \tag{6}$$

When the state of the hidden cell was fixed, activating probability of the ith hidden element was

$$P(v_i = 1 \mid h, \theta) = \sigma\left(a_i + \sum_j h_j W_{ij}\right). \tag{7}$$

The binary state of all hidden layer units was calculated from equation (6). After the state of all hidden layer units was determined, the ith visible unit v_i value of 1 probability according to equation (7) was determined, and a reconstruction of the visible layer was created

(3) The parameter updated formula in the data training process was as follows:

$$\begin{aligned} \Delta W_{ij} &= \epsilon\left(\left\langle v_i h_j \right\rangle_{\text{data}} - \left\langle v_i h_j \right\rangle_{\text{recon}}\right), \\ \Delta a_i &= \epsilon\left(\left\langle v_i \right\rangle_{\text{data}} - \left\langle v_i \right\rangle_{\text{recon}}\right), \\ \Delta b_j &= \epsilon\left(\left\langle h_j \right\rangle_{\text{data}} - \left\langle h_j \right\rangle_{\text{recon}}\right), \end{aligned} \tag{8}$$

where ε was the learning rate, and $\langle \bullet \rangle_{\text{recon}}$ was the distribution that represented the reconstructed model definition.

3.2. The Softmax Classifier. In the above process, what is finally obtained was the feature values of $x^{(i)}$. However, in the prediction of input varieties, it was necessary to categorize output and to add a softmax classifier [22] to the output layer to organize the learned feature values. The diagrammatic drawing of the softmax classifiers was presented in Figure 6. The marked training set $\{(x^{(1)}, y^{(1)}), (x^{(2)}, y^{(2)}), \ldots, (x^{(m)}, y^{(m)})\}$, among $y^{(j)} \in \{1, 2, \ldots, k\}$ representative training sample $x^{(i)}$ is k. The given test input $x^{(i)}$, which is the classification model calculates the probability that it belongs to each category.

Thus, to a sample set with k types, output k-dimensional vector to represent the probability vector. The jth element in the probability vector represents the probability of belonging to the jth category, and the sum of values of elements is 1. Specifically, our hypothesis function $h_\theta(x)$ is shown as

$$\begin{aligned} h_\theta\left(x^{(i)}\right) &\begin{bmatrix} p\left(y^{(i)} = 1 \mid x^{(i)}; \theta\right) \\ p\left(y^{(i)} = 2 \mid x^{(i)}; \theta\right) \\ \vdots \\ p\left(y^{(i)} = k \mid x^{(i)}; \theta\right) \end{bmatrix} \\ &= \frac{1}{\sum_{j=1}^{k} e^{\theta_j^T x^{(i)}}} \begin{bmatrix} e^{\theta_1^T x^{(i)}} \\ e^{\theta_2^T x^{(i)}} \\ \vdots \\ e^{\theta_k^T x^{(i)}} \end{bmatrix} = \begin{bmatrix} p_1 \\ p_2 \\ \vdots \\ p_k \end{bmatrix}. \end{aligned} \tag{9}$$

Among $\theta_1, \theta_2, \theta_3, \ldots, \theta_k$ are network model parameters, as

$$\theta = \begin{bmatrix} -\theta_1^T - \\ -\theta_2^T - \\ \vdots \\ -\theta_k^T - \end{bmatrix}, \frac{1}{\sum_{j=1}^{k} e^{\theta_j^T x^{(i)}}}, \tag{10}$$

this item mainly restricts the probability values from 0 to 1, which the sum of the probability values is 1.

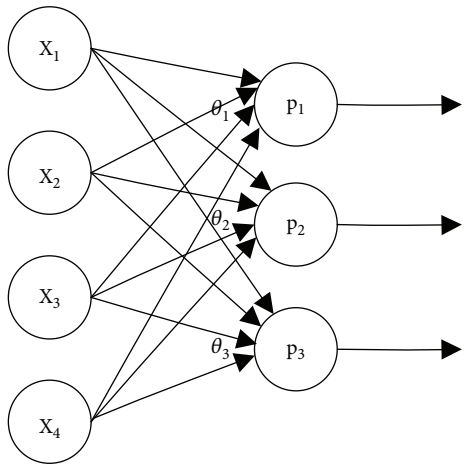

Figure 6: The softmax classifier.

In equation (9), the probability of the sample $x^{(i)}$ output by the classifier belonging to class j is ($1\{\text{true}\} = 1, 1\{\text{false}\} = 0$):

$$p\left(y^{(i)} = j \mid x^{(i)}; \theta\right) = \frac{e^{\theta_j^T x^{(i)}}}{\sum_{j=1}^{k} e^{\theta_j^T x^{(i)}}} = p_1 = \prod_{j=1}^{k} p_j^{1\{y^{(i)}=j\}}. \quad (11)$$

The likelihood function corresponding to training samples is

$$L(\theta) = \prod_{i=1}^{m} p\left(y^{(i)} = j \mid x^{(i)}; \theta\right) = \prod_{i=1}^{m} \prod_{j=1}^{k} p_j^{1\{y^{(i)}=j\}},$$

$$l(\theta) = \log L(\theta) = \sum_{i=1}^{m} \sum_{j=1}^{k} 1\left\{y^{(i)} = j\right\} \log\left(p_j\right)$$

$$= \sum_{i=1}^{m} \sum_{j=1}^{k} 1\left\{y^{(i)} = j\right\} \log\left(\frac{e^{\theta_j^T x^{(i)}}}{\sum_{l=1}^{k} e^{\theta_l^T x^{(i)}}}\right). \quad (12)$$

The parameter θ that maximizes the likelihood function as the optimal parameter of the softmax classifier. The cost function of the softmax regression model is

$$J(\theta) = -\frac{1}{m}\left[\sum_{i=1}^{m} \sum_{j=1}^{k} 1\left\{y^{(i)} = j\right\} \log\left(\frac{e^{\theta_j^T x^{(i)}}}{\sum_{l=1}^{k} e^{\theta_l^T x^{(i)}}}\right)\right]. \quad (13)$$

The cost function is minimized by the gradient descent method; the gradient function is as follows:

$$\nabla_{\theta_j} J(\theta) = -\frac{1}{m}\left[\sum_{i=1}^{m} x^{(i)}\left(1\left\{y^{(i)} = j\right\} - p\left(y^{(i)} = j \mid x^{(i)}; \theta\right)\right)\right]. \quad (14)$$

The softmax classifier has an unusual feature: it has a "redundant" set of parameters [23]. To illustrate the feature, if the vector μ was subtracted from the parameter vector θ_j, each θ_j becomes $\theta_j - \mu (j = 1, 2, \ldots, k)$. The function is shown as

$$p\left(y^{(i)} = j \mid x^{(i)}; \theta\right) = \frac{e^{\left(\theta_j - u\right)^T x^{(i)}}}{\sum_{l=1}^{k} e^{(\theta_l - u)^T x^{(i)}}} = \frac{e^{\theta_j^T x^{(i)}} e^{-\mu^T x^{(i)}}}{\sum_{l=1}^{k} e^{(\theta_l - u)^T x^{(i)}} e^{-\mu^T x^{(i)}}}$$

$$= \frac{e^{\theta_j^T x^{(i)}}}{\sum_{l=1}^{k} e^{\theta_l^T x^{(i)}}}. \quad (15)$$

In equation (15), we can see that the parameters $\theta_j - \mu$ and θ_j can both gain the same result. In other words, when θ_j is the optimal parameter, $\theta_j - \mu$ can also have the same effect. It is the disadvantage of having redundant parameters in the softmax classifier. The loss function of the softmax classifier is distinctly nonconvex. Although there is a minimum point, the minimum value is in "flat" space and not at a single point. That is, all points in the area can get a minimum value. To make the cost function a strictly convex function, we need to add a weight attenuation term, as follows:

$$J(\theta) = J(\theta) + \frac{\lambda}{2} \sum_{i=1}^{m} \sum_{j=1}^{k} \theta_{ij}^2,$$

$$\nabla_{\theta_j} J(\theta) = \nabla_{\theta_j} J(\theta) + \lambda \theta_j. \quad (16)$$

3.3. Modeling. In establishing the model, the collected data were first normalized, and then DBN was used for unsupervised training to extract features. However, these features were not directly applicable to classification [24–26], so the softmax classifier was added to the output to perform supervised classification training. The flow diagram is shown in Figure 7.

4. Experiment Design

In this experiment, we used six agricultural inputs, including phosphate (P_2O_5, SinoChem, China), potassium (K_2O, SinoChem, China), compound fertilizer (carbamide, nitrogen phosphorus potassium, SouthRanch, China), Podol pesticide (TaoChun, China), imidacloprid (Bayer, Germany), and oxamoxime (HeYi, China), purchased from local stores in Guangzhou, China. The first three of these inputs were chemical fertilizers, the latter three were pesticides, and their aqueous solutions were placed in dilution ratios (500 : 1) for use. Eighteen pots of soil-filled bottom drainable basins were prepared and set in an open-air environment. The EC sensors, pH sensors, and moisture sensors were inserted into the soil, and the power was turned on to enable to collect the sensor data in real time. During the period from October 2016 to March 2017, 200 ml of each inputs aqueous solution was sprayed into three pots of soil. Over 50 experiments, the soil parameter data before and after the input, including moisture proportion (before input), conductivity (before input), the pH value (before input), moisture ratio (after input), conductivity (after input), and the pH value (after input) were recorded. 150 data were collected for

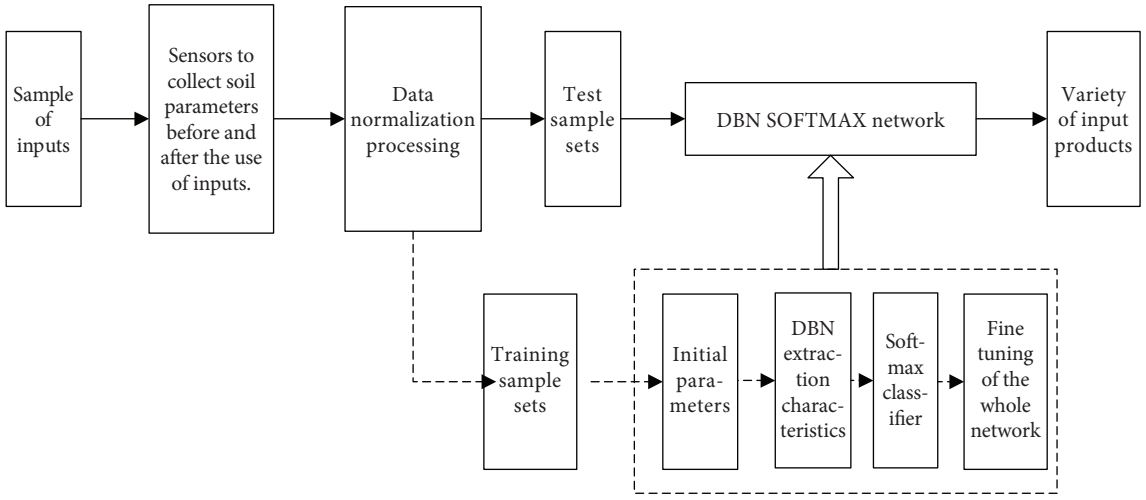

Figure 7: The flow diagram of modeling.

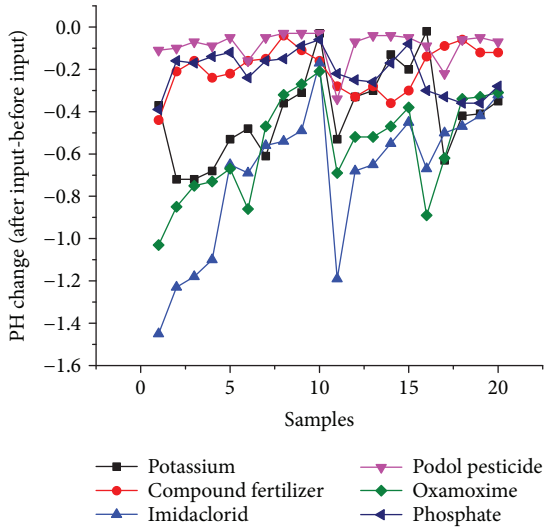

Figure 8: Changes in pH before and after input.

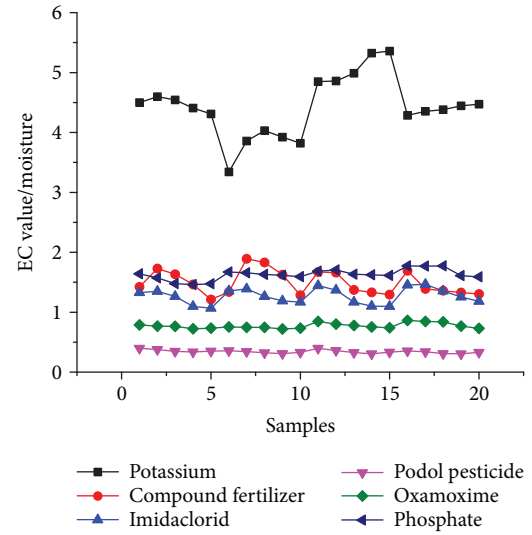

Figure 9: Changes in EC/moisture before and after input.

each type of input product, and the total number of data was 900.

5. Results and Discussion

5.1. Data of Sensors. The sensor data before input were not the same in each experiment; the collected sensor data after input minus before input could better explain the characteristics of the input. Six agricultural inputs were sprayed into the soil, respectively, and pH, conductivity, and moisture data were collected before and after the input. In this paper, 20 times of experimental data were randomly selected for observation.

Observing the collected pH values, before input they were close to 7, which was neutral. After applying six agricultural inputs, the pH value decreased. As shown in Figure 8, the changes of pH at different inputs were similar and overlapped with each other. It indicates that there was no significant difference in the power of hydrogen during several agricultural inputs applied.

Further observation of changes in electrical conductivity (EC), since the EC value was very sensitive to moisture content, there was a significant error in the shift in the EC value observed separately. The EC value divided the moisture content, and the obtained ratio was counted as shown in Figure 9. Observation shows that in general, EC changes in pesticides, including podol pesticide, imidacloprid, and oxamoxime were smaller, while fertilizers were comparatively larger. Changes of potassium had the most considerable EC value, and its value was more significant than the three; however, the EC value changes of pesticide were less than 1.5.

5.2. Modeling and Analysis. Sensors collected the trained and relevant experimental data of the agricultural inputs

Table 1: The characteristic data table.

y^a	Feature data					
1	0.261774	0.51821	0.363377	0.333239	0.40386	0.748109
1	0.249594	0.569245	0.360975	0.317917	0.442481	0.728785
1	0.25111	0.560419	0.361024	0.32006	0.437188	0.730672
2	0.811001	0.796877	0.348194	0.270687	0.189169	0.231068
2	0.839929	0.777112	0.698331	0.380023	0.302937	0.187739
2	0.822922	0.811853	0.321081	0.268463	0.183998	0.220862
3	0.397166	0.347973	0.591175	0.642555	0.696136	0.526804
3	0.441901	0.3287	0.630434	0.696979	0.742546	0.464949
3	0.417766	0.325697	0.646081	0.692987	0.75344	0.477638
4	0.716266	0.526859	0.587048	0.715965	0.590975	0.389491
4	0.764408	0.593614	0.599644	0.594801	0.447832	0.317517
4	0.735743	0.50656	0.56267	0.718762	0.570059	0.368529
5	0.221322	0.570325	0.261664	0.264869	0.386502	0.750886
5	0.226302	0.555085	0.258739	0.26812	0.375292	0.751574
5	0.23323	0.578087	0.251799	0.265587	0.376804	0.743913
6	0.760376	0.252841	0.753006	0.841325	0.298932	0.814017
6	0.752798	0.194803	0.781346	0.848471	0.26095	0.846151
6	0.760472	0.275192	0.74997	0.839426	0.310604	0.809583

[a] y is for the types of agricultural inputs. 1: potassium fertilizer; 2: compound fertilizer; 3: imidacloprid; 4: Podol liquid; 5: oxamoxime; 6: phosphate fertilizer.

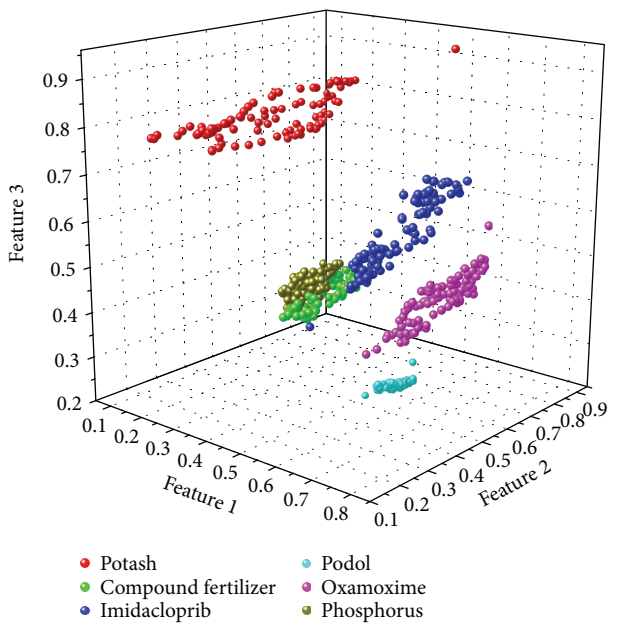

Figure 10: Three-dimensional distribution of feature values.

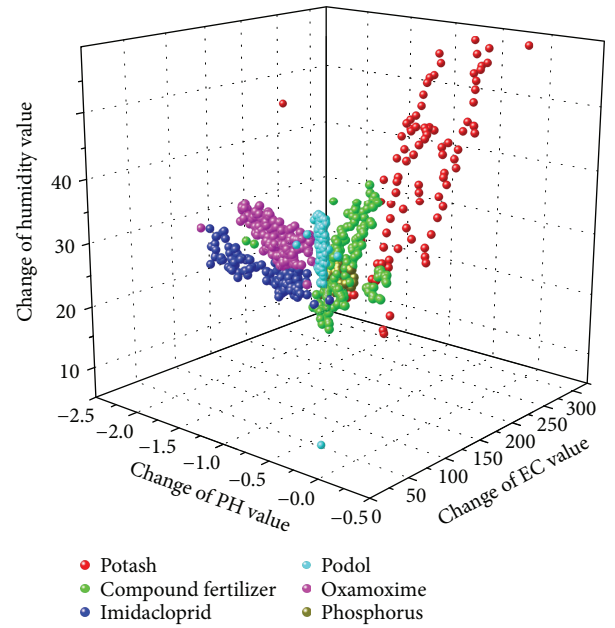

Figure 11: Three-dimensional distribution of original values.

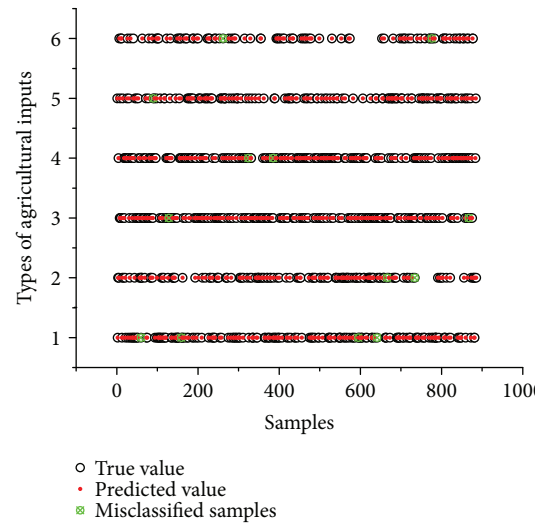

Figure 12: The predicted results of DBN-SOFTMAX for test sets. In the ordinate, 1: potassium fertilizer; 2: compound fertilizer; 3: imidacloprid; 4: Podol liquid; 5: oxamoxime; and 6: phosphate fertilizer.

prediction models. The main content of each data sample is input product category, the moisture proportion (before input), conductivity (before input), the pH value (before input), moisture ratio (after input), conductivity (after input), and pH value (after input). In establishing the model, the leave-one-out method [27] was used for the cross-validation to test the model's performance. Each of the 900 samples was taken separately, and then the remaining 899 samples were used to build the model. The model independently tested each sample, and the results were averaged to obtain the average performance of the method.

When using DBN for feature extraction, a four-layer neural network was established, the number of neurons in each layer was 300, 100, 20, and 6, respectively. The activation function of the hidden layer was "logsig", the training method was the L-BFGS algorithm [28], and the output layer function was a softmax function. In DBN feature extraction,

Table 2: The forecast accuracy comparison table.

Training data	Model	Input layer (neuron)	Hidden layer (neuron)	Output layer (neurons)	Accuracy
Raw data	BP	6	10	6	84.7%
Raw data	DBN-BP	6	300-100-20-6	6	97.8%
Raw data	DBN-SOFTMAX	6	300-100-20-6	6	98.5%

RBM used an unsupervised learning method to train each layer of RBM networks separately, ensuring that the feature information was preserved as much as possible during the mapping process. After the training was completed, a classifier was set at the last level of the DBN; using supervised fine-tuning, the best training results were obtained. Since each layer of RBM network only adjusted the weights in its own layer, it did not guarantee that the feature vector mapping of the entire DBN was optimal. After supervised fine-tuning, the process of RBM network training could be regarded as the initialization process of weight parameters of a deep neural network, which enabled the DBN network to overcome the disadvantages of the traditional BP network due to random initialization weight parameters and easy to fall into local optimum and long training time.

During the training, the number of iterations was 400, the learning rate was 0.1, and the training error target was set to 0.001. After the training, the extracted feature data were shown in Table 1:

Through unsupervised training of DBN and nonlinear mappings, the features were obtained from the input data, such as pH, moisture, and conductivity. After extracting features, the cohesion of the same types of agricultural inputs and the variances of different farm inputs could be better demonstrated. After dimensional reduction by the principal component analysis (PCA) method [29], the three-dimensional distribution of feature values and the three-dimensional distribution of original values were shown in Figures 10 and 11. It could be observed that the feature values extracted by DBN can be separated, but the initial input values without feature extraction were scattered and there were some confusion. Therefore, it was evident that using the extracted feature values for classification could achieve better prediction results.

We used this model for predicting the agricultural inputs. First, by applying the RBM-based DBN model, unsupervised training on raw data was carried out to improve the robustness of the network. Second, the feature data were obtained, and the softmax classifier was added to the back of DBN, the feature data were taken as the input, and the categories of inputs were taken as the output. Thirdly, the feature data and the tagged samples were combined to fine-tune the softmax classifier, and finally, the model was established to predict the accuracy. The result was shown in Figure 12. When 900 samples were predicted, thirteen samples were wrongly predicted with the model accuracy of 98.5%.

To evaluate the performance of the DBN-softmax model, BP-neural network and DBN-BP model were also established and the prediction accuracy of the input products was compared.

Table 3: DBN model performance comparison with BP-NN and SVM.

Models	R^2_{cal}	RMSEC	R^2_{CV}	RMSECV
DBN	0.99	0.03	0.99	0.15
BP-NN	0.99	0.09	0.94	0.40
SVM	0.99	0.09	0.98	0.21

As shown in Table 2, the DBN-BP accuracy was higher than that of the BP neural network, because DBN adopted the unsupervised layer-wise [16] mechanism training mode. The weights gained through DBN were obtained by learning the structure of input data, which were close to the optimal global values. However, BP neural network, whose initial values were randomly set, was prone to problems such as local optimal and gradient diffusion, so it required manual adjustment parameters [30]. When DBN-BP was compared with DBN-SOFTMAX, we used the same DBN structure to extract features with different classifiers, so the prediction accuracy was the same. It indicated that the prediction accuracy depended mainly on the quality of feature extraction, and the results obtained by different classifiers were not very different.

Further research on the determination coefficient (R-Square) and root mean square error (RMSE) when testing model performance. This paper compared conventional modeling methods such as BP-NN and support vector machine (SVM) [31]. When establishing the SVM model, the nu-SVM algorithm was selected, and the radial basis function (RBF) was selected as the kernel function. The error penalty coefficient γ and the kernel function parameter nu were 0.255 and 1, which were determined by grid searching technique [32]. In the process of modeling, the calibration sets were used to build the model, and the leave-one-out method was used for cross-validation to test the robustness and adaptability of the model further.

As shown in Table 3, when the BP-NN model was observed, the performance of the calibration sets was the same as SVM. However, the determination coefficient of cross-validation was smaller than SVM, and the root mean square error was more extensive than SVM, revealing that the model was not as accurate and stable as the SVM model. When the DBN model was observed, it could be seen that after feature extraction, the determination coefficients of calibration sets and cross-validation were the largest compared to BP-NN and SVM, reaching 0.99 and 0.99, respectively. Meanwhile, the RMSE of calibration sets and cross-validation in the DBN model were the smallest, which were 0.03 and 0.15, respectively. So in general, compared to SVM

and BP-NN, DBN was still considered to be the optimal modeling method.

6. Conclusions

Based on the self-developed monitoring equipment and DBN-SOFTMAX model, we have developed a platform for intelligent monitoring of agricultural inputs; perform online and real-time monitoring on farms. When the agricultural inputs were applied in farms, we could compare the types of inputs and application time with the data entered by the administrators in the traceability system. Once the producers do not record the traceability information or input the wrong information, our system can capture related data timely and accurately, then automatically provides safety warning to the producers, to ensure that the traceability information is true and accurate. The intelligent monitoring platform will pave a new way for the development of traceability systems.

Data Availability

The data used to support the findings of this study are available from the corresponding author upon request.

Conflicts of Interest

The authors declare no conflict of interest.

Authors' Contributions

Ling Yang, Ting Wu, and Li Lin conceived and designed the experiments; Ling Yang performed the experiments; Ting Wu, Juan Zhou, Xu Can Cai, and V Sarath Babu analyzed the data; Ling Yang, Ting Wu, and Li Lin wrote and finalized the manuscript.

Acknowledgments

This study was jointly supported by the National Natural Science Fund (61501531); fund for Science and Technology from Guangdong Province (2015A020209173, 2017A020225007); fund from Guangzhou Science and Technology Bureau (201704020030, 201803020033); and "Innovation and Strong Universities" special funds (KA170500G) from the Department of Education of Guangdong Province. V. Sarath Babu was supported by Chinese Postdoctoral Science Foundation.

References

[1] A. Regattieri, M. Gamberi, and R. Manzini, "Traceability of food products: general framework and experimental evidence," *Journal of Food Engineering*, vol. 81, no. 2, pp. 347–356, 2007.

[2] T. Bosona and G. Gebresenbet, "Food traceability as an integral part of logistics management in food and agricultural supply chain," *Food Control*, vol. 33, no. 1, pp. 32–48, 2013.

[3] H. Y. Deng, W. Xie, Z. Q. Zhou, B. Li, and Q. T. Jiang, "Determination of 11 benzoylurea insecticides residues in vegetable by LC-MS/MS," *Journal of Instrumental Analysis*, vol. 28, no. 8, pp. 970–974, 2009.

[4] J. H. Zheng, G. F. Pang, C. L. Fan, and M. L. Wang, "Simultaneous determination of 128 pesticide residues in milk by liquid chromatography-tandem electrospray mass-spectrometry," *Chinese Journal of Chromatography*, vol. 27, no. 3, pp. 254–263, 2009.

[5] M. Y. Selisker, D. P. Herzog, R. D. Erber, J. R. Fleeker, and J. Itak, "Determination of Paraquat in fruits and vegetables by a magnetic particle based enzyme-linked immunosorbent assay," *Journal of Agricultural and Food Chemistry*, vol. 43, no. 2, pp. 544–547, 1995.

[6] M. J. Alcocer, P. P. Dillon, B. M. Manning et al., "Use of phosphonic acid as a generic hapten in the production of broad specificity anti-organophosphate pesticide antibody," *Journal of Agricultural and Food Chemistry*, vol. 48, no. 6, pp. 2228–2233, 2000.

[7] S. Kumaran and C. Tran-Minh, "Insecticide determination with enzyme electrodes using different enzyme immobilization techniques," *Electroanalysis*, vol. 4, no. 10, pp. 949–954, 2010.

[8] S. H. Chough, A. Mulchandani, P. Mulchandani, W. Chen, J. Wang, and K. R. Rogers, "Organophosphorus hydrolase–based amperometric sensor: modulation of sensitivity and substrate selectivity," *Electroanalysis*, vol. 14, no. 4, pp. 273–276, 2015.

[9] J. Burrell, T. Brooke, and R. Beckwith, "Vineyard computing: sensor networks in agricultural production," *IEEE Pervasive Computing*, vol. 3, no. 1, pp. 38–45, 2004.

[10] M. Srbinovska, C. Gavrovski, V. Dimcev, A. Krkoleva, and V. Borozan, "Environmental parameters monitoring in precision agriculture using wireless sensor networks," *Journal of Cleaner Production*, vol. 88, pp. 297–307, 2015.

[11] D. D. Chaudhary, S. P. Nayse, and L. M. Waghmare, "Application of wireless sensor networks for greenhouse parameter control in precision agriculture," *International Journal of Wireless & Mobile Networks*, vol. 3, no. 1, pp. 140–149, 2011.

[12] H. J. Jia and Z. H. Guo, "Research on the technology of rs485 over ethernet," in *2010 International Conference on E-Product E-Service and E-Entertainment*, pp. 1–3, Henan, China, November 2010.

[13] M. Aref and A. Sikora, "Free space range measurements with Semtech Lora™ Technology," in *2014 2nd International Symposium on Wireless Systems within the Conferences on Intelligent Data Acquisition and Advanced Computing Systems*, pp. 19–23, Offenburg, Germany, September 2014.

[14] N. Azmi, S. Sudin, L. M. Kamarudin et al., "Design and development of multi-transceiver Lorafi board consisting LoRa and ESP8266-Wifi communication module," *IOP Conference Series: Materials Science and Engineerin*, vol. 318, article 012051, 2018.

[15] G. E. Hinton, "A practical guide to training restricted Boltzmann machines," in *Neural Networks: Tricks of the Trade*, G. Montavon, G. B. Orr, and K. R. Müller, Eds., vol. 7700 of Lecture Notes in Computer Science, pp. 599–619, Springer, Berlin Heidelberg, 2012.

[16] Y. Bengio, "Learning deep architectures for AI," *Foundations and Trends® in Machine Learning*, vol. 2, no. 1, pp. 1–127, 2009.

[17] B. Schölkopf, J. Platt, and T. Hofmann, "In Greedy layer-wise training of deep networks," *International Conference on Neural Information Processing Systems*, pp. 153–160, 2006.

[18] G. E. Hinton and R. R. Salakhutdinov, "Reducing the dimensionality of data with neural networks," *Science*, vol. 313, no. 5786, pp. 504–507, 2006.

[19] N. Li, J. Shi, and M. Gong, "Change detection in synthetic aperture radar images based on fuzzy restricted Boltzmann machine," in *Bio-inspired Computing – Theories and Applications. BIC-TA 2016*, M. Gong, L. Pan, T. Song, and G. Zhang, Eds., vol. 681 of Communications in Computer and Information Science, pp. 438–444, Springer, Singapore, 2016.

[20] G. V. Tulder and M. D. Bruijne, "Combining generative and discriminative representation learning for lung CT analysis with convolutional restricted Boltzmann machines," *IEEE Transactions on Medical Imaging*, vol. 35, no. 5, pp. 1262–1272, 2016.

[21] P. M. Long and R. A. Servedio, "Random classification noise defeats all convex potential boosters," *Machine Learning*, vol. 78, no. 3, pp. 287–304, 2010.

[22] L. Chen, M. Zhou, W. Su, M. Wu, J. She, and K. Hirota, "Softmax regression based deep sparse autoencoder network for facial emotion recognition in human-robot interaction," *Information Sciences*, vol. 428, pp. 49–61, 2018.

[23] K. Duan, S. S. Keerthi, W. Chu, S. K. Shevade, and A. N. Poo, "Multi-category classification by soft-max combination of binary classifiers," in *Multiple Classifier Systems. MCS 2003*, T. Windeatt and F. Roli, Eds., vol. 2709 of Lecture Notes in Computer Science, pp. 125–134, Springer, Berlin, Heidelberg, 2003.

[24] B. Liao, J. Xu, J. Lv, and S. Zhou, "An image retrieval method for binary images based on DBN and Softmax classifier," *IETE Technical Review*, vol. 32, no. 4, pp. 294–303, 2015.

[25] A. Nagabandi, G. Kahn, R. S. Fearing, and S. Levine, "Neural network dynamics for model-based deep reinforcement learning with model-free fine-tuning," *2018 IEEE International Conference on Robotics and Automation (ICRA)*, 2017, pp. 7559–7566, Brisbane, Australia, May 2018.

[26] J. Yang, Y. Bai, F. Lin, M. Liu, Z. Hou, and X. Liu, "A novel electrocardiogram arrhythmia classification method based on stacked sparse auto-encoders and softmax regression," *International Journal of Machine Learning and Cybernetics*, vol. 9, no. 10, pp. 1733–1740, 2017.

[27] M. Kearns and D. Ron, "Algorithmic stability and sanity-check bounds for leave-one-out cross-validation," *Neural Computation*, vol. 11, no. 6, pp. 1427–1453, 1999.

[28] D. C. Liu and J. Nocedal, "On the limited memory BFGS method for large scale optimization," *Mathematical Programming*, vol. 45, no. 1–3, pp. 503–528, 1989.

[29] S. Wold, K. Esbensen, and P. Geladi, "Principal component analysis," *Chemometrics and Intelligent Laboratory Systems*, vol. 2, no. 1–3, pp. 37–52, 1987.

[30] B. Yang, X. H. Su, and Y. D. Wang, "Bp neural network optimization based on an improved genetic algorithm," in *Proceedings. International Conference on Machine Learning and Cybernetics*, vol. 61, pp. 64–68, Beijing, China, November 2002.

[31] C. Cortes and V. Vapnik, "Support-vector networks," *Machine Learning*, vol. 20, no. 3, pp. 273–297, 1995.

[32] L. I. Bing, Q. Z. Yao, Z. M. Luo, and Y. Tian, "Gird-pattern method for model selection of support vector machines," *Computer Engineering & Applications*, vol. 44, no. 15, pp. 136–138, 2008.

Hindawi
Journal of Sensors
Volume 2018, Article ID 3528296, 13 pages
https://doi.org/10.1155/2018/3528296

Review Article

The State-of-the-Art of Knowledge-Intensive Agriculture: A Review on Applied Sensing Systems and Data Analytics

Barun Basnet and Junho Bang

Department of IT Applied System Engineering, Chonbuk National University, Jeollabuk-do, Republic of Korea

Correspondence should be addressed to Junho Bang; jhbang@jbnu.ac.kr

Received 16 March 2018; Revised 7 July 2018; Accepted 26 July 2018; Published 19 September 2018

Academic Editor: Wesley Beccaro

The application of sensors and information and communication technology (ICT) in agriculture has played a vital role in improving agricultural production and the value chain. Recently, the use of data analytics has shifted agriculture from input-intensive to knowledge-intensive as a large amount of agricultural data can be stored, shared, and analyzed to create information. In this paper, we have reviewed existing sensors and data analytics techniques used in different areas of agriculture. We have classified agriculture into five categories and reviewed the state-of-the-art technology in practice and ongoing research in each of these areas. Also, we have presented a case study of Korean scenario compared with other developed nations and addressed some of the issues associated with it. Finally, we have discussed current and future challenges and provided our views on how such issues can be addressed.

1. Introduction

The Food and Agriculture Organization of the UN (FAO) predicts that the global population will reach 9.2 billion by 2050, and food production must increase by 70 percent to keep the pace [1]. The income distribution in the world is uneven and hugely divided. In one part of the world, prosperity exists, and there is always demand for high-quality food. While in another part of the world, hunger and war exist, and there is always demand for a large quantity of foods. With limited farming land and freshwater resources, this quality and quantity crisis in food can only be addressed by the application of ICT in agriculture. Both small- and large-scale farming can benefit from introducing ICT into the agriculture value chain, having their productivity increased, quality improved, services extended, and costs reduced. Furthermore, ICT facilitates information- and knowledge-based approach rather than only focusing on input-intensive agriculture. As a result, agriculture becomes more networked, and decision making and resource utilization could significantly be leveraged.

ICT in agriculture is interchangeably used as e-agriculture, smart agriculture, precision agriculture (PA), or IoT (internet of things) in agriculture depending upon the context. Modern agriculture is hugely automated, controlled, and constantly monitored. Sensors are the heart of ICT, and various sensing devices used for this purpose generate a large volume of data continuously. The application of data analytics helps in solidifying the research in agriculture. It provides insights into various issues in the agriculture like weather prediction, crop and livestock disease, irrigation management, and supply and demand of agriculture inputs and outputs and helps in solving those problems. It can also provide valuable information for optimum resource utilization and production boosting. Our work reviews research articles focused on agricultural data and provides insights on several agricultural issues.

A wide variety of review literature is available, covering the topic: sensors and ICT in agriculture. Ojha et al. [2] reviewed the use and the state-of-the-art of wireless sensor networks (WSNs) in agriculture. Their work covers applications, design, standards, and technologies of WSNs used in agriculture. Also, another article by same authors [3] reviewed and proposed a sensor-cloud framework for the efficient addressing of various agricultural problems and applications. Another review article included key vision control techniques and their potential applications in fruit or vegetable harvesting robots [4]. In particular, it looked

at various vision schemes and recognition approaches for harvesting robots. Similarly, Zion [5] reviewed on the use of computer vision technologies in aquaculture. The review highlighted on the measurement, stock identification, and monitoring of different gender and species of aquatic animals. Other reviews included the keywords "ICT" and "agriculture" but were more focused on models and architectures in agriculture absorbing ICT [6, 7]. A recent article by Wolfert et al. [8] reviewed the state-of-the-art of big data applications in smart farming and identifying socio-economic challenges associated with it. The article slightly touched the technological part but largely focused on socio-economic and governance issues for the design of suitable business models. Another recent article by Lan et al. [9] reviewed the state-of-the-art in precision agricultural aviation technology highlighting remote sensing, aerial spraying, and ground verification technologies. Likewise, a large number of research articles do exist, combining the use of artificial intelligence (AI), database, and advanced statistical tools in the agriculture [10–12]. However, a review article focused on sensors and data analytic techniques in the area of agriculture is still scarce in the literature.

This article aims to review the use of ICT especially sensors and data analytic techniques in the area of agriculture. Agriculture in this paper is used in a broader sense and covers research in crop cultivation, horticulture, animal husbandry, apiculture, and aquaculture. Our classification closely resembles the scientific classification of agriculture. By breaking agriculture into different subfields, and reviewing applied sensors and data analytics, we intend to complement existing reviews. The objective of this paper is to review research and development in the area of agriculture from the technological perspective highlighting its various subfields. Also, we intend to facilitate readers in comparing one subfield with the other subfields easily.

1.1. Associated Technical Terminologies. We briefly explain certain terms which frequently appears when we talk about ICT, sensors, and data analytics.

Sensors are electronic devices that measure a physical change in its environment and convert it into a suitable electrical form. Sensors like environmental sensors, airflow sensors, location sensors, electrochemical sensors, mechanical sensors, and optical sensors are used for acquiring various kinds of agricultural data. *Smart sensors* are capable of not only acquiring data but also store, process, and integrate such data. *Sensor fusion* is a combination of two or more sensor data to get additional insights or overcome the weakness of a single sensor. *Wireless sensor networks* (WSNs) are networks of such sensors connected wirelessly.

An *embedded system* is a microprocessor/controller embedded into an electro-mechanical system for performing a particular task. It is programmable and has limited memory and processing power. Most of the embedded systems are based on *sensing systems* consisting of sensors and actuators.

Internet of things (IoT) is a complex interconnected network of things that continuously exchange data. Here, "things" refer to any physical devices like sensors, cameras, wearables, vehicles, cell phones, and houses that are connected to the internet.

Cloud computing is an internet-based computing service where one can store, manipulate and retrieve data, and utilize resources from anywhere without actually owning the required hardware or software.

Data analytics techniques include analyzing and processing of acquired large datasets from the field and providing meaningful information so that any interested party may utilize them for their future work. Those large data sets are called *big data*, and the analytic technique is called *data mining*. A separate field of study called *data science* has emerged recently which combines computer algorithms and statistical methods for data analytics [13].

2. Research Methodology and Motivation

The primary purpose of this paper is to review the use of sensors and data analytics in different branches of agriculture. We frequently use ICT and sensors interchangeably in this paper as sensors are a key to the-state-of-the-art ICT, and sensor data are raw materials for any sort of data analytics. The terminology *sensor* used in this survey actually refers to *sensing systems* rather than the sensor devices itself. Likewise, agriculture is an enormous and vast area, and we do not attempt to review the use of ICT tools and techniques in every process, steps, fields, and subfields of agriculture. To narrow down, we have excluded *prefield* (genetics, seed/egg development) and postfield (distribution, processing, and consumer) and only reviewed the use of ICT tools and techniques for *In-field* applications, that is, planting/raising and harvesting. Also, the classification of the areas of agriculture in Section 3 is a general classification and might not exactly match with other sorts of classifications elsewhere. Figure 1 shows the evolution of different technologies used in the areas of the agriculture. However, we have excluded other (e.g., chemical, genetics, bioengineering) types of advancements made in the field of agriculture.

At large, only peer-reviewed research articles are provided as a reference for preparing this paper. However, reports and publications of various government and nongovernment organizations were also referred for understanding the perspectives outside academia in regard to challenges and future work direction. Also, our review does not contain research in agricultural machinery and robots but might cover certain underlying technologies if only they are relevant to sensors and data analytics tools.

3. Sensors and Data Analytics in Agriculture

3.1. Agronomy/Crop Farming. The general use of wireless sensor networks in crop monitoring and data acquisition can be found in various research and review articles [14–16]. Modern agronomical research and practice are becoming more and more data intensive. Data are continually collected, analyzed, and simulated to understand and predict crop growth and behavior under various circumstances.

Driemeier et al. [10] proposed a computational environment to support research in sugarcane precision agriculture.

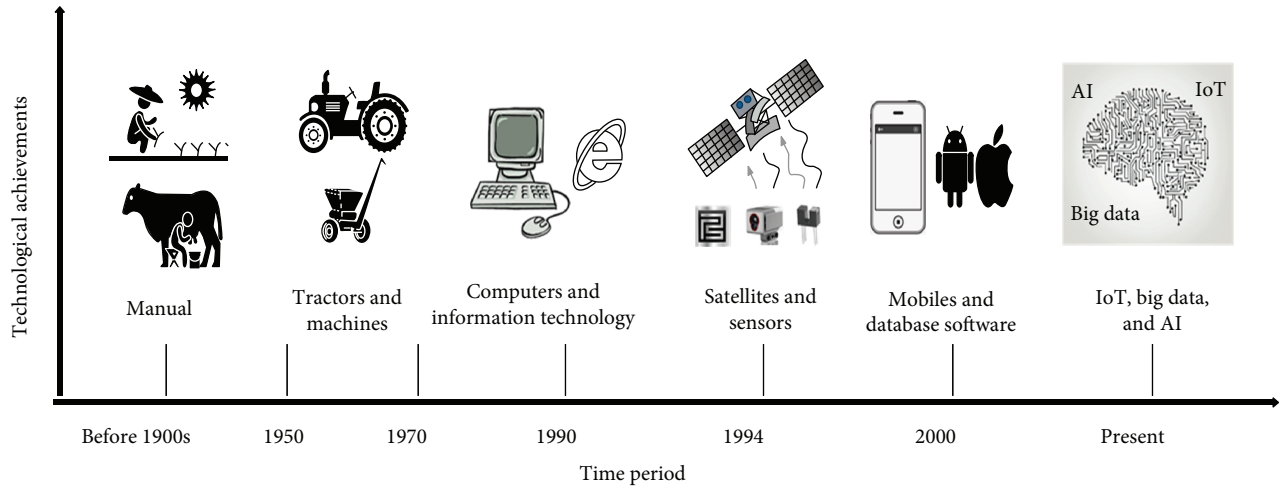

Figure 1: Evolution of different technologies used in the areas of the agriculture.

The work presented a data analysis workflow model for data acquisition, formatting, and verification. The model was employed to analyze three joint experiments comprised of soil attributes, sugarcane quality, and sugarcane yield. Yang et al. [11] reported the use of airborne multispectral and hyperspectral imagery and high-resolution satellite imagery for monitoring growth and estimating crop yield. They presented several application examples to demonstrate the advantages and limitations of different remote sensing and imagery analysis techniques. Similarly, Dong et al. [17] studied the feasibility of deriving spatially variable crop maximum light use efficiency ($LUE_{\max}$) from satellite remote sensing data to improve crop biomass estimation. This study offered a new way to derive $LUE_{\max}$ for specific production efficiency models (PEM) and to improve the accuracy of biomass estimation using remote sensing. Equations (1), (2), and (3) represent an accuracy assessment model based on three statistical criteria.

$$\mathrm{RMSE} = \sqrt{\left(\frac{1}{n}\right) \times \sum_{i=1}^{n} (E_i - M_i)^2}, \quad (1)$$

$$\mathrm{nRMSE} = \frac{\mathrm{RMSE}}{\bar{M}} \times 100, \quad (2)$$

$$\mathrm{dindex} = 1 - \frac{\sum_{i=1}^{n} (E_i - M_i)^2}{\sum_{i=1}^{n} \left(\left|E_i - \bar{M}\right| + \left|M_i \bar{M}\right|\right)^2}. \quad (3)$$

Here, RMSE, nRMSE, and d-index represent the root-mean-square error, the normalized RMSE, and the index of agreement, respectively. A smaller value for both RMSE and nRMSE gives the higher estimation accuracy. The parameters inside the equations n, M_i, E_i, and $\bar{M}$ represent the number of observations, the measured value, the estimated value, and the mean of all measured values.

Similarly, Ge et al. [18] reported a study to characterize the temporal dynamics of maize plants' growth and water use through RGB (red, green, blue) images and automated pot weights. These methods proved to help in quantifying plant leaf water content. Figure 2 represents the hyperspectral image analysis to extract leaf pixels and the average leaf reflectance to predict plant leaf water content. Kristen et al. [19] reported sensor-based approaches to facilitate cost-effective and site-specific management for soil health. The authors applied a sensor fusion approach (partial least square analysis) to estimate soil health indicators and soil management assessment framework (SMAF) scores using visible and near-infrared (VNIR) spectra in conjunction with electrical conductivity (EC_a) sensor data. The fusion of EC_a and CI data with VNIR improved estimation of the physical category and subsequently the overall SMAF soil health. However, chemical and fertility-related soil properties were not well estimated by this sensor fusion combination.

3.2. Horticulture/Plant Farming. Horticulture can sometimes be considered as a branch of agronomy concerned with the cultivation of plants, fruits, and vegetables rather than crops. The sensing technologies used in both areas are of similar nature. Various papers report design of greenhouse horticulture monitoring and control systems with WSN and commercially available embedded systems or IoT prototyping platforms [20–24].

Kim and Glenn [25] reported the development of a multimodal sensing system to identify the onset and severity of plant stress in young apple trees under different water treatments in a greenhouse. The data analysis result determined the spectral signature, and canopy temperature was highly correlated to plant water stress. Figure 3 represents thermal images of five different apple trees in the temperature range of 22.3°C to 40.7°C. The rectangle in each image indicates the region of interest (ROI) for the calculation of canopy temperature. In a similar manner, Tian et al. [26] reported the design of a growth cabinet using an LED light source for hydroponics cultivation of rape plants. The work's focus was to design a light source made up of blue and red LEDs to predict and provide enough energy required by plants for photosynthesis at different growth stages. The designed system could also control microclimatic parameters like temperature, humidity, light intensity, and

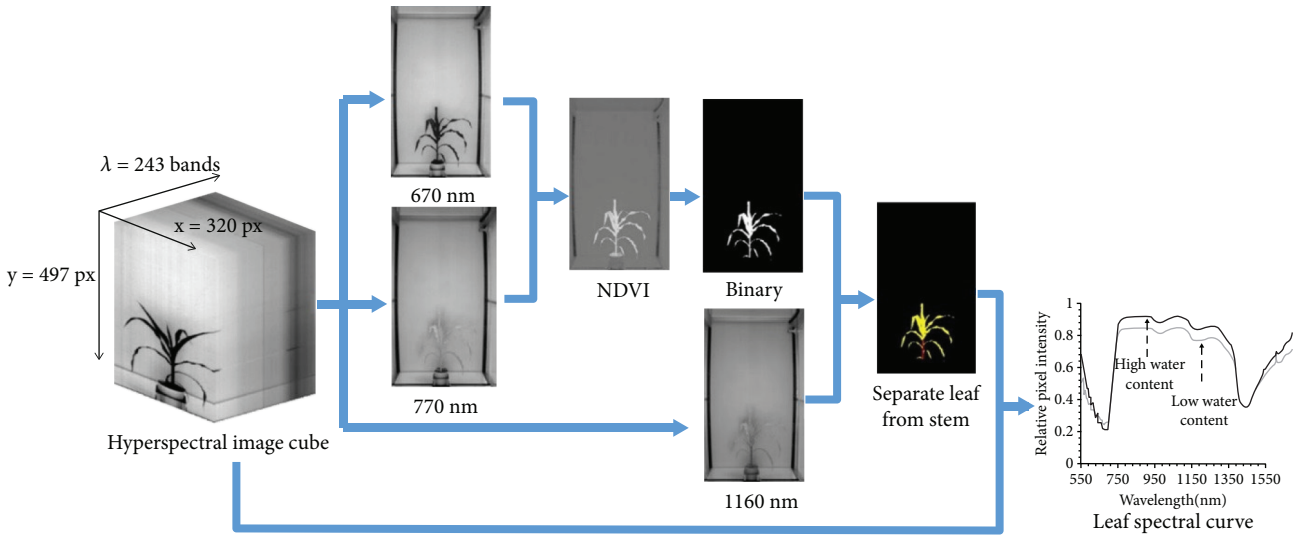

Figure 2: Hyperspectral image analysis to extract leaf pixels and the average leaf reflectance (pixel intensity) to predict plant leaf water content (Ge et al. [18]).

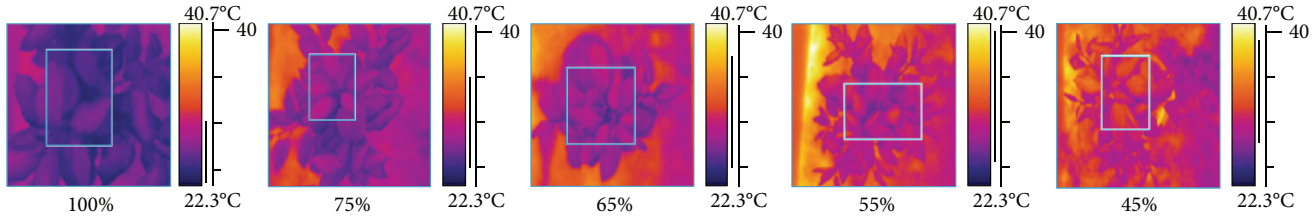

Figure 3: Thermal images of young apple trees in five different water treatments (Zhao et al. [4]).

CO_2 concentration level inside the growth cabinet. Their experimental results demonstrated that the plants grew very well and even superior to the plants that grew in the natural environments in terms of height, growth time, and taste. Basnet et al. adopted [27] a moving average algorithm for smoothing out variations in sensed data for a greenhouse automation system. The algorithm could greatly help in stabilizing fluctuations caused by rapid change in the environment or imprecise sensors and thus bringing stable output.

$$\begin{aligned} \text{Avg}_{t1} &= \frac{1}{n-1}\left[x_0^{t1} + x_1^{t1} + x_2^{t1} + \cdots + x_{n-1}^{t1}\right], \\ \text{Avg}_{t2} &= \frac{1}{n}\left[x_1^{t1} + x_2^{t1} + x_3^{t1} + \cdots + x_{n-1}^{t2}\right]. \end{aligned} \tag{4}$$

Equation (4) represents the mathematical expression of the moving average algorithm presented in the work.

Rose et al. [28] researched the collection, classification, and quantization of phenotypic data of multiple vine rows using commercial multi-view-stereo software. Using a moving sensor platform (a track-driven vehicle, camera, GPS, and data acquisition hardware), morphological data of multiple vine rows were acquired. The authors claimed to complement existing 2D research with 3D solution-based image processing and demonstrated different data processing stages for predicting yields. Similarly, Zhao et al. [4] reviewed key techniques in vision-based control for harvesting fruits and vegetables. Their work presented an overview of various vision schemes (binocular, spectral, thermal, laser, etc.) and image processing algorithms (AdaBoost, Bayesian, fuzzy neural, etc.) for fruit recognition system.

Jesus et al. [29] proposed a field programmable gate array- (FPGA-) based wireless smart sensor for real-time photosynthesis monitoring system. A case study to monitor the photosynthetic response of chili pepper.

Capsicum annuum L. is made where the smart sensor acquires and fuses the primary sensor signals to measure temperature, relative humidity, solar radiation, CO2, air pressure, and air flow. The measurements are used to calculate net photosynthesis in real time and transmit the data via wireless communication to a sink node. In addition, the proposed smart sensor was equipped with signal processing ability, such as average decimation and *Kalman filters*, to the primary sensor readings so as to decrease the amount of noise in them as shown in Figure 4.

3.3. Animal Husbandry/Livestock Farming. Traditional animal husbandry requires the raising of a large flock of animals or cattle by experienced herdsmen. Modern animal husbandry called precision livestock farming (PLF) is about monitoring, tracking, and acquiring all sorts of data of livestock in real-time with the application of sensing systems and ICTs. These data are further processed and analyzed to

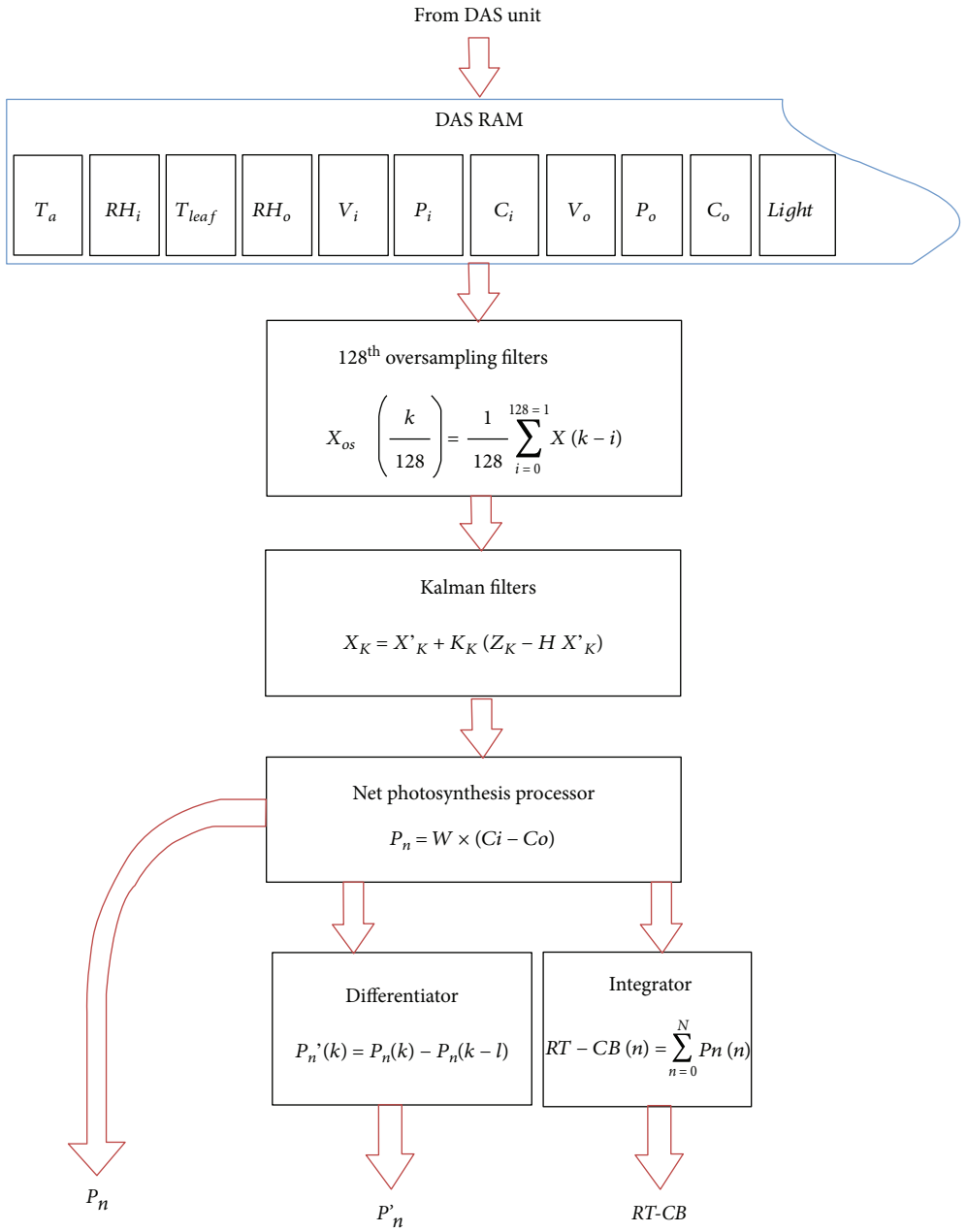

Figure 4: FPGA signal processing and smart processor unit (Jesus et al. [29]).

help in the decision-making process and provide a solution to various problems.

Aydin [30] reported a study to automatically assess the lameness of broiler by observing locomotion behaviors with the use of 3D vision camera and image process algorithm. The work is presented as a first attempt at assessing the lameness of broiler chickens with the use of 3D cameras having depth sensors as shown in Figure 5. Experiments were conducted to determine the *number of lying events* and *latency to lie down* of broiler chickens. The *gait scores* from 0 to 4 were chosen to rank lameness in the chicken. The proposed system had a high correlation between the output parameters against the manual labeling. Authors, therefore, asserted their work would be useful for developing an automatic animal monitoring and behavior analysis system to assess the health and welfare of broilers. Hongqian et al. [31] proposed a cloud-based data management system (CDMS) for automatic data collection for laying-hen farms. The CDMS facilitated asynchronous data transmission (*Kafka*-based), file distribution (*Hadoop*-based), information collection and management (*MySQL*-based) for the farms located in different areas. The system was set with 8 networking nodes and experimented at a commercial egg farm. The work expected to enhance the modern poultry in the efficient management of big data and record-keeping in real-time. Nkwari et al. [32] presented an article where a cow behavior is modeled using data collected from GPS sensors to get the expected position of it. The authors used the *continuous-time*

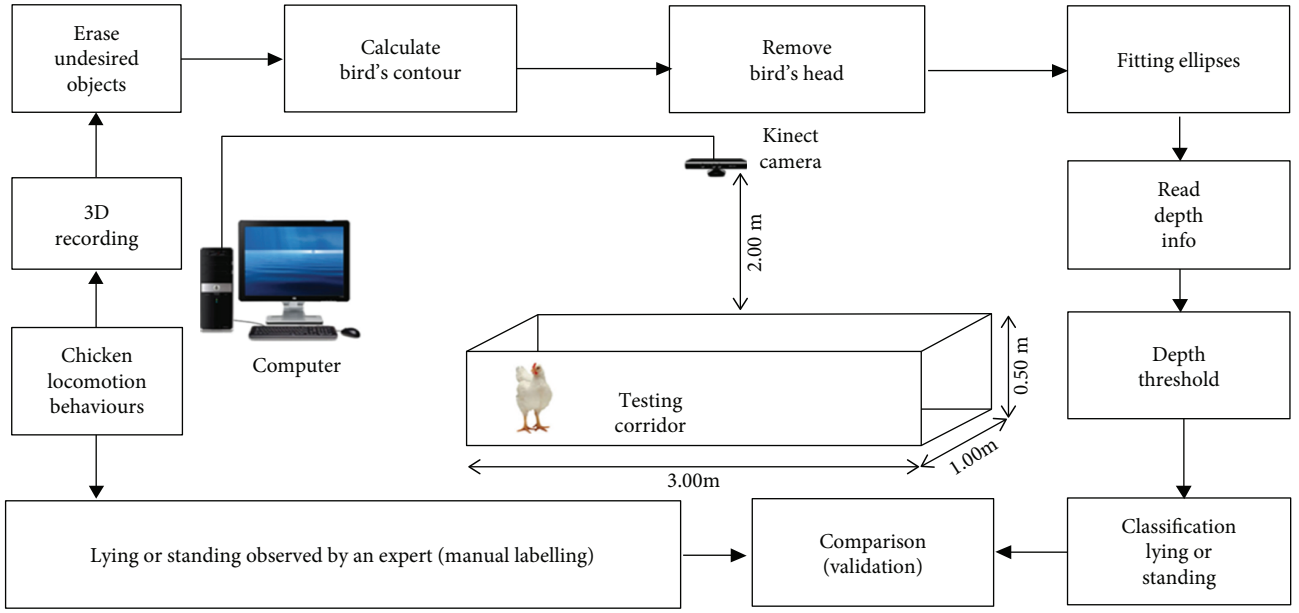

Figure 5: Flowchart of the image analysis and classification procedure using 3D vision camera (Aydin A 2017).

Markov process (CTMP) in order to model the random movement pattern (stochastic process) as shown in

$$\begin{aligned} P_{ij}^{(n)} &= P_r(X_n = j | X_0 = i), \\ p_b &= p_1 + p_2 + p_3 + p_4, \\ p_1 &= P[a_1 \le r \le b_1 = \sum_k \frac{1}{n}. \end{aligned} \tag{5}$$

Here, P_{ij} is the total probability that the cow moves from the location i to j. $P_{ij}^{(n)}$ represents the probability P_{ij} after the cow has taken n steps. p_1, p_2, p_3, and p_4 represent the probability the cow is in four different boundaries. a_1 and b_1 represent point limit of each boundary. By calculating which cow has a greater probability to get stolen, the work expects to help in preventing cattle rustling in farms.

Manteuffel et al. [33] presented a study which can help in preventing fatal piglet crushing events by mother sow. The work focuses on the extensive study of distress-specific vocalization to detect crushing events and thereby triggering for a mechanism to induce posture changes. Another study conducted by Feiyang et al. [34], a wireless network with the RFID tag collectors and weight sensors was employed to monitor chickens on a farm. The system detected sick chickens in the farm and classified them by studying their behaviors and parameters like the ability to snatch food, resting time, moving speed, and weight. The classification thus made and the extracted information is expected to facilitate precise husbandry and epidemic warning.

$$\begin{aligned} &\text{Stay}(i) = \text{Stay}_{\text{last}}(i) - \text{Stay}_{\text{first}}(i), \\ &D(i,j) = \sqrt{\sum_{p=1}^{n} (x_{ip} - x_{jp})^2}, \quad i = (x_{i1}, x_{i2}, \dots, x_{ip}), j = (x_{j1}, x_{j2}, \dots, x_{jp}). \end{aligned} \tag{6}$$

Equation (6) represents the formula for chickens' resting time and the *Euclidean distance* formula applied in the *K-means clustering* method for the recognition of chickens' disease and quality, respectively. Here, $\text{Stay}(i)$ represents the total resting time of chicken i from the beginning, that is, $\text{Stay}_{\text{first}}(i)$ to last period of stay, that is, $\text{Stay}_{\text{last}}$. In the same manner, $i = (x_{i1}, x_{i2}, \dots, x_{ip})$ and $j = (x_{j1}, x_{j2}, \dots, x_{jp})$ are two p-dimension objects with $D(i, j)$ Euclidean distance between them. The parameters $x_{i1}, x_{i2}, \dots, x_{ip}$ are the chicken's ability to snatch food, weight, speed, and resting time of the chicken i. The same concept goes for another chicken j. Smaller Euclidean distance represents chickens of similar characteristics.

3.4. Apiculture/Beekeeping. Apiculture or beekeeping is a branch of agriculture where bee colonies are maintained in hives for harvesting honey. Various ICT technologies especially WSN were used previously to monitor the beehives and get various environmental data through sensors [33, 35–37]. Due to various environmental changes, their population is reported to be rapidly decreasing, and various interdisciplinary researches are going on to understand this phenomenon and provide possible solutions as well.

Murphy et al. [12] proposed a threshold-based algorithm and decision tree algorithms based on a biological study of bees to detect important hive changes and alert the beekeeper in a WSN for monitoring bee health. It classified hives as being in one of the ten possible states ranging from "normal" to "dead" which might or might not require an immediate response from the beekeeper. With the knowledge acquired, the beekeeper can automatically apply established beekeeping knowledge to the collected data, allowing early identification of poor health for improved colony health as well as analysis of the behavior. Figure 6 represents a *decision tree algorithm* to classify hive states of the bee colonies. Here,

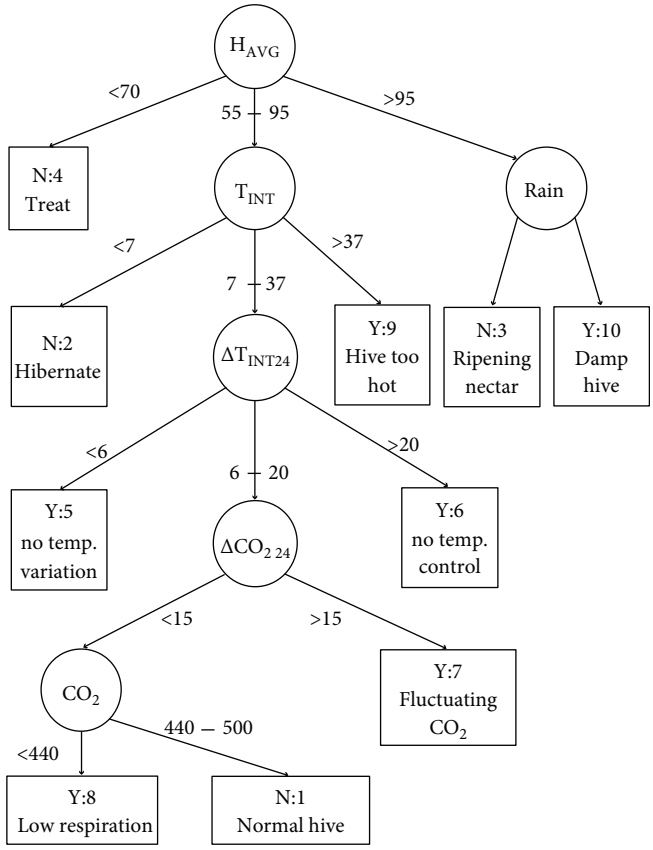

Figure 6: Decision tree induced from the training set for the hive classification (Murphy et al. [12]).

H_{AVG}, T_{INT}, ΔT, and ΔCO_2 represent average humidity, internal temperature, change in temperature, and change in CO_2 concentration level, respectively.

Similarly, another work presented by Kviesis et al. [38], a hierarchical three-level model consisting of a wireless node, a local data server, and a cloud data server called WBee is designed for monitoring honey bee colonies. The main distinguishing work presented in the paper is the design of the system acquiring synchronized samples from all the hives and being able to save data at each level in case there is a communication failure.

3.5. Aquaculture/Fishkeeping. Aquaculture outputs have high demands in the global food market, and the application of ICT has helped to increase its quality and the production in recent years. Water quality is the most important parameter in aquaculture since health, appetite, growth, and other activities of aquatic animals depend on it. Various subparameters like dissolved oxygen (DO), pH level, temperature, salinity, turbidity, and ammonia nitrogen content affect the quality of water. Monitoring of such parameters and recirculating water periodically is essential in maintaining the quality of water.

Lebrero et al. [39] reported the design of multiparameters monitoring system where DO sensor, pH electrode, pt1000 temperature sensor, and NH3-N sensor were used to monitor aquaculture water quality. The system would trigger an aerator ON or OFF if the sensor would read below or above the threshold (4 to 5.5 mg/L) of DO. Similar work by Hongpin et al. [40] reported on aquaculture monitoring system and control based on virtual instruments, additional features of power management, and networking solutions. The work has implemented sensor network nodes (dissolved oxygen sensor, temperature sensor, water level sensor, and pH sensor) in fish ponds for maximizing monitoring, control, and recording of the aquaculture system. With such benefits, the work reported on effectively reducing the probability of high risk of fish mortality, increase on economic benefit and consumer confidence, safety, and low energy consumption. The working concept of the designed system is presented in a flowchart as given in Figure 7.

Simbeye et al. [42] presented a multiple fish tracking systems in 3D space with structured-light (SL) sensor for acquisition of detailed information required for behavioral studies. Similarly, Saberioon and Cisar [41] used near-infrared imaging technique to observe feeding process and behavior of fish. Their work [41, 42] can help to quantify such behavior of fish and can help in developing an automatic feeding system in the future. Figure 8 represents the work of infrared imaging technique to observe the feeding process of fish. Zion reviewed the use of computer vision technologies in aquaculture and reported the satisfactory level of works done in the area of edible or ornamental fish farms [5]. However, in the case of sea cage farms, the author points out the challenges in the application of the technology because of various parameters like deep water level, high

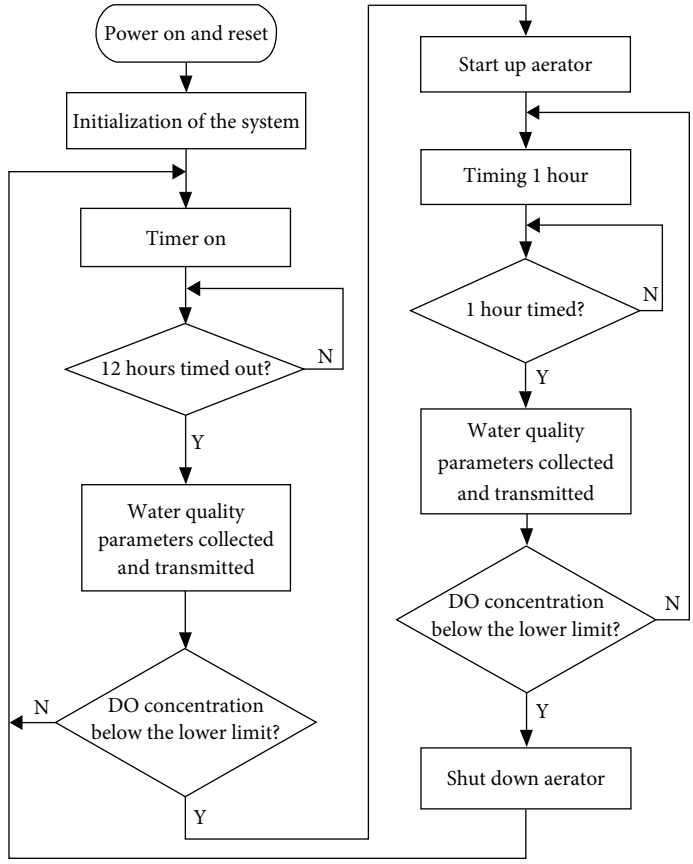

Figure 7: Flowchart of the remote monitoring system of aquaculture (Hongpin et al. [40]).

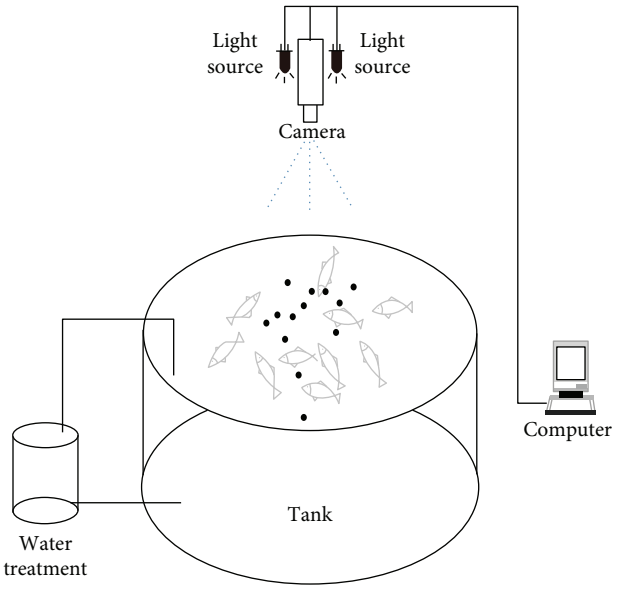

Figure 8: Infrared imaging technique to observe the feeding process (Saberioon and Cisar [41]).

turbidity, the presence of other aquatic animals, adjustment difficulty of feeding location, and lightening.

3.6. Chapter Conclusion. In this chapter, we reviewed various sensor-based technologies and data analytics techniques used in the field of agriculture. As mentioned in the previous chapters, agriculture is a very vast field and we do not attempt to review the application and development of different technologies in every process, steps, fields, and subfields of agriculture. We have only covered *In-field* applications.

There are other types of technological advancements made which has revolutionized the field of agriculture. Some of the noticeable things are advances in chemical fertilizers and pesticides, genetic engineering, soil and irrigation technology, agricultural tools and machinery, and production and distribution technology. However, review of such technologies is beyond the scope of this article. Table 1 shows the state-of-the-art use of different sensors and data analytics techniques presented in this work ([11–42]). Tables 2 and 3 show the state-of-the-art technology of different sensing system platforms and big data applications in smart farming and key issues, respectively.

4. Korean Scenario

South Korea is a highly industrialized country and hosts some of the world's huge leading tech-giants like Samsung, LG, and Hyundai. The Korean government has initiated steps in transferring the technology used in the industrial sector for the development of the agricultural sector as well. A report published by the Korean Rural Economic Institute emphasized the role of Korean agriculture in the nation's

Table 1: Use of sensors and data analytic techniques in different areas of agriculture.

Analytics and ICT	Sensors used	Purpose	Area	References
Image processing	Satellite data Sensors	Monitoring/estimating yield, water content check, feeding process observation	Agronomy, aquaculture	[4, 11, 17, 41]
Computer vision	3D camera, depth sensors	Lameness assessment, harvesting fruit	Animal husbandry, horticulture	[27, 28, 34]
Pattern recognition	GPS/sensors, RFID/ weight sensors, structured light sensor	Preventing cattle rustling classifying/epidemic warning, behavioral studies	Animal husbandry, apiculture	[31, 32, 42]
WSN	Environmental sensors	Detect hive changes, monitoring	Apiculture, aquaculture	[35, 38, 40]
Cloud computing	Smart devices, wireless nodes	Remote access, monitoring bee colonies	Animal husbandry, apiculture	[30, 39]
Others	Satellite LED and sensors	Crop biomass estimation hydroponics cultivation	Agronomy, horticulture	[18, 26]

Table 2: The state-of-the-art of the sensing platforms in agriculture (Ojha et al. [2]).

Feature	MICAZ	TelosB	IRIS	LOTUS	Imote2	SunSPOT
Processor	ATmega128	IMSP430	ATmega128	Cortex M3 LPC 17xx	Marvell/ XScalePXA271	ARM 920T
Clock speed (MHz)	7.373	6.717	7.373	10–100	13–416	180
Bus width (bits)	8	16	8	32	32	32
System memory (kB)	4	10	4	64	256	512
Operating frequency band (MHz)	2400	2400	2400	2400	2400	2400
Transceiver chip	CC2420	CC2420	Atmel RF230	Atmel RF231	CC2420	802.15.4
Number of channels	Programmable	Programmable	Programmable	—	In steps of 5 MHz	—
Data rate (kbps)	250	250	250	250	250	250
I/O connectivity	UART, I2C, SPI, DIO	UART, I2C, SPI, DIO	UART, I2C, SPI, DIO	3xUART, SPI, I2C, I2S, GPIO, ADC	UART3x, SPI2x, I2C, I2S, GPIO, DIO, JTAG	DIO, I2C, GPIO

Table 3: The state-of-the-art of big data applications in smart farming and key issues (Wolfert et al. [8]).

Stages of the data chain	State of the art	Key issues
Data capture	Sensors, open data, unmanned aerial vehicles (UAV), biometric sensing, genotype information, reciprocal data	Availability, quality, formats
Data storage	Cloud-based platform, Hadoop Distributed File System (HDFS), hybrid storage systems, cloud-based data warehouse	Quick and safe access to data
Data transfer	Wireless, cloud-based platform, Linked Open Data	Safety, agreements on responsibilities and liabilities
Data transformation	Machine learning algorithms, normalization, visualization and anonymization	Heterogeneity of data sources, automation of data cleansing and preparation
Data analytics	Yield models, planting instructions, benchmarking, decision ontologies, cognitive computing	Semantic heterogeneity, real-time analytics, scalability
Data marketing	Data visualization	Ownership, privacy, new business models

economic growth for the past 70 years [43]. It also reported the country's policy in investing in new technologies including ICT to cope with global warming, lack of resources, and changes in human consumption patterns. Similarly, the Electronics and Telecommunications Research Institute (ETRI) reported emerging ICT technologies to combine agricultural products at each stage in smart farms [44].

Koo et al. [45] reviewed Korean and international research trend related to ICT-based horticultural facilities. With keywords precision agriculture, smart farm, ICT, and IoT, the paper has thoroughly investigated technologies used in Korean agricultural scenario as shown in Table 4. It has also provided various case studies on failures and given directions and solutions from several perspectives. It emphasizes

Table 4: Core technologies for the realization of smart farm based on ICT (Koo et al. [45]).

Research objectives	Research content
Standardization and open common platform	Standardization of sensor technology and device. Building an open service platform. User-oriented interface development.
Sensor and instrumentation technology	Development of crop monitoring technology through image processing. Development of measuring device for soil and crop biomaterial information. Developed a high-efficiency sensor and measuring device. Real-time monitoring of electricity usage in the greenhouse complex. Monitoring and responding to load on the surrounding ecosystem and environment. Establishment of a sensor network system and improvement of battery or signal amplification technology of wireless measurement equipment.
Control and automation	Development of greenhouse complex environment control system algorithm. Developed smart grid integrated greenhouse control algorithm linked with energy saving technology (renewable energy). Development of differentiated ventilation fan and circulation fan control system. Development of additional forced ventilation operation algorithm through ventilation analysis.
Big data utilization and performance evaluation	ICT-based big data standardization, DB construction method development database analysis and application software development. Smart farm model performance analysis program development.
Web and mobile services	Provides real-time management and production information through the web system. Development of pest detection system and alarm system using image processing.
Renewable energy and energy load reduction technology	Developing appropriate capacity of the unit farmhouse considering the economy. Energy saving technology development for greenhouse structure and operation. Development of energy efficient operation technology using renewable energy.

the development of an intelligent service system for management and control of all the process of agricultural production. Yeo [46] reported the development of a moving monitor and control system for crops in the greenhouse. The movable sensing units gather continuous data and the connection is made through the Wi-Fi where the data are saved and processed on the server as shown in Figure 9. The movable sensing units consist of high-resolution IP camera, environmental sensors, and Wi-Fi repeater and controlling units contain embedded PC, programmable logic controller (PLC), and BLDC motors. This work expects to provide a better solution in monitoring scheme and management of plants and crops in a greenhouse.

Another recent article published by Kim [47] researched on the estimation of the factors influencing the future prices of corn and wheat through *Bayesian model* averaging as shown in (7). With the application of probabilistic factors, the results of the study facilitate the improvement in the ability to forecast grain future prices.

$$\Pr(A|B) = \frac{\Pr(B|A)\,\Pr(A)}{\Pr(B)}. \tag{7}$$

Here, $\Pr(A)$ and $\Pr(B)$ represents the probabilities of the occurrence of the events A and B, respectively. Whereas, $\Pr(A \mid B)$ and $\Pr(B \mid A)$ represents a conditional probability of the likelihood of the occurrence of the event A given B is true and vice-versa.

5. Challenges and Future Work Direction

The use of sensors and data analytics gives a better hope for the agricultural sector, but challenges still remain. The factors associated with them which still need further attention are listed as Sections 5.1–5.6.

5.1. Sustainable Agriculture. While technological efforts are made in increasing the productivity of the agriculture, environmental and social factors are often not taken into account. In particular, developing countries prioritize on adopting technologies for fast development rather than a sustainable one [48]. Initiatives from the different sectors of society should be taken with a view to developing the sustainability of farming systems along with the adoption of the various technologies including sensors technology and ICT. Also, technology interventions should be designed to select appropriate and environment-friendly technologies for collecting, storing, recycling, and treating and disposing of e-waste [1].

5.2. Technological Constraint. Technology at hand determines the progress in each area of its application. The improvement in technology will add more precision, accuracy, speed, and reliability whereas reducing cost in the future. Standardization in technology is vital for the improvement in communication between farm equipment. Also, research and open source projects should be encouraged more to improve the overall quality of technological solutions [49].

5.3. End-User Oriented. Technological solutions should always be user-friendly. It should suit local contexts and needs. In the case of agricultural application, solution providers should take special care in making their products and solutions as easy, readable, and understandable as possible.

5.4. Big Data. Intelligent processing and analysis of a large amount of unstructured and heterogeneous data are required. Research show *dimensional reduction* in big data is necessary for core value extraction, and also the work is also equally challenging [50]. Open access to research and publication of these data are very important. But there exists ownership ambiguity of whom they belong to. Farmers?

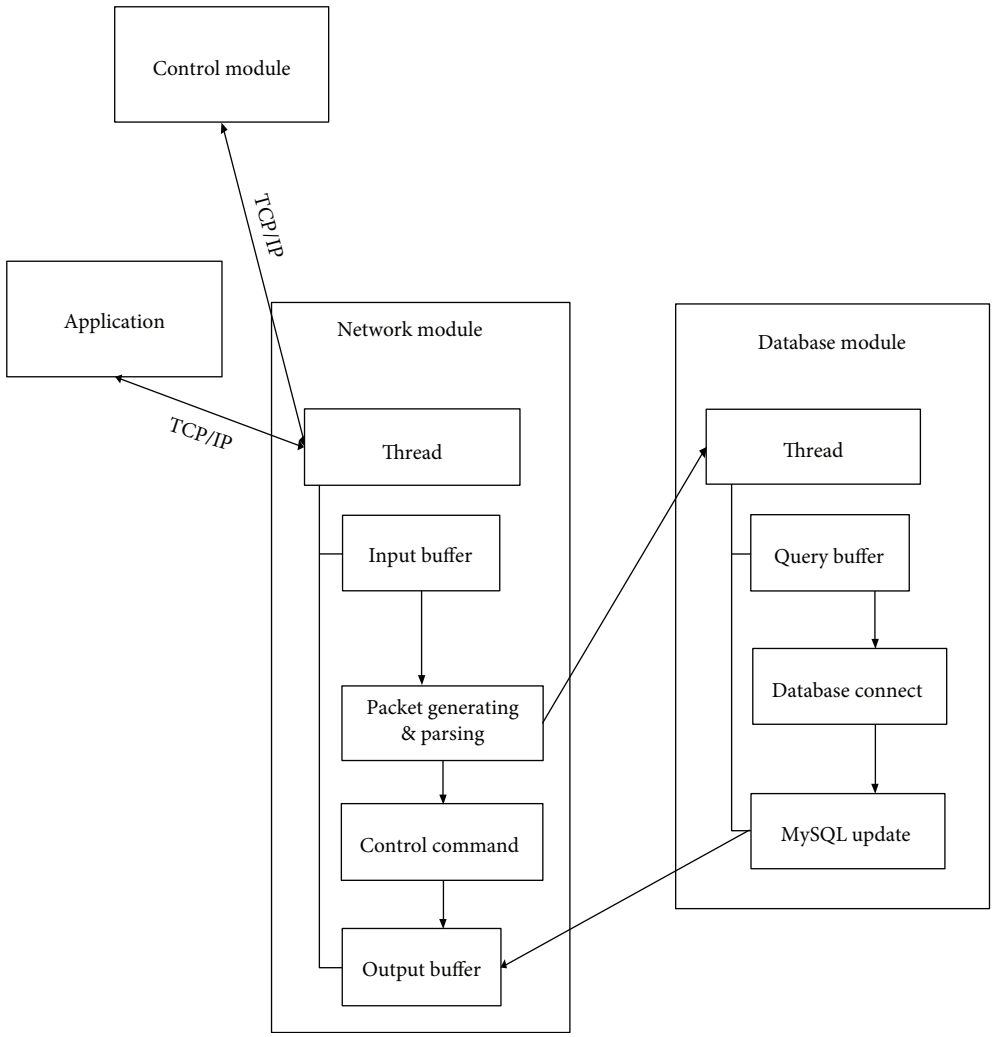

Figure 9: Server architecture proposed by Yeo et al. [46].

Companies? Or government? The problem should be addressed, but again if it is addressed too strictly, it can slow down innovations. Also, it is important to improve the understanding of big data usage. It is necessary to systematically promote the concept, its practical use, necessity, and value of use by expanding the education and sensitization of big data utilization [8].

5.5. Cost and Investment. Investing in the technology should not only make things easier to do but also help in increasing the return. Reduced cost increases the willingness to embrace the technology. Therefore, the cost of sensing systems and ICTs needs to be reduced, and their use needs to be financially sustainable. Farmers should be briefed about the economic consequences before and after the use of the technology [51].

5.6. Multidiscipline Collaboration. Not only through sensors technology and ICT but also many issues in the agriculture can be approached from various other disciplines. They can offer better solutions, enhance productivity, and provide other insights that agriculture scientists and other concerned parties might have overlooked. Collaboration and cooperation among experts from different fields will help in the betterment of the agricultural industry.

6. Discussions and Conclusions

In this paper, we presented a broad overview of the use of various sensors and data analytic techniques used in the area of agriculture. We divided the agriculture into five different subfields and reviewed on the state-of-the-art technology and research trends associated with each subfields. Sensor technologies especially IoTs and smart sensors have led to the exponential growth in sensor-based applications in agriculture. Our survey found the application of AI-based data analytics to be very active as many research was focused on these areas. As agriculture is becoming more data-intensive, these improvements in the technology have helped in the advancement of the area of agriculture. Many challenges still remain as we discussed in the "Challenge and Future work direction" section. However, at large, positive trends were identified, and we conclude that as sensors and data analytic techniques improve, it will bring more insights in solving a wide variety of agricultural issues.

Conflicts of Interest

The authors declare that there are no conflicts of interest regarding the publication of this paper.

Acknowledgments

This work is a part of a research project (1801000664) supported by the National Research Foundation of Korea. The authors also would like to thank Dr. R. P. Tasho and the reviewers for their suggestions on improving the quality of this paper.

References

[1] N. Alexandratos and J. Bruinsma, "World agriculture towards 2010/2050," in *The 2012 Revision*, , pp. 1–3, Food and Agriculture Organization of the United Nations, 2012, Chapter 1.

[2] T. Ojha, S. Misra, and N. S. Raghuwanshi, "Wireless sensor networks for agriculture: the state-of-the-art in practice and future challenges," *Computers and Electronics in Agriculture*, vol. 118, pp. 66–84, 2015.

[3] T. Ojha, S. Misra, and N. S. Raghuwanshi, "Sensing-cloud: leveraging the benefits for agricultural applications," *Computers and Electronics in Agriculture*, vol. 135, pp. 96–107, 2017.

[4] Y. Zhao, L. Gong, Y. Huang, and C. Liu, "A review of key techniques of vision-based control for harvesting robot," *Computers and Electronics in Agriculture*, vol. 127, pp. 311–323, 2016.

[5] B. Zion, "The use of computer vision technologies in aquaculture – a review," *Computers and Electronics in Agriculture*, vol. 88, pp. 125–132, 2012.

[6] S. J. C. Janssen, C. H. Porter, A. D. Moore et al., "Towards a new generation of agricultural system data, models and knowledge products: Information and communication technology," *Agricultural Systems*, vol. 155, pp. 200–212, 2017.

[7] J. W. Kruize, J. Wolfert, H. Scholten, C. N. Verdouw, A. Kassahun, and A. J. M. Beulens, "A reference architecture for farm software ecosystems," *Computers and Electronics in Agriculture*, vol. 125, pp. 12–28, 2016.

[8] S. Wolfert, L. Ge, C. Verdouw, and M. J. Bogaardt, "Big data in smart farming- a review," *Agricultural Systems*, vol. 153, pp. 69–80, 2017.

[9] Y. Lan, S. Chen, and K. F. Bradley, "Current status and future trends of precision agricultural aviation technologies," *International Journal of Agricultural and Biological Engineering*, vol. 10, no. 3, pp. 1–17, 2017.

[10] C. Driemeier, L. Y. Ling, G. M. Sanches, A. O. Pontes, P. S. G. Magalhaes, and J. E. Ferreira, "A computational environment to support research in sugarcane agriculture," *Computers and Electronics in Agriculture*, vol. 130, pp. 13–19, 2016.

[11] C. Yang, J. H. Everitt, Q. du, B. Luo, and J. Chanussot, "Using high-resolution airborne and satellite imagery to assess crop growth and yield variability for precision agriculture," *Proceedings of the IEEE*, vol. 101, no. 3, pp. 582–592, 2013.

[12] F. Edwards-Murphy, M. Magno, P. M. Whelan, J. O'Halloran, and E. M. Popovici, "B+WSN: smart beehive with preliminary decision tree analysis for agriculture and honey bee health monitoring," *Computers and Electronics in Agriculture*, vol. 124, pp. 211–219, 2016.

[13] H. Wimmer and L. M. Powell, "A comparison of open source tools for data science," in *Proceedings of the Conference on Information Systems Applied Research*, vol. 8, pp. 4–12, Wilmington, NC, USA, 2015.

[14] Z. Liqiang, Y. Shouyi, L. Leibo, Z. Zhen, and W. Shaojun, "A crop monitoring system based on wireless sensor network," *Procedia Environmental Sciences*, vol. 11, pp. 558–565, 2011.

[15] A. Sivasankari and S. Gandhimathi, "Wireless sensor based crop monitoring system for agriculture using Wi-fi network dissertation," *International Journal of Computer Science and Information Technology Research*, vol. 2, pp. 293–303, 2014.

[16] K. Y. Bendigeri and J. D. Mallapur, "Advanced remote monitoring of a crop in agriculture using wireless sensor network topologies," *International Journal of Electronics and Communication Engineering & Technology*, vol. 6, pp. 30–38, 2015.

[17] T. Dong, J. Liu, B. Qian et al., "Deriving maximum light use efficiency from crop growth model and satellite data to improve crop biomass estimation," *IEEE Journal of Selected topics in Applied Earth observations and Remote sensing*, vol. 10, no. 1, pp. 104–117, 2017.

[18] Y. Ge, G. Bai, V. Stoerger, and J. C. Schnable, "Temporal dynamics of maize plant growth, water use, and leaf water content using automated high throughput RGB and hyperspectral imaging," *Computers and Electronics in Agriculture*, vol. 127, pp. 625–632, 2016.

[19] K. S. Veum, K. A. Sudduth, R. J. Kremer, and N. R. Kitchen, "Sensor data fusion for soil health assessment," *Geoderma*, vol. 305, pp. 53–61, 2017.

[20] J. A. Enokela and T. O. Othoigbe, "An automated greenhouse control system using Arduino prototyping platform," *Australian Journal of Engineering Research*, vol. 1, no. 1, pp. 64–73, 2015.

[21] V. S. Jahnavi and S. F. Ahamed, "Smart wireless sensor network for automated greenhouse," *IETE Journal of Research*, vol. 61, no. 2, pp. 180–185, 2015.

[22] A. Salleh, M. K. Ismail, N. R. Mohamad, M. A. Aziz, M. A. Othman, and M. H. Misran, "Development of greenhouse monitoring uisng wireless sensor network through Zigbee technology," *International Journal of Engineering Science Invention*, vol. 2, pp. 2319–6734, 2013.

[23] R. Pahuja, H. K. Verma, and M. Uddin, "A wireless sensor network for greenhouse climate control," *IEEE Pervasive Computing*, vol. 12, no. 2, pp. 49–58, 2013.

[24] K. A. Eldhose, R. Antony, P. K. Mini, M. N. Krishnapriya, and M. S. Neenu, "Automated greenhouse monitoring system," *International Journal of Engineering and Innovative Technology*, vol. 3, pp. 164–166, 2014.

[25] J. Y. Kim and D. M. Glenn, "Measurement of photosynthetic response to plant water stress using a multi-modal sensing system," *Transactions of the ASABE*, vol. 58, no. 2, pp. 233–240, 2015.

[26] L. Tian, Q. Meng, L. Wang, and J. Dong, "A study on crop growth environment control system," *International Journal of Control and Automation*, vol. 7, no. 9, pp. 357–374, 2014.

[27] B. Basnet, I. Lee, M. Noh, H. Chun, A. Jaffari, and J. Bang, "An smart greenhouse automation system applying moving average algorithm," *The Transactions of The Korean Institute of Electrical Engineers*, vol. 65, no. 10, pp. 1755–1760, 2016.

[28] J. Rose, A. Kicherer, M. Wieland, L. Klingbeil, R. Töpfer, and H. Kuhlmann, "Towards automated large-scale 3D phenotyping of vineyards under field conditions," *Sensors*, vol. 16, no. 12, pp. 2–15, 2016.

[29] J. R. Millan-Almaraz, I. Torres-Pacheco, C. Duarte-Galvan et al., "FPGA-based wireless smart sensor for real-time photosynthesis monitoring," *Computers and Electronics in Agriculture*, vol. 95, pp. 58–69, 2013.

[30] A. Aydin, "Using 3D vision camera system to automatically assess the level of inactivity in broiler chickens," *Computers and Electronics in Agriculture*, vol. 135, pp. 4–10, 2017.

[31] C. Hongqian, H. Xin, T. Guanghui et al., "Cloud-based data management system for automatic real-time data acquisition from large-scale laying-hen farms," *International Journal of Agricultural & Biological Engineering*, vol. 9, no. 4, pp. 106–115, 2016.

[32] P. K. M. Nkwari, S. Rimer, and B. S. Paul, "Cattle monitoring system using wireless sensor network in order to prevent cattle rustling," in *IST-Africa 2014 Conference Proceedings*, Le Meridien Ile Maurice, Mauritius, May 2014.

[33] C. Manteuffel, E. Hartung, M. Schmidt, G. Hoffmann, and P. C. Schon, "Online detection and localisation of piglet crushing using vocalisation analysis and context data," *Computers and Electronics in Agriculture*, vol. 135, pp. 108–114, 2017.

[34] Z. Feiyang, H. Yueming, C. Liancheng, G. Lihong, D. Wenjie, and W. Lu, "Monitoring behavior of poultry based on RFID radio frequency network," *International Journal of Agricultural and Biological Engineering*, vol. 9, no. 6, pp. 139–147, 2016.

[35] J. F. Odoux, P. Aupinel, S. Gateff, F. Requier, M. Henry, and V. Bretagnolle, "ECOBEE: a tool for long-term honey bee colony monitoring at the landscape scale in West European intensive agroecosystems," *Journal of Apicultural Research*, vol. 53, no. 1, pp. 57–66, 2015.

[36] F. E. Murphy, E. Popovici, P. Whelan, and M. Mango, "Development of an heterogeneous wireless sensor network for instrumentation and analysis of beehives," in *2015 IEEE International Instrumentation and Measurement Technology Conference (I2MTC) Proceedings*, Pisa, Italy, May 2015.

[37] D. W. Fitzgerald, F. E. Murphy, W. M. D. Wright, P. M. Whelan, and E. M. Popovici, "Design and development of a smart weighing scale for beehive monitoring," in *2015 26th Irish Signals and Systems Conference (ISSC)*, Carlow, Ireland, June 2015.

[38] A. Kviesis, A. Zacepins, M. Durgun, and S. Tekin, "Application of wireless sensor networks in precision apiculture," *Engineering for Rural Development*, vol. 20, pp. 440–445, 2015.

[39] S. Gil-Lebrero, F. J. Quiles-Latorre, M. Ortiz-López, V. Sánchez-Ruiz, V. Gámiz-López, and J. J. Luna-Rodríguez, "Honey bee colonies remote monitoring system," *Sensors*, vol. 17, p. 55, 2017.

[40] L. Hongpin, L. Guanglin, P. Weifeng, S. Jie, and B. Qiuwei, "Real-time remote monitoring system for aquaculture water quality," *International Journal of Agricultural and Biological Engineering*, vol. 8, no. 6, pp. 136–143, 2015.

[41] M. M. Saberioon and P. Cisar, "Automated multiple fish tracking in three-dimension using a structured light sensor," *Computers and Electronics in Agriculture*, vol. 121, pp. 215–221, 2016.

[42] D. S. Simbeye, J. Zhao, and S. Yang, "Design and deployment of wireless sensor networks for aquaculture monitoring and control based on virtual instruments," *Computers and Electronics in Agriculture*, vol. 102, pp. 31–42, 2014.

[43] C. Zhou, B. Zhang, K. Lin et al., "Near-infrared imaging to quantify the feeding behavior of fish in aquaculture," *Computers and Electronics in Agriculture*, vol. 135, pp. 233–241, 2017.

[44] Korea Rural Economic Institute, *Agriculture in Korea*, 2015.

[45] H. S. Koo, J. H. Min, and J. Y. Park, "2015 electronics and telecommunications trends," in *Survey of ICT-Agriculture Convergence*, ETRI, 2014.

[46] U.-h. Yeo, I.-b. Lee, K.-s. Kwon et al., "Analysis of research trend and core technologies based on ICT to materialize smart-farm," *Protected Horticulture and Plant Factory*, vol. 25, no. 1, pp. 30–41, 2016.

[47] H. J. Kim, "Development of a moving monitor system for growing crops and environmental information in green house," *The Journal of Korea Institute of Information, Electronics, and Communication Technology*, vol. 9, no. 3, pp. 285–290, 2016.

[48] B. R. Prasad and S. Agarwal, "Comparative study of big data computing and storage tools: a review," *International Journal of Database Theory and Application*, vol. 9, no. 1, pp. 45–66, 2016.

[49] S. G. Dutia, *Agtech: Challenges and Opportunities for Sustainable Growth*, Ewing Marion Kauffman Foundation, 2014.

[50] T. H. M. d. Oliveira, M. Painho, V. Santos, O. Sian, and A. Barriguinha, "Development of an agricultural management information system based on open-source solutions," *Procedia Technology*, vol. 16, pp. 342–354, 2014.

[51] K. Sabarina and N. Priya, "Lowering data dimensionality in big data for the benefit of precision agriculture," in *International Conference on Intelligent Computing, Communication & Convergence*, Odisha, India, 2015.

Hindawi
Journal of Sensors
Volume 2018, Article ID 5231810, 7 pages
https://doi.org/10.1155/2018/5231810

Research Article

Applicability of a 3D Laser Scanner for Characterizing the Spray Distribution Pattern of an Air-Assisted Sprayer

F. Javier García-Ramos, Alfredo Serreta, Antonio Boné, and Mariano Vidal

Escuela Politécnica Superior, University of Zaragoza, C/Cuarte, s/n, 22004 Huesca, Spain

Correspondence should be addressed to F. Javier García-Ramos; fjavier@unizar.es

Received 10 May 2018; Accepted 2 August 2018; Published 12 September 2018

Academic Editor: Annachiara Berardinelli

Three-dimensional (3D) laser technology has been tested for assessing the performance of air-assisted spraying. A static test using an air-assisted sprayer equipped with two axial fans (front and back) with opposing directions of rotation was developed. The sprayer was adjusted to spread water in a static mode, at a pressure of 10 bars, with four air volumetric flow rates. Measurements were performed using a Leica HDS6000 3D laser scanner. In addition, the flow and velocity of air generated by the air-assisted sprayer were measured using a hot-wire anemometer and a 3D sonic anemometer with the objective of estimating the influence of air flow on the spatial distribution of spray droplets. To carry out the analysis, all of the droplets detected by the laser were considered to be of the same size. The distribution of products was asymmetric when the machine only worked with the back fan, with 41% of the product distributed on the left side versus 59% on the right side, as referenced to the direction of the machine's advance. This asymmetry was corrected when the machine functioned with the two fans activated. These spray data were concordant with the measured air flow generated by the machine in the different working conditions. For the different regulation settings of the machine, taking the vertical of the machine as 0°, the angular region comprised between 40° and 60° was the one that received the highest quantity of product. The increase of the air flow produced a greater distance of the product. For the highest air flow configuration, 99% of the product detected by the laser was detected within a distance of 16 m from the axis of the machine.

1. Introduction

Air-assisted sprayers used in fruit production must be carefully and effectively regulated to ensure that crops are successfully treated. Four main factors affect the deposition efficiency [1, 2]: the nozzle type, fluid pressure, ground speed, and volumetric flow rate of the air. The combination of these parameters determines the applied volume rate. This factor directly influences the quality of the treatment [3].

The use of experimental methods to characterize the product distribution by a sprayer would be difficult and expensive [4]. The characteristics of the plume generated by the sprayer can be simulated by applying integrated computational fluid dynamics (CFD) [5, 6]. However, experimental methods are required to validate such simulations and to determine two critical physical features: first, the deposition of the product as a function of distance, which is related to the spray drift, and second, the product distribution in the vicinity of the machine, which must be in accordance with the position and geometry of the tree to be treated.

To determine the deposition of the product as a function of distance, quantification tests of the deposition are required through the use of collector elements. Distance of deposition defines the spray drift which is considered as the main source of contamination of pesticide applications in tree crops [7]. Currently, spray drift is measured based on the use of collector elements according to international standards [8]. Alternatively, various technologies can be implemented: laser techniques to obtain the droplet size spectrum and testing with wind tunnels are comparable technologies to predict the field spray deposition [9]. From such measurements, it was reported in [7] that the percentage of deposition in the

ground is reduced exponentially with distance. For this goal, four types of nozzles were tested, both in a wind tunnel and in an axial sprayer working in a citrus orchard.

The pattern of spray deposition is affected by droplet size and air flow. Droplets in flight are often measured using laser-based spatial (number-density weighted) and temporal (number-flux weighted) techniques [10].

The distribution of the spray in the vicinity of the sprayer is often estimated by measuring the air flow generated by the fans. In this sense, the air flow generated by the sprayer can be characterized using high-precision anemometers such as sonic anemometers (two-dimensional or three-dimensional) which are used to measure the velocity components for different heights, sections, and distances from the sprayer [11, 12].

Laser technology has been used successfully to measure the tree canopy geometry in real time with the goal of implementing variable application rate techniques [13–17]; in these measurements, the sensor is embedded on the tractor that performs the crop treatment. Furthermore, laser technology allows real-time monitoring of airborne spray drift, obtaining range-resolved images of the spray plume while requiring fewer personnel and consuming less time than traditional methods, as in the case of light detection and ranging (LIDAR) technology [18]. This technology has been successfully applied to measure the pesticide plumes in fruit orchards [5].

Another application of laser technology is its use in validating equipment design and for analysis of different regulations prior to field trials, as a validation tool for the design of the manufactured prototypes. In this case, the laser can be used statically to analyze the distribution of the product [19].

In conclusion, methodologies used to measure the spray drift and the spray distribution are expensive, time consuming and, in many cases, not practical for the manufacturer's day-to-day tests. For these tests, manufacturers require rapid measurement methods with a reasonable precision to test different configurations of their machines, which, in most cases, have been previously simulated through the use of computational fluid dynamics (CFD). Therefore, an easy estimation of the spray plume generated in the vicinity of the sprayer (maximum distance of deposition of the product and its spatial distribution) for a specific configuration of air flow, nozzle pressure, and nozzle orientation would be of great help to validate key design parameters of the sprayer such as nozzle position, nozzle type, air conducts geometry, and fan regulation.

The present study is aimed at analyzing the viability of using three-dimensional (3D) laser scanner technology to assess the effectiveness of an air-assisted sprayer used in fruit orchards in terms of the two aforementioned critical criteria: the deposition of the product as a function of distance and the product distribution in the vicinity of the machine.

2. Materials and Methods

2.1. Instrumentation. The operation of an air-assisted sprayer equipped with two reversed-rotation axial fans (Gar-melet S.L., Huesca, Spain), one placed behind the tank and the other placed in front, was analyzed. The diameter of the front fan was 800 mm and that of the back fan was 830 mm. When viewed from the tractor, the front fan spins anticlockwise and the rear fan clockwise. Each fan sucks air axially from the outer area of the machine and expels it radially (Figure 1).

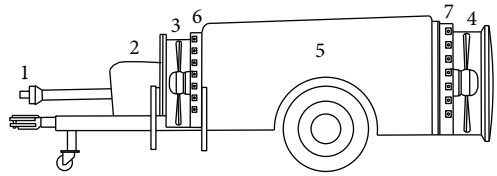

Figure 1: Air-assisted sprayer equipped with two reversed-rotation axial fans (1: PTO; 2: pump; 3: front fan; 4: rear fan; 5: tank; 6: front nozzles; 7: rear nozzles).

Figure 2: Leica HDS6000 3D laser scanner. (a) Global view; (b) relative position of laser and sprayer during testing.

A Leica HDS6000 3D laser scanner (Figure 2) was used to assess the functioning of this sprayer. The 3D laser scanner [19] consists of a pulsed, high-speed laser scanner, with survey-grade accuracy, range, and field of view. It uses a visible green laser beam, with a range of 150–300 m, depending on surface conditions. According to the manufacturer's specifications, the spatial accuracy is 4 mm. The instrument includes a digital camera, which is used to visually determine the region to be scanned in spherical coordinates.

During the scan, the instrument head automatically rotates while a mirror oscillates in the vertical direction. Both movements can be programmed to cover the selected area with user-specified vertical and horizontal angular steps. The angular accuracy (vertical and horizontal) is 60 μrad. Scanner operations were controlled by a computer, where job specifications were set and data were received and stored. The time required to complete a scanning job depends on the extent of the selected region and on the survey point density.

Under the experimental conditions used in the present study, the equipment surveyed about 1500 points s-1. The laser spot varies according to the distance; at a distance of 50 m, the laser spot is 4 mm in diameter. To detect a particle, the laser scanner must receive about 35% of the emitted energy. Because of this fact, the density of the cloud of drops present in the laser spot affects the sensitivity of the measurement. Tests carried out using LIDAR sensors have shown the difficulty of the laser beam to impact on a less dense cloud, even if these droplets have bigger size [20]. This might result in an underestimation of the amount of droplets at the far end.

Table 1: Air flows generated by the sprayer with different configurations of settings and PTO working at 540 rpm.

Activated fans	Fan gear box setting	Blade setting	Air flow (m^3/h)
Back	Low	3	31,981
		4.5	37,624
Back	High	3	38,654
		4.5	42,831
Back	Low	3	31,981
Front	Low	3	26,635

The scanner registers Cartesian coordinates of the laser reflection point. The precision of the scanner was adjusted such that at a distance of 30 m, data would be recorded every 20 mm. The scanned area was defined through a rectangular window.

Back and front fans can be regulated, in a range labelled 1–5, to supply different air flows from rotating fan blades. The air flows in the present study were measured according to the method given in [21], considering two settings of the fan blade regulation: 3 and 4.5. The air flow corresponding to the back fan was measured at its inlet, using a TESTO 0635 1041 hot-wire anemometer (accuracy 0.03 m/s; range 0–20 m/s). The air flow rate of the front fan was measured at the outlet of the fan because of the presence of the power take off (PTO) of the tractor. Measurements were carried out with the PTO working at 540 rpm.

In addition, the velocity of the air generated by the sprayer was measured in the absence of any wind using a WindMaster 3D sonic anemometer (Gill Instruments, UK) according to the methodology developed by [11]. The accuracy of the sonic anemometer was 1.5% (for wind speeds of up to the maximum measurable value) with an air velocity range of 0 to 45 m/s and a resolution of 0.01 m/s. The air velocity data was recorded at a frequency of 1 Hz. Measurements were carried out with the sprayer static, establishing the same regulations of the fans as those that were selected for the laser tests. The air velocity was measured, based on previous research [22], in the plane corresponding to the back fan of the sprayer. Measurements were made on both sides of the machine at 1.5, 2.5, and 3.5 m from the center of the sprayer for several heights: 1, 2, 3, and 4 m.

2.2. Measurements of Spraying Distribution. Laser measurements were carried out with the sprayer static, establishing three regulations of the fans (Table 1). The sprayer was equipped with 32 Albuz ATR 80° orange nozzles, 16 at the rear and 16 at the front. Tests were carried out at a pressure of 10 bars (1, 39 L/min per nozzle). For each configuration, the laser performed one complete scan.

The droplets (or group of droplets) detected by the laser scanner in each test, referenced with Cartesian coordinates (x, y, z), were transformed to polar coordinates (V, φ, θ) according to Figure 3, using the center of the rear fan of the sprayer as the center of the coordinate system.

The sprayer was positioned so that the rear fan coincided with the xz plane. In this frame of reference, the machine was aligned with the y-axis, so that the tractor was placed in a positive section of that axis and the rear fan of the machine was at the 0 coordinate of the y-axis. The laser was aligned with the machine and located in the negative section of the y-axis, at a distance of 12 m and at a height of 5 m above the sprayer (Figure 2).

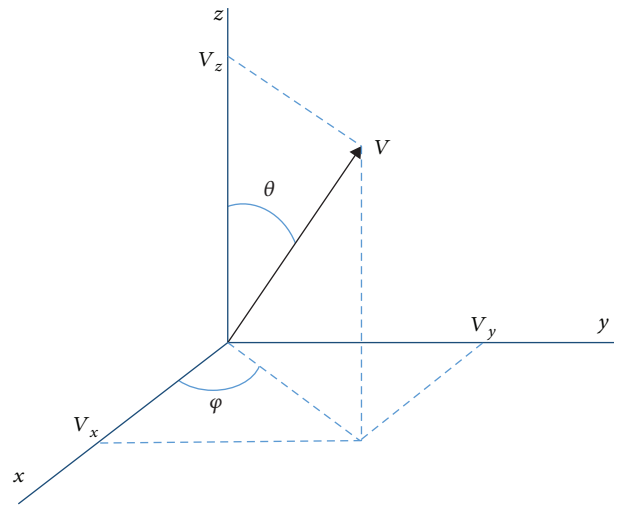

Figure 3: Polar coordinates versus Cartesian coordinates.

Tests carried out on sprayers using LIDAR technology, which has common characteristics to the one used in this test, have shown that measurements cannot be linked to droplet size [23]. In this sense, the 3D scanner cannot differentiate the size of the drops detected. All the drops detected by the laser were considered, as an approximation, to be the same size. Therefore, quantification of products present in the different areas of the 3D space was obtained by counting the number of drops present in each zone.

Considering all drops of the same size requires prior analysis to correctly interpret the information provided by the laser. The droplet population generated by a nozzle presents a great variability in sizes and, at the same time, is conditioned by the working pressure. Among the various parameters used in characterizing the range of droplet sizes in a spray, the most commonly used is the volumetric median diameter (VMD or D50). Additionally, relative span is an indicator of the distribution uniformity. Larger droplets are deposited at a closer distance than smaller ones that are more susceptible to drift. For a specific air velocity, the percentage of product deposited at a given distance is related to an inverse function with D50 [24], being higher for small-diameter droplets.

In order to establish direct correlations between the information supplied by the laser and the volume of product applied at different distances, it would be necessary to carry out quantification tests to collect the quantity of product deposited in different areas near the sprayer. In this article, a first step has been taken to demonstrate the feasibility of the 3D scanner technique in providing relevant information. However, the authors plan to carry out quantification trials in the future in order to obtain complete information to establish precise models for estimating product deposition from the information provided by the laser.

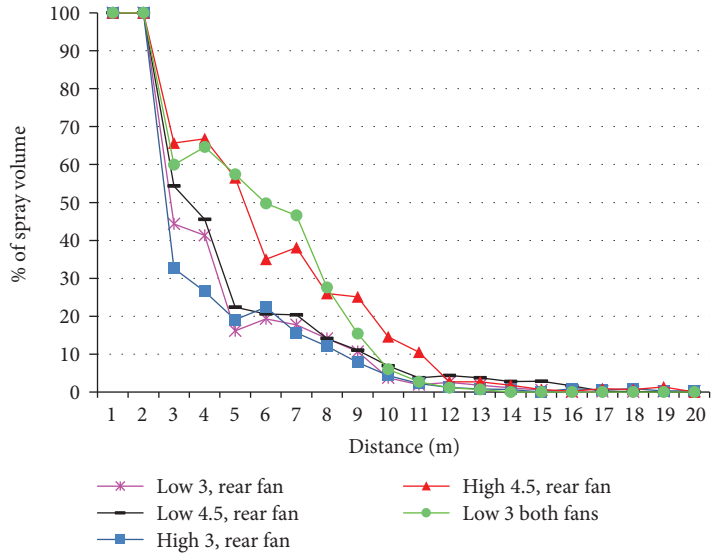

Figure 4: Percentage of spray volume detected by the laser within circular crowns of 1 m width for five air flow regulation settings.

Analysis of the experimental data has been carried out leading to three key results: (1) spray deposition as a function of the distance from the machine, (2) symmetry of spray distribution, and (3) spray distribution in angular sectors in a plane (rear fan) perpendicular to the longitudinal axis of the machine.

3. Results and Discussion

3.1. Spray Deposition as a Function of the Distance to the Machine. Considering the center of the rear fan as the coordinate axis, the amount of product applied by the sprayer in circular crowns of 1 m in width was measured.

This methodology allowed the analysis of the spray deposition distance as a function of the regulation of the sprayer. A 100% output of the product from the nozzles was assumed, and using this, the percentage of product that reached the volume of each circular crown was computed.

Figure 4 represents the percentage of product applied as a function of distance for each of the selected regulation settings of the machine. Observing this figure, it becomes clear that the laser technique allows determination of the spray deposition as a function of distance and the quantity of product that reaches distances greater than 16 m was found to be less than 1%. This technique, therefore, should facilitate the establishment of safety distances for the application of phytosanitary products as a function of the regulation of the sprayer.

Moreover, Figure 4 illustrates that the distance of spray deposition varies with regulation of the machine, showing that the air flow directly affects the reach of the sprayer. It can also be seen that the use of two fans allows a greater overall reach of the machine, for the same position of the fan blades (position 3). This fact reveals the interaction between the air flow emitted by the rear fan and that emitted by the front fan.

Results were concordant with those obtained using other methodologies. In [7], the authors report curves of

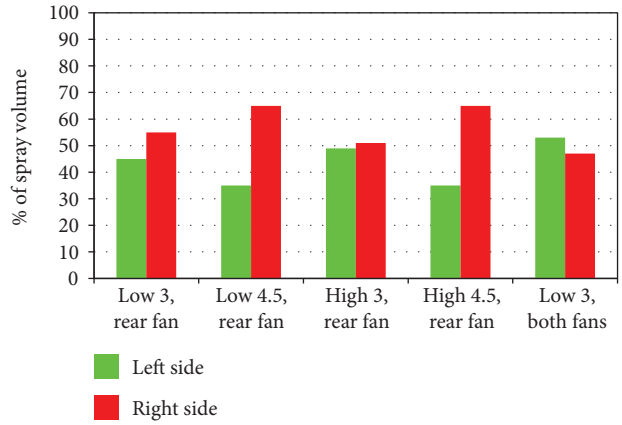

Figure 5: Percentage of spray volume detected by the laser on the right and left sides of the sprayer.

sedimenting deposit as percentage of sprayed volume with structures similar to those of Figure 4 (values decreased with distance) from analysis of 10 types of nozzles (5 Albuz ATR 80 Grey and 5 Albuz TVI 8003 Blue) in a wind tunnel and also as validated in field trials. In the same line, [25] reports values of deposition decreasing with the distance via an acquisition device and a pesticide deposition optical measurement system with an air-assisted spraying system.

3.2. Symmetry of Spray Distribution. The axial fans, due to their direction of rotation, distribute the air flow with some asymmetry, usually applying greater volume of air to the area coincident with the direction of rotation. This fact produces an asymmetry in the spray distribution.

Laser technology was used to assess the symmetry of the spray distribution by quantifying the amount of product applied by the machine to the left and right sectors.

For the data shown in Figure 5, we designate the "right sector" as the one located to the right of the direction of the

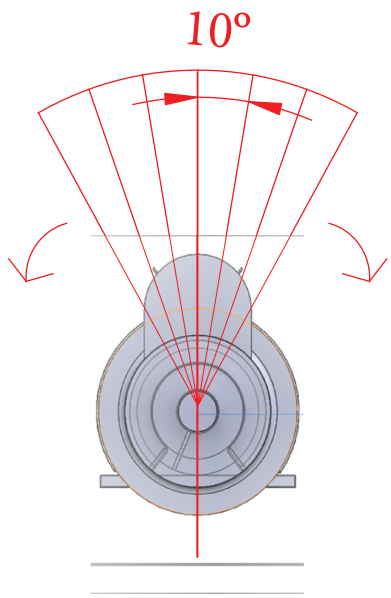

Figure 6: Angular sectors used in the analysis of spray direction.

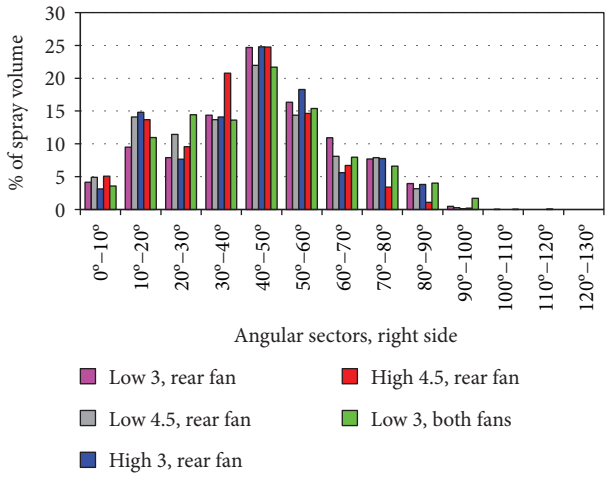

Figure 7: Percentage of spray volume for each angular sector for the right side of the sprayer.

advance of the machine. The rear fan of the machine rotates clockwise from the perspective of an observer located at the rear of the machine. Therefore, considering the forward direction of the machine, the rear fan rotates clockwise, theoretically releasing more air to the row of trees located to the right of the advance of the machine.

These results were concordant with those shown in [11], which reported the assessment of the function of a similar sprayer. The asymmetry of the spray distribution was greater working at a blade setting of 4.5 in comparison with a blade setting of 3. The use of two fans with inverted rotation corrected the asymmetry, showing that a design consisting of two fans with opposing rotation improves the homogeneity of the treatment.

3.3. Spray Distribution in Angular Sectors. The amount of products applied by the sprayer in angular sectors of a plane

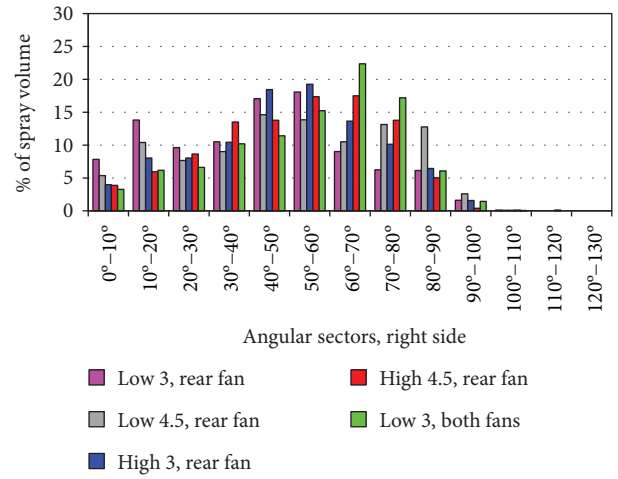

Figure 8: Percentage of spray volume for each angular sector for the left side of the sprayer.

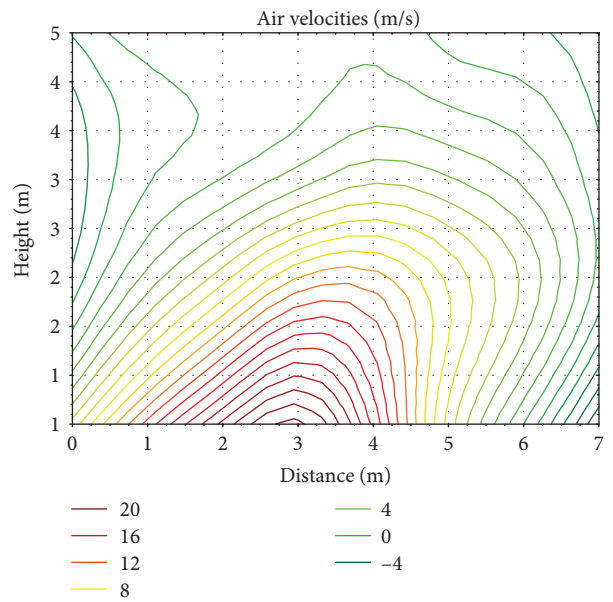

Figure 9: Magnitude of air velocity at the plane of the back fan of the sprayer from 3D anemometer measurements, obtained with the sprayer in a low gear and with a blade setting of 4.5.

located at the rear fan was analyzed. For this goal, angular sectors of 10° were used for the left and right sides of the machine, considering the vertical as 0° (Figure 6). The center of the fan was located at 900 mm above the ground.

Figures 7 and 8 show the distribution of spray in the different angular sectors. On both the left and right sides, the greatest amount of product was distributed in the angular sector between 40° and 60°. Considering the geometry of a fruit tree and the designed function of the sprayer, this result is quite logical, because the largest amount of product is directed to the area of greatest vegetation.

According to this result, the laser technique is a useful tool to regulate correctly the position of the nozzles and the direction of the air flow generated by the fans, with the aim

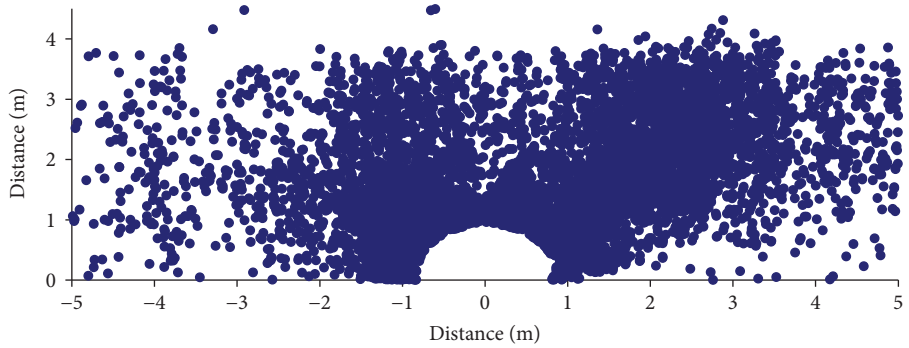

Figure 10: Droplets detected by the laser scanner in the plane of the back fan of the sprayer functioning in a low gear and with a blade setting of 4.5.

of directing the pesticide to the canopy of the tree, reducing the spray drift and increasing the efficiency of the treatment.

3.4. Spray Volume versus Air Flow. The laser sensor was capable of estimating the spray volume in the different areas surrounding the sprayer. The measured movement of the product detected by the laser was in agreement with the air flow generated by the sprayer. Figure 9 shows the air velocity pattern generated by the back fan of the sprayer, operating with a low gear and a blade setting of 4.5. The air velocities show an asymmetry with higher velocities on the right side of the machine because of the clockwise rotation of the fan. Figure 10 shows the particles of product detected by the laser for the same configuration. The comparison of the air velocity pattern and the spray volume detected by the laser show a clear correlation between both parameters in accordance with previous studies [26, 27], which have shown that the droplets are blown into the fruit tree canopy by the forced air.

The flow rate of liquid supplied by the equipment was constant during all the tests as the working pressure was set at 10 bars. However, when comparing the number of droplets obtained for different air flows, the number of droplets detected at high speed of the fan was 36.8% lower than that at low speed for blade setting 3 and 40.4% lower considering blade setting 4.5. Analyzing the number of droplets detected at a distance of 7 to 12 m, the number of droplets detected at high speed of the fan was 32.7% lower than that at the low one, at blade setting 3, and 53.4% considering blade setting 4.5. These data are consistent with those obtained by [20], which in tests conducted with a LIDAR on board a vehicle detected a greater number of spray droplets for low air flows than for high ones. This fact could also support the fact that the lower the density of the droplet cloud, the greater the difficulty of the laser in determining it, as also it was concluded by [20].

4. Conclusions

The laser technique examined in this study provides useful information on of air-assisted sprayers for evaluating their function with the aim of improving efficiency of application in the field.

Measurements using the laser sensor allowed the quantification of the maximum distance of deposition of the product. Such data facilitates quantification of the risk of drift and, therefore, the risk of contamination of elements adjacent to the treatment plot: water channels, populations, roads, farms, orchards, and so on.

The left-right asymmetry of the spraying can be estimated in a straightforward manner for the different configurations of the fans. Furthermore, the laser allows quantification of the amount of products applied in different areas in the vicinity of the sprayer. The results of this study also showed that information supplied by the laser on the spraying pattern is concordant with the air flow pattern of the sprayer as measured using 3D anemometers.

When considered together, our results indicate that laser technology can be used for the validation of sprayer machine design. Moreover, as the next step, the regulation of the function of the sprayer, depending on the vegetative state of the crop and the geometry of the orchard, can be established and checked. The air flow, air direction, fan setting, pressure, nozzle type, and nozzle position can be optimized using this laser technique.

Data Availability

The "excel spreadsheet format" data used to support the findings of this study may be released upon application to the main author of the research (F. Javier García-Ramos), who can be contacted by email at fjavier@unizar.es or by post mail at Escuela Politécnica Superior, University of Zaragoza., C/Cuarte, s/n, 22004, Huesca, Spain.

Conflicts of Interest

The authors declare that they have no conflicts of interest.

References

[1] M. Farooq, R. Balachandar, D. Wulfshon, and T. M. Wolf, "PA—precision agriculture: agricultural sprays in cross-flow and drift," *Journal of Agricultural Engineering Research*, vol. 78, no. 4, pp. 347–358, 2001.

[2] Y. M. Koo, M. Salyani, and J. D. Whitney, "Spray variable effects on abscission of oranges fruits for mechanical harvesting," *Transactions of the ASAE*, vol. 43, no. 5, pp. 1067–1073, 2000.

[3] J. V. Cross, P. J. Walklate, R. A. Murray, and G. M. Richardson, "Spray deposits and losses in different sized apple trees from an axial fan orchard sprayer: 1. Effects of spray liquid flow rate," *Crop Protection*, vol. 20, no. 1, pp. 13–30, 2001.

[4] D. Dekeyser, A. T. Duga, P. Verboven, A. M. Endalew, N. Hendricks, and D. Nuyttens, "Assessment of orchard sprayers using laboratory experiments and computational fluid dynamics modelling," *Biosystems Engineering*, vol. 114, no. 2, pp. 157–169, 2013.

[5] A. M. Endalew, C. Debaer, N. Rutten et al., "Modelling pesticide flow and deposition from air-assisted orchard spraying in orchards: a new integrated CFD approach," *Agricultural and Forest Meteorology*, vol. 150, no. 10, pp. 1383–1392, 2010.

[6] F. J. García-Ramos, H. Malón, A. Javier Aguirre, A. Boné, J. Puyuelo, and M. Vidal, "Validation of a CFD model by using 3D sonic anemometers to analyse the air velocity generated by an air-assisted sprayer equipped with two axial fans," *Sensors*, vol. 15, no. 2, pp. 2399–2418, 2015.

[7] X. Torrent, C. Garcerá, E. Moltó et al., "Comparison between standard and drift reducing nozzles for pesticide application in citrus: part I. Effects on wind tunnel and field spray drift," *Crop Protection*, vol. 96, pp. 130–143, 2017.

[8] ISO 22866, 2005, *Equipment for Crop Protection - Methods for Field Measurement of Spray Drift*, International Organization for Standardization, Geneva, Switzerland, 2000.

[9] D. Nuyttens, M. De Schampheleire, K. Baetens, and B. Sonck, "Comparison of different drift risk assessment means," *Aspects of Applied Biology*, vol. 84, 2008.

[10] E. Hilz and A. W. P. Vermeer, "Spray drift review: the extent to which a formulation can contribute to spray drift reduction," *Crop Protection*, vol. 44, pp. 75–83, 2013.

[11] F. J. García-Ramos, M. Vidal, A. Boné, H. Malón, and J. Aguirre, "Analysis of the air flow generated by an air-assisted sprayer equipped with two axial fans using a 3D sonic anemometer," *Sensors*, vol. 12, no. 6, pp. 7598–7613, 2012.

[12] F. Lebeau, A. Verstraete, C. Stainier, and M. F. Destain, "RTDrift: a real time model for estimating spray drift from ground applications," *Computers and Electronics in Agriculture*, vol. 77, no. 2, pp. 161–174, 2011.

[13] S. D. Tumbo, M. Salyani, J. D. Whitney, T. A. Wheaton, and W. M. Miller, "Investigation of laser and ultrasonic ranging sensors for measurements of citrus canopy volume," *Applied Engineering in Agriculture*, vol. 18, no. 3, pp. 367–372, 2002.

[14] P. Balsari, G. Doruchowski, P. Marucco, M. Tamagnone, J. C. van de Zande, and M. Wenneker, "A system for adjusting the spray application to the target characteristics," *Agricultural Engineering International CIGR*, vol. 10, pp. 1–11, 2008.

[15] J. Llorens, E. Gil, J. Llop, and A. Escolà, "Ultrasonic and LIDAR sensors for electronic canopy characterization in vineyards: advances to improve pesticide application methods," *Sensors*, vol. 11, no. 2, pp. 2177–2194, 2011.

[16] P. Berk, M. Hocevar, D. Stajnko, and A. Belsak, "Development of alternative plant protection product application techniques in orchards, based on measurement sensing systems: a review," *Computers and Electronics in Agriculture*, vol. 124, pp. 273–288, 2016.

[17] H. Liu and H. Zhu, "Evaluation of a laser scanning sensor in detection of complex-shaped targets for variable-rate sprayer development," *Transactions of the ASABE*, vol. 59, no. 5, pp. 1181–1192, 2016.

[18] E. Gregorio, J. R. Rosell-Polo, R. Sanz et al., "LIDAR as an alternative to passive collectors to measure pesticide spray drift," *Atmospheric Environment*, vol. 82, pp. 83–93, 2014.

[19] F. J. García-Ramos, A. Boné, A. Serreta, and M. Vidal, "Application of a 3-D laser scanner for characterising centrifugal fertiliser spreaders," *Biosystems Engineering*, vol. 113, no. 1, pp. 33–41, 2012.

[20] E. Gil, J. Llorens, J. Llop, X. Fàbregas, and M. Gallart, "Use of a terrestrial LIDAR sensor for drift detection in vineyard spraying," *Sensors*, vol. 13, no. 1, pp. 516–534, 2013.

[21] ISO 9898, 2000, *Equipment for Crop Protection—Test Methods for Air-Assisted Sprayers for Bush and Tree Crops*, Geneva, Switzerland, International Organization for Standardization, 2000.

[22] A. de Moor and J. Langenakens, "Dynamic air velocity measurements of air-assisted sprayers in relation to static measurements," *Aspects of Applied Biology*, vol. 66, pp. 309–322, 2002.

[23] R. Sanz-Cortiella, J. Llorens-Calveras, J. R. Rosell-Polo, E. Gregorio-Lopez, and J. Palacin-Roca, "Characterisation of the LMS200 laser beam under the influence of blockage surfaces. Influence on 3D scanning of tree orchards," *Sensors*, vol. 11, no. 3, pp. 2751–2772, 2011.

[24] J. P. Douzals and M. P. Chalendard, "Vertical and horizontal spray distribution of hollow cone nozzles in a wind tunnel: a preliminary study to mitigate spray drift in orchard applications," in *SuproFruit 2015, 13th Workshop on spray application techniques in fruit growing*, vol. 448, pp. 32–34, Lindau, Germany, July 2015.

[25] Z. Changyuan, Z. Chunjiang, W. Xiu, L. Wei, L. Wei, and Z. Ruixiang, "Nozzle test system for droplet deposition characteristics of orchard air-assisted sprayer and its application," *International Journal of Agricultural and Biological Engineering*, vol. 7, no. 2, pp. 122–129, 2014.

[26] N. Pai, M. Salyani, and R. D. Sweeb, "Regulating airflow of orchard air-blast sprayer based on tree foliage density," *Transactions of the ASABE*, vol. 52, no. 5, pp. 1423–1428, 2009.

[27] F. F. Dai, "Selection and calculation of the blowing rate of air assisted sprayers," *Plant Protection*, vol. 34, no. 6, pp. 124–127, 2008.

Hindawi
Journal of Sensors
Volume 2018, Article ID 8743179, 16 pages
https://doi.org/10.1155/2018/8743179

Research Article

Urban Lawn Monitoring in Smart City Environments

José Marín,[1] Lorena Parra,[2] Javier Rocher,[2] Sandra Sendra,[2,3] Jaime Lloret,[2] Pedro V. Mauri,[4] and Alberto Masaguer[1]

[1]*Universidad Politécnica de Madrid, Calle Ramiro de Maeztu 7, 28040 Madrid, Spain*
[2]*Instituto de Investigación para la Gestión Integrada de Zonas Costeras, Universitat Politècnica de València, C/ Paraninf 1, 46730 Grao de Gandia, Valencia, Spain*
[3]*Departamento de Teoría de la Señal, Telemática y Comunicaciones, ETS Ingenierías Informática y de Telecomunicación, Universidad de Granada, C/ Periodista Daniel Saucedo Aranda, s/n, 18071 Granada, Spain*
[4]*IMIDRA, Finca "El Encin", A-2, Km 38, 2, 28800 Alcalá de Henares, Madrid, Spain*

Correspondence should be addressed to Jaime Lloret; jlloret@dcom.upv.es

Received 7 March 2018; Revised 18 May 2018; Accepted 24 June 2018; Published 19 July 2018

Academic Editor: Martin E. Omaña

Control over water usage for irrigation purposes is a key factor in order to achieve the sustainability in agriculture. The irrigation of urban lawns represents a high percentage of the urban water usage. The use of information and communication technology (ICT) offers the possibility of monitoring the grass state in order to adjust the irrigation regime. In this paper, we propose an Arduino-based system with a camera set on a drone. The drone flies along the garden taking pictures of the grass. Those pictures are processed with a rule-based algorithm that classifies them according to the grass quality. Pictures can be tagged in three categories: high coverage, low coverage, or very low coverage. After designing our algorithm, twelve pictures are used to verify its correct operation. The results show a 100% hit rate. To analyze the suitability of using drones to perform this task, we carried out a comparative study for gardens with different sizes, where the drone and a similar system mounted on a small autonomous vehicle have been used. The results show that, for gardens bigger than 1000 m^2, the use of drone is needed due to the time consumed by the vehicle to cover the entire surface. Finally, we show the results of sending the image information after processing it in different manners.

1. Introduction

Water is a scarce resource; less than 3% of the worldwide water is freshwater, and only 1% is available in rivers, lakes, and aquifers [1] and can be used for irrigation, industry, and human use. However, the increase of water consumers, the floods and droughts due to climate change, and the water pollution endanger the continuity of the current water use models. Efficiency in the use of water is nowadays crucial. The Food and Agriculture Organization of the United Nations (FAO) estimates that in 2050, there will be enough water to ensure food production for the worldwide population. However, poverty and food insecurity will remain in several regions and countries [2]. Nevertheless, water availability can diminish in some areas. For these reasons, it is necessary to promote new techniques to ensure water efficiency is maximized in as many areas as possible. The optimization of irrigation techniques is a vital process to improve sustainability and the rational use of the water in agriculture. Many techniques have been developed for different crops [3]. Most of these techniques are applied in agricultural areas. Nevertheless, urban lawns demand high amount of water, and no technique has been designed for this special issue.

We can define the urban lawns as the group of green areas in the city. These green areas include domestic or private gardens, public gardens, recreational green areas dedicated to sports, and roundabouts. Some of the urban lawns can be only formed by grass while others can have shrubs or trees. In this paper, we focused our efforts on the grass classification for its irrigation, although the shrubs and trees are irrigated by other methods. Thus, it is necessary

to promote precision gardening in order to improve the sustainability in water usage. The use of precision gardening implies the use of information and communication technology (ICT) for monitoring the plots and achieving a more sustainable culture [4]. In smart cities, the monitoring of the water requirements in urban lawns can be used to define the irrigation process. Also, in these cities, many other processes are monitored and it is possible to identify the best moment to irrigate depending on the water and energy use in the grid.

Different technologies can be used for monitoring the grass. The main ones are based on remote sensing systems and the use of drones and wireless sensor networks (WSNs). The use of satellite images for remote sensing is useful for monitoring the changes in the land coverages [5]. Nevertheless, the spatial resolution of the current available images is too low. Nowadays, the highest spatial resolution is offered by the WorldView-4 satellite sensor which has a precision of 1.24 m. This satellite has a period of 4.5 days [6]. However, these characteristics do not fulfil with our needs. For a continuous grass monitoring, we need to monitor the state of the grass at least once per day. In addition, we should consider that some days, cloudy conditions may make the image not useful. Mulla [7] indicates that the use of remote sensing based on satellite images is not useful for precision gardening. The second option is the use of drones with a camera to take pictures of the whole garden. The spatial resolution will depend on the camera's characteristics and on the flight height. In this case, the main disadvantages are that the drone is not able to fly in windy days and the legislation in some countries may limit flights in urban and inhabited areas. The use of drones for monitoring purposes is increasing, and they can be used even for emergency rescue systems [8]. The last option for grass monitoring is the use of wireless sensor networks (WSNs) with RGB sensors [9]. The system is based on one small automated vehicle (SAW) that moves along the garden taking data about the grass coverage with the RGB sensors. However, it is necessary to evaluate the time consumed to cover the garden and estimate the required time in different gardens and its viability. The use of a WSN for environmental monitoring is widely used, and many examples can be found in [10]. For our objectives, satellite remote sensing cannot be used because we need daily control and more precision than the current satellites can offer. The use of soil moisture sensors will not indicate when the grass needs to be replanted. In order to know when it is necessary to plant, we must use sensors that measure the electromagnetic radiation (cameras). The use of sensors based on fixed cameras means that many must be placed, which leads to a bigger cost. For this reason, we need to place the sensors in a vehicle. An airplane is discarded due to high cost of daily flights. Another option is the use of SAW, but this may damage the grass. Therefore, the only option left is the use of a drone.

This paper presents a smart system able to monitor the state of the grass and to decide the irrigation and planting needs. The system is capable of classifying the grass into different categories, that is, high coverage, low coverage, and very low coverage. The proposed system is composed of an Arduino node with a CMOS sensor. Our system is based on the idea developed by [9]. We will verify this system and will compare it with the proposed solution based on a drone. This proposal is part of a bigger study where the images will be locally processed by the drones, and they will only send the tag for a specific area. Thus, this paper will present the design, implementation, and verification of the drone operation and how it collects the pictures. After collecting the images, they will be processed to analyze the color composition, and finally our designed algorithm will classify them. In the next step of our study, it has been planned to add some moisture soil sensors to help us decide the irrigation regime. Our proposal will include the deployment of two moisture sensors placed at 5 meters to the east and west of each sprinkler. The number of used moisture sensors will depend on the size of the monitored area. Each pair of moisture sensors will be connected to a wireless node. The wireless node will be in charge of sending the data gathered by the moisture sensors to the base station via WiFi connection. In order to ensure that all the nodes can reach the base station, or the sink, a multihop protocol is proposed. With the moisture soil sensors, it is possible to monitor the remaining water in the soil, and with the CMOS sensor, it is possible to identify the grass coverage using the green histograms of the obtained pictures. Further studies will integrate these functions.

The main beneficiaries of the system proposed in this paper are the cities that can use this proposal to plan the irrigation of their urban lawns.

The rest of the paper is structured as follows. Section 2 shows a different work, similar to our system, as well as presents the material and methods. In Section 3, the entire proposal is detailed. The verification of the proposed system to classify the grass coverage with the camera pictures is performed in Section 4. Section 5 presents the results of our proposal applied at different garden sizes. Finally, conclusion and future work are shown in Section 6.

2. Related Works

This section presents some of the current systems focused on monitoring gardens and crops.

Many authors proposed different solutions for monitoring the needs of gardens and crops. Firstly, we will talk about the WSN. Tripathy et al. [11] proposed a system with temperature, light, and water sensors for urban gardens. This system required the deployment of different sets of sensors for monitoring big areas, that is, to detect a small area with needs of replantation inside a bigger area. Due to this, a large number of sensors would be required.

There are some other systems that include the use of cameras along with other sensors. Macedo-Cruz et al. [12] used a picture taken with a CCD-based technology camera. These authors used a combination of three thresholding strategies (the Otsu method, the isolate algorithm, and the fuzzy thresholding method) for determining the frost damage. Lloret et al. [13] designed a WSN based on the use of cameras for detecting unusual status in the leaves of vineyards. The camera took images, and the sensor node processed them for detecting anomalies and reported them

to the farmer. These studies are based on the use of cameras on the soil. Therefore, we can conclude that our system presents the same problem as we explained in the case of the WSN. For monitoring a big area, we will require the use of aerial pictures.

There are three alternatives in remote sensing; these are the use of unmanned aerial vehicles (UAVs), aircraft, and satellite images. Matese et al. [14] compared the use of UAVs, aircraft, and satellite images in vineyards. They concluded that the economic breakeven exists between 5 and 50 ha in the case of UAVs versus the other systems studied. Moreover, the different systems provided comparable results in coarse vegetation gradients and large vegetation clusters, but on the opposite situation, the satellite images fail. Torres et al. [15] used the analysis of satellite pictures captured by QuickBird. The different wavelength images are used to obtain the green vegetation indexes, near-infrared spectroscopy (NIR), normalized difference vegetation index (NDVI), panchromatic index, and ratio vegetation index (RVI). These indexes are used to characterize the size and potential of each olive. Xu et al. [16] used moderate resolution imaging spectroradiometer (MODIS) for determining the production of grasslands in China, and they measured the NDVI of different areas of China. In the case of the satellite images, this technology has different gaps. The cost of satellite images is expensive, and as we mentioned earlier, it is only economically viable in large areas. Another problem is the periodicity of images that prevents a daily control of the area that we want to monitor. In addition, the satellite image has low resolution.

To solve the problem of monitoring big areas and the needs of better resolution than satellite remote sensing, different authors proposed the uses of UAVs and aircrafts. Yang [17] designed an airborne multispectral digital imaging system. This system is based on 4 cameras that capture images in blue (430–470 nm), green (530–570 nm), red (630–670 nm), and near-infrared (NIR, 810–850 nm). The results confirmed that this system is suitable for monitoring crop pests and growing conditions, mapping invasive weeds, and assessing wetland ecosystems. Mutanga and Skidmore [18] studied the variation of N in the grass of the Kruger National Park, in South Africa. They used the images obtained from HYMAP MKII scanner (a type of spectrophotometer in an aircraft) and a neural network for classifying the images. They concluded that the 60% of variation can be explained by the image of their system.

The use of drones is currently a very popular method to obtain aerial images since it is an economical option (in areas smaller than 5 ha [14]) and easier to manage than an aircraft. Candiago et al. [19] used a drone equipped with a Tetracam ADC Micro camera for acquiring images in the red (R), green (G), and near-infrared (NIR) bands, allowing to calculate the NDVI, the green normalized difference vegetation index (GNDVI), and the soil adjusted vegetation index (SAVI). Cambra et al. [20] proposed another system with the use of drones. This system consists of a network made up of a drone and a pressure sprayer. The videos captured by drones are transferred to a PC which will perform an analysis of them through the OpenCV library. The system enables a set of sprayers in a determined area with weeds. We can observe in these cases that the UAVs can be used for monitoring an area smaller than 5 ha.

Finally, Kumar et al. [21] presented a smart autonomous gardening rover that is able to identify and classify different species of plants using extraction algorithms and a neural network. Once the plant is identified, the rover introduces its arm containing the sensors, and according to the measurements, it takes its spray water and fertilizers from this arm. In this case, the author does not use aerial vehicles. For our proposal, we cannot use terrestrial vehicles because they could damage the grass and flowers of gardens which are more sensitive than grass.

As a summary, the use of a WSN is not the best option for monitoring big areas since many sets of sensors are required to identify problems in smaller areas within. The use of cameras on soil presents the same problem because it is not possible to take pictures of big areas with the necessary resolution. For solving this problem, we can use remote sensing. Satellite imaging has important gaps, and the use of this technology is not possible in our case (low precision and high round-trip time to the same point [7]). Aircrafts present the best resolution and the periodicity of taking pictures is better than satellite. However, the cost of this alternative is very high for monitoring small areas. Finally, in this paper, we present a drone that has a camera to measure the reflectance of grass, and our algorithm allows a way of identifying those areas that present low coverage of grass or require water. Additionally, our system stores information in a database for statistical analysis and further uses.

3. Scenario and System Description

This section details the employed material, including the vegetal species and the electronic elements that compose our designed and developed sensor. The methodology followed to process the data is also presented.

3.1. Vegetal Material to Verify the Grass Coverage Classification. In this subsection, we are going to describe the vegetal material used to verify the proposed classification system [9] in the previous work.

The vegetal material has been obtained from a country estate called El Encín. This space is placed in the IMIDRA research center where the agrifood and agroenvironmental research projects of the Community of Madrid (Spain) are carried out. It is located in Alcalá de Henares, Madrid (Spain) (see Figure 1). Currently, IMIDRA is developing a study of the water demand of different grass species. The plots of these experiments are employed to find a relation between the coverage and the response of our developed device. Different combinations of grass species are used in the plots. Each plot has a surface of 1.5 m^2.

3.2. Scenarios Used to Test the Developed System. This subsection shows the description of the gardens used to test the system. The aim of using different sizes of gardens is to evaluate the feasibility of using a type of system or another to monitor

Figure 1: Plots from where the vegetal material is obtained, in the IMIDRA facilities.

each garden, as well as the required energy consumption and consumed bandwidth for each scenario.

In order to test our system, four different gardens have been used. The selected gardens do not have any inclination or irregularities in the terrain. The smallest garden has a surface of 180 m^2, and the biggest one has a surface of 160,000 m^2. The rest of the gardens have a surface of 900, 4600, and 7000 m^2, respectively. All of them are covered with only grass, that is, there are no trees nor shrubs. The gardens of 900, 4600, and 7000 m^2 have a rectangular shape, and the other two gardens have an "L" shape. The selected gardens have good grass coverage in the entire area.

3.3. System for Image Capturing. In order to gather the different images of grass, we have developed a camera-based system which will be installed on the drone. The system for image capturing is composed of an Arduino module and an OV7670 camera able to take pictures with a resolution of 640×480 VGA. It presents a high sensitivity for low-light operation and requires a low operating voltage which makes the OV7670 camera module suitable for embedded portable applications.

Figure 2 shows a basic schematic diagram of the camera connection. The camera module works with a single +3.3 V power supply. This camera needs an external oscillator to generate the clock signal (XCLK pin) of the camera. We can select different communication protocols, although the use of the I2C protocol is recommended. Through the I2C bus, we can control and update both the pixel clock signals (PCLK) and the camera data (data (9:0)). If integrated camera modules are selected, such as MCU STM32F2 or STM32F4 series, no additional module is required. For hosts that do not have a camera interface, additional hardware is needed to store a complete file before reading them with low-speed MCUs.

The system for capturing the images of grass must be installed in a drone, so we should choose modules of small sizes but capable of performing the tasks of image capturing and processing. The final goal of our system is to perform the processing of images in the drone, while it is covering the trip. There are different devices specially designed for the development of integrated systems and Internet of Things (IoT) deployments. In our case, we are going to use an Arduino model. Arduino is an open-source platform that provides both hardware solutions and its own integrated development environment (IDE). Arduino modules are characterized by their simplicity in programming and system management. Table 1 shows a comparison of characteristics of some of its simplest and most used modules that would suit our needs. In our case, we are going to select an Arduino UNO Rev. 3 module. Arduino Uno is an electronic platform based on the ATmega328 processor. It has 14 digital pin inputs/outputs (6 analog inputs, a 16 MHz crystal oscillator). It allows programming through its USB connection and can be powered through the USB connection, from a PC or using a Li-ion battery. The reason of selecting these modules is due to its weight and price, which is the cheapest one available. This module is the second with the smallest weight of 25 g. This is important because when we work with drones, the total weight of the system impacts the flight autonomy.

Additionally, we will provide our system with an ESP-01 wireless module which can be deactivated if we do not need its use and a microSD memory module which allows us to save data and even images, if needed. Figure 3(a) shows the complete system and the main connections among them, while Figure 3(b) shows the 3D design of the support to fix the camera at the bottom part of the drone. The camera is directed towards the ground.

4. Proposal

This section presents the proposed system to gather information about the described grass. First, the sensor and the node are described; the SAV and its components are shown. Finally, the operation process of our system is detailed.

4.1. General Description of the Architecture. The proposed architecture is based on a programmed drone that crosses the field to be analyzed (see Figure 4). The path must be previously designed using software compatible with the chosen drone model.

At the same time the drone moves, it periodically takes pictures of the lawn. For each image taken, the capture system processes each image and decomposes it into its 3 RGB components. As a result of this process, 3 data matrices are obtained, one per component, with data on the red color information, green color information, and blue color information values of each pixel that form each picture. From each matrix, we can extract the histogram from which we can determine the status of that parcel. Finally, after applying our classification algorithm, each picture will be labelled as a parcel of high coverage, a parcel of low coverage plot, or a parcel of very low coverage. We can have a unique base from where the drone takes off and lands. However, to optimize the battery lifetime, we opted for a 2-base system. The first one will be the base from which the drone will take off and the second one will be the drone's landing point.

On the other hand, to reduce battery consumption caused by data transmission and possible packet loss due

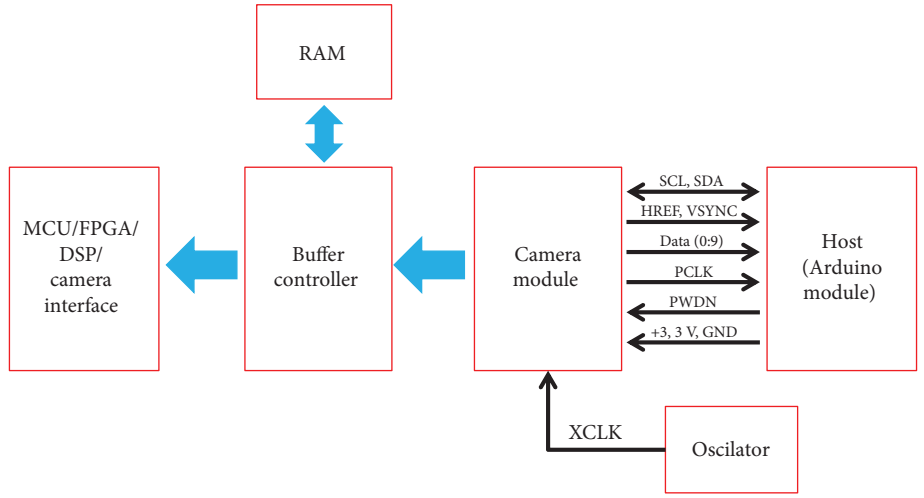

Figure 2: Basic schematic diagram of the camera connection.

Table 1: Characteristics of different nodes.

	Uno	Mega	101	Wemos D1 Pro + Wifi
Revision	R3	R3	R1	R2
CPU	ATmega328	ATmega2560	Intel Curie	Ensilica 32-bit RISC CPU Xtensa LX106
Flash memory	32 KB	256 KB	196 KB	4 Mbytes
Voltage	5.10 V	5.10 V	5.10 V	3.3 V
Power consumption	734 mW	403 mW	336 mW	500 mW
Clock speed	16 Mhz	16 Mhz	32 Mhz	80 MHz/160 MHz
Power/speed	46 mW/Mhz	26 mW/Mhz	11 mW/Mhz	6.25 mW/MHz/3.125 mW/MHz
Digital I/O pins	14	54	14	11
Analog in pins	6	16	4	1
Weight (g)	25	37	34	9.07
Cost (€)	2.82	11.20	37.60	5.60

to the drone movement, the data related to parcel information will be transmitted when arriving at the landing base. That is, the system will take the images and will locally process them, and after arriving to the landing base, the data will be wirelessly transmitted through a WiFi connection.

The information collected by each database will be sent to a central server located in the cloud. Finally, the owners will be able to see the status of their fields in real time.

4.2. Drone and Flight Planning. To implement our system, we have selected a commercial drone with capacity to support our small electronic device to collect the images. Table 2 summarizes the main features of some commercial models that could be used to implement our proposal. To implement our proposed system, we have selected the DJI Phantom 4 Pro which is considered as one of the widely used devices for taking aerial images for semiprofessional purposes. This model incorporates an advanced visual stereo positioning system (VPS) that allows the drone performing a precise stationary flight, even without satellite positioning, making flights easier and safer.

Although the drone can be manually controlled, to monitor the surfaces and collect the pictures, we have used a flight planning software. To plan the flight of a drone, there are several applications with support for different operating systems. In our case, we have selected free software specially designed for Android devices. DroneDeploy [22] is a software platform designed for drone flight planning. The DroneDeploy application provides a simple interface for data capture and automated flights that allows you to explore and share high-quality interactive maps directly from our mobile device. DroneDeploy allows you to generate high-resolution maps and 3D models.

DroneDeploy is compatible with several commercial drone models such as the following:

(i) Mavic Pro

(ii) Phantom 4 Pro

(iii) Phantom 4

(iv) Phantom 3 Pro

(v) Phantom 3 Advanced

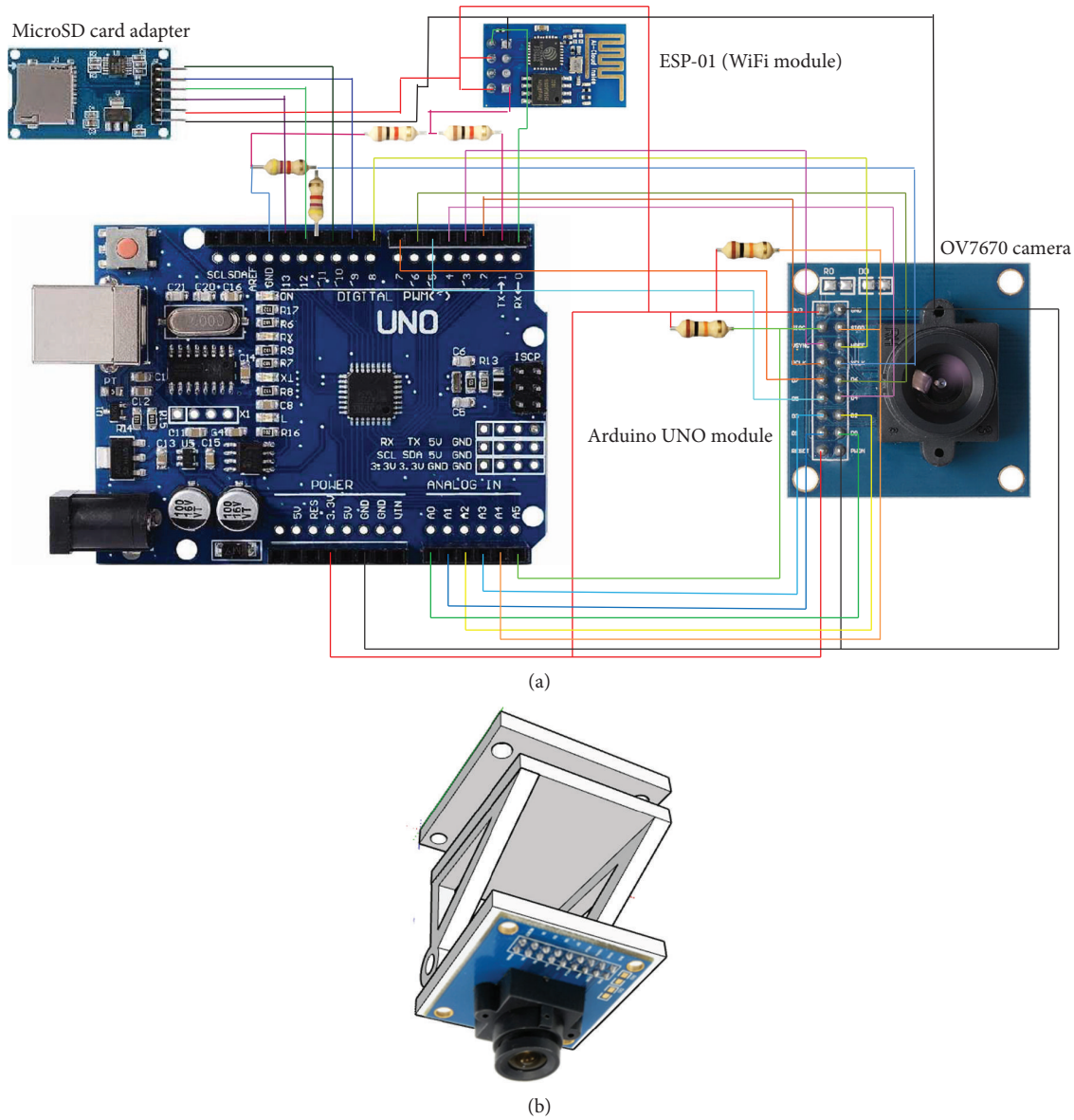

Figure 3: System of camera: (a) complete system and the connections; (b) support for camera.

(vi) Inspire 1 e Inspire 1 Pro

(vii) Inspire

(viii) Matrice 100

(ix) Matrice 200

(x) Matrice 600

For drones equipped with cameras, the application allows exploring interactive maps; measuring distance, area, and volume; analyzing elevation and NDVI images; and sharing maps and annotations through instant messaging applications. Figure 5 shows the example of a planned flight in a real scenario, and Figure 6 shows the drone during a flight.

4.3. Control Algorithm. To start taking measurements by the drone, we must consider that the device is going to move from coordinator node 1 to coordinator node 2 which is the one that has the possibility of transmitting the data to the cloud or to a server. It is also important to consider that the drone has to have enough autonomy to cover the entire route. Therefore, these checks must autonomously be carried out before starting the flight.

As shown in Figure 7, before starting the flight, the drone should receive the data related to the field under the study and check if its battery allows full field coverage. If its energy autonomy allows it, the drone will take off and will start taking pictures. For each image taken, the drone analyzes the image and processes it in its RGB components. After that, the drone keeps the green component and saves the results with the relative position of the extracted data from the flight plan. After taking the image, the drone checks if it has reached the end of the route and keeps moving forward for the next measurement. When

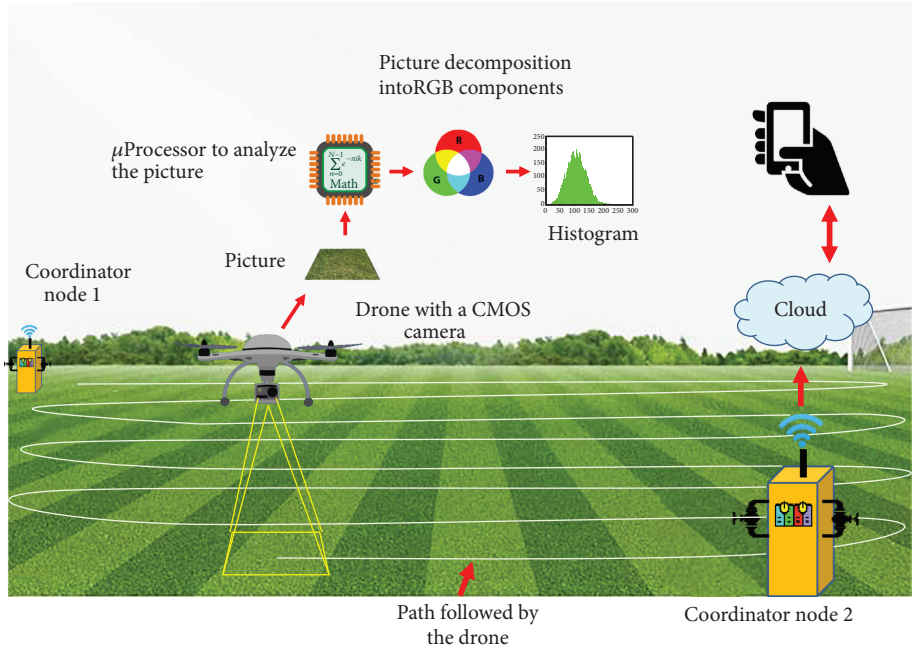

Figure 4: Proposed architecture.

Table 2: Characteristics of different commercial nodes.

Model	Weight (g)	Max. flight speed (km/h)	Autonomy (min)	Max. distance (m)	Price (€)
Parrot Bebop 2	500	46	25	300	540
Parrot Disco FPV	500	80	40	Not applicable	499
DJI Phantom 2	1500	Not applicable	25	1000	622
DJI Phantom 4 Pro	1380	72	28	6000	1600
DJI Phantom 3 Pro	1280	57	23	2000	1080
DJI Phantom 3 Advanced	1280	57	23	Not applicable	1070
Syma X8C Venture	600	Not applicable	9	100	150
Parrot AR Drone 2.0	436	Not applicable	36	50	250
DJI Inspire 1 V2	2935	78	18	Not applicable	3399
DJI Mavic Pro	726	65	27	6000	1100
Yuneec Typhoon H Pro	2060	60	22	Not applicable	907
Syma X5C Explorers	960	20	8	50	68
Quadron Evo	839	Na	10	100	56
JJRC H20	200	Na	6	40	50

the drone completes its flight, it lands on the base of the coordinator node 2. When at the base, the drone wirelessly connects to the coordinator node 2 and transmits all the data obtained from the field. After finishing its function, the drone will switch to standby mode.

On the other hand, after receiving the data of the flight plan and the size of the field to be analyzed, the drone determines if it has energy enough to complete the route. If the battery level is not high enough, the drone sends a message to the user asking for flight acceptance. If the user does not accept the flight, the drone will remain in standby mode in the base of the coordinator node 1. However, if the user accepts the flight, the drone will start flying and capturing images. After each measure, the drone checks if its autonomy is sufficient to take one more measurement and reach the coordinator node 2. As long as this condition is maintained, the path will be followed. When the condition is not kept, the drone will leave the flight plan and will directly go to the base of the coordinator node 2. After that, the drone will wirelessly connect to the coordinator node 2 and will transmit all the data obtained from the field as well as the position where it left to take measures. After finishing its operation, the drone will switch to standby mode.

4.4. Process to Analyze the Pictures. In this section, we present the verification process to apply to the system developed by

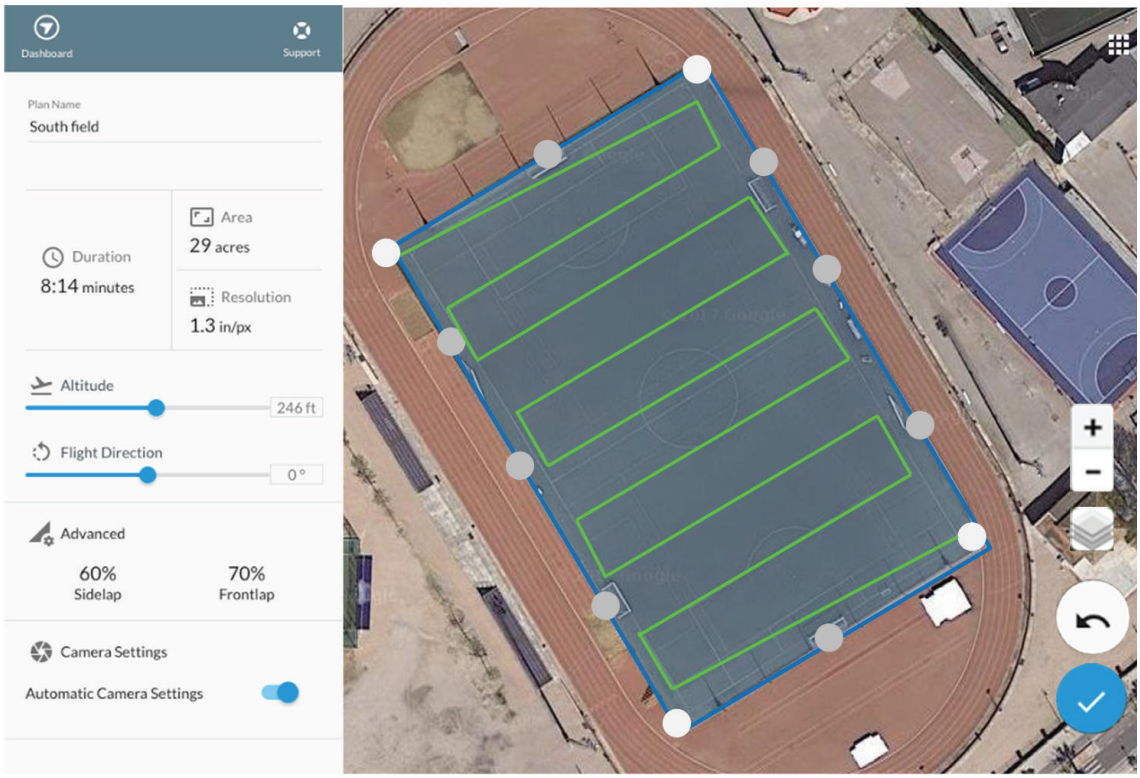

Figure 5: Example of planned flight over a real scenario performed with DroneDeploy App.

Figure 6: Our drone during a flight with the developed system for gathering pictures.

[9]. In order to verify it, we used new grass plots, and using the pictures obtained with the Arduino camera, we extracted the desired values used to perform the comparison.

Different pictures were taken to the grass plots (see Figure 8(a)). After obtaining the picture, it is cut in order to extract the part related to the grass and ensure that the

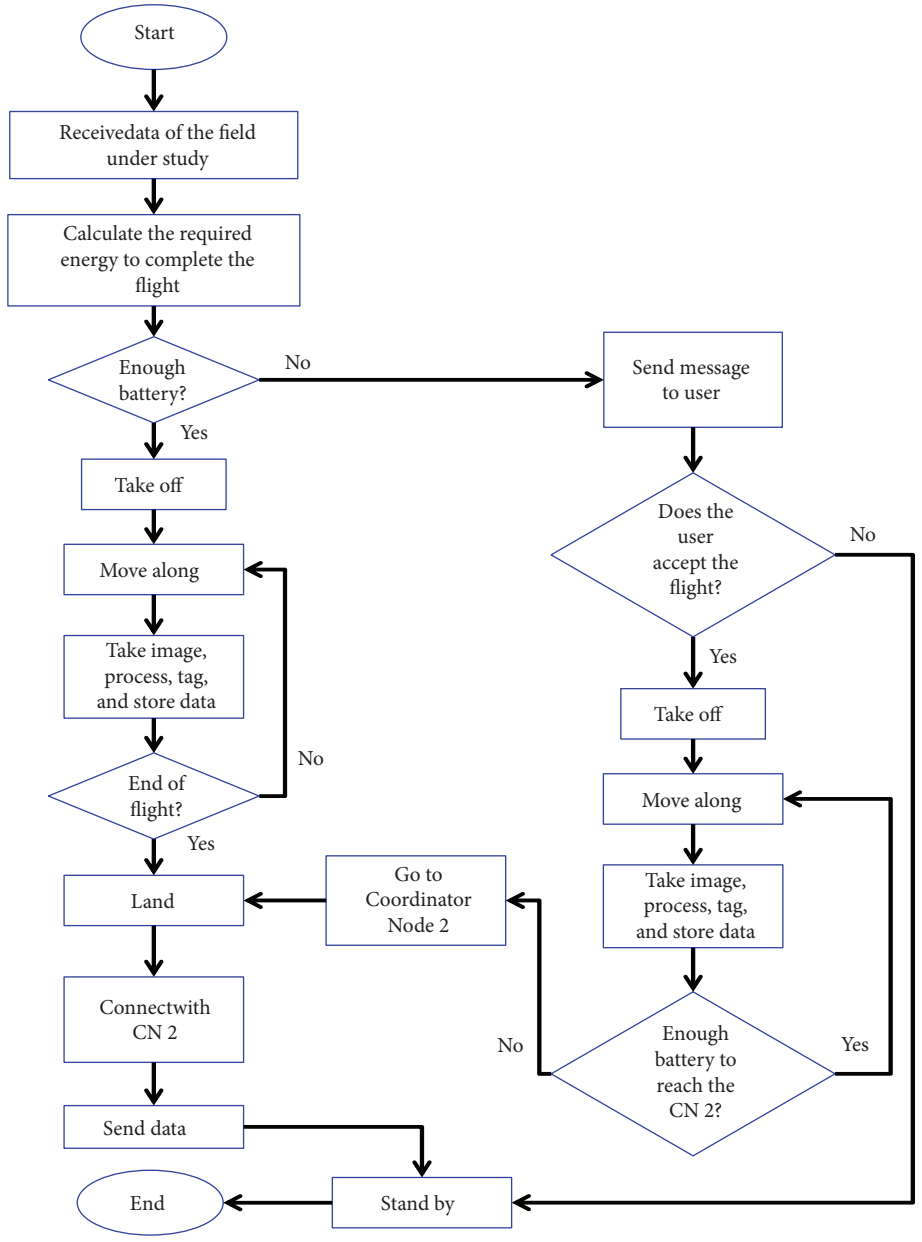

Figure 7: Control algorithm.

number of pixels of the pictures was 1500×1000 pixels (see Figure 8(b)). Then, the resolution of the picture was reduced to 10%. The picture has consequently 150×100 pixels (see Figure 8(c)).

Once we have the picture with a size of 100×150 pixels, we can obtain the values of brightness from each pixel. To obtain it, we use the MATLAB software (see Algorithm 1).

An image can be understood as a matrix of row × column pixels. In order to analyze each pixel, we should go through each row, accessing each cell that represents the columns. There are several ways to do this task, but the simplest one is to use 2 nested "FOR" loops, so that the outer "FOR" loop locates the cursor at the beginning of a row and the inner "FOR" loop allows the cursor to go through all the squares of that row until reaching the last column. Finally, we created a vector of 256 positions that corresponds to the brightness levels of each color, and for each level of brightness, we counted how many pixels contain that brightness color. Finally, we saved the result in the variable His_G that is used to store the results of the histogram.

Once we have the matrix of the green component with the values of brightness, it is possible to apply the methodology described by [9]. So, firstly, we obtain the green histograms shown in Figure 8. As we can see, all the new histograms follow the trend of the mean histograms from different grass coverages. After that, we can obtain the number

```
%Read Picture.
x=imread (picture);
GREEN= x (:,:,3);
[Rows, Columns]= size (GREEN (:,:,1));
%calcule blue histogram
    for f=1:256
        h_G(f)=0;
    end.
    for g=1:Rows.
      for h=1:Columns
        V_Green= GREEN(g,h);
        h_G(V_Green+1)= h_G(V_Green+1)+1;
      end
    end
%Vector of histogram component green.
    His_G=h_G;
```

Algorithm 1: Part of MATLAB code to extract RGB components.

of pixels with brightness values between 40 and 60. We selected this range based on the results shown by [9].

Finally, since the flight height of the drone is fixed with respect of the ground, the focus of the camera is manually set before the flight.

5. Results and Discussion

This section shows the results and the discussion about the extracted values. First, the grassland classification method for analyzing pictures instead of RGB sensors is presented. Then, the results of the simulations to apply the proposed system (with drone) or our previous system (with the SAW) in 5 gardens with different sizes are evaluated. Finally, a comparison between our system and the current proposals is discussed.

5.1. Grassland Classification. In order to carry out our classification, we only need to sum the number of pixels with brightness values between 40 and 60 in the green component of the picture. Then, we will analyze the classification assigned to each picture to check if the classification process assigned the tags correctly.

After processing the pictures, the matrix with the data of green brightness is used. The pictures were not previously tagged according to their type of coverage; they are just named as new samples (NS) 1 to 12. They are named based on the summation of the pixels with brightness values between 40 and 60.

In the previous work, the plots were assigned according to three categories: high coverage (HC), low coverage (LC), and very low coverage (VLC). Figure 9 represents the obtained histograms of the NS 1 to NS 12 and the average value of the obtained histograms of HC, LC, and LVC by [9]. In solid colors, we can see the average value of the tagged histograms: HC in green, LC in orange, and VLC in red. The data from the NS 1 to NS 12 is shown with black dashes. It is possible to see that all the histograms follow the same behaviour of one of the average values from the previous work. The summation of pixels with brightness values between 40 and 60 is compared with the results obtained in the previous work [9], and the ranges of values were set to tag the different pictures. Results can be seen in Figure 10. The HC plots, with good grass coverage, have a summation lower than 500. Then, the plots named as NS 1 to NS 4 are classified as HC plots. The NS 5 to 9 have a summation lower than 1500 but higher than 500. They are classified as LC. Finally, the NS 10 to 12, which have a summation higher than 1500, are classified as VLC. Taking into account the 12 pictures under study, 4 of them were tagged as HC, 5 as LC, and 3 as VLC.

The next step is to verify if the classification was correctly done. Figure 11 shows the pictures and their classification according to our proposed algorithm. The results show that the classifications have been correctly done. The plots tagged as HC present a grass coverage of 100% (see Figures 11(a)–11(d)). On the other hand, the plots classified as LC present a lower grass coverage, and most of the grass presents a yellowish color which indicates a poor grass state. Those plots (see Figures 11(f)–11(i)) present an irrigation deficit. Finally, the plots tagged as VLC (see Figures 11(j)–11(l)) present a very low coverage, and most of the plot has no grass, and only the brown soil is observed. In those plots, the irrigation is not immediately required. However, a seeding process will be necessary to restore the grass coverage. Thus, we can indicate that the methodology presented by [9] with RGB sensors can be used to evaluate the grass state in the picture. This is due to the fact that the operation of the sensors inside the cameras and the image postprocessing is similar to the operation of the RGB sensors.

The only limitation is that the system must operate with matrices of 100×150 values of brightness. However, we can divide the summation of pixels and the total number of pixels. If the result is a value lower than 0.03, the assigned category will be HC. The plots with values between 0.03 and 0.1 will be tagged as LC. Finally, the plots with values higher than 0.1 will be classified as VLC. By following this process, it is possible to apply this method with pictures of different sizes.

5.2. Study of Feasibility of Using This Method in Different Garden Sizes. In this subsection, we are going to detail the simulations of using our proposal (with a drone) in gardens of different sizes that were presented in Section 2. The results are compared with the simulation results of using a SAW. The parameters evaluated are the time required to gather the data from the entire garden and the volume of information generated. The amount of gathered data, the number of turns, and the total distance travelled are also considered for these simulations.

To calculate the number of turns (P), it is necessary to divide the shorter side (SS) of the field between the width of each turn (WP) (1). On the one hand, the width of each turn with the SAW (WP_{SAW}) is the SAW width (WI_{SAW}). Sensors are located covering the width of the vehicle (2). On the other hand, the width of each turn in the case of the drone

(a) (b) (c)

Figure 8: Processing of pictures.

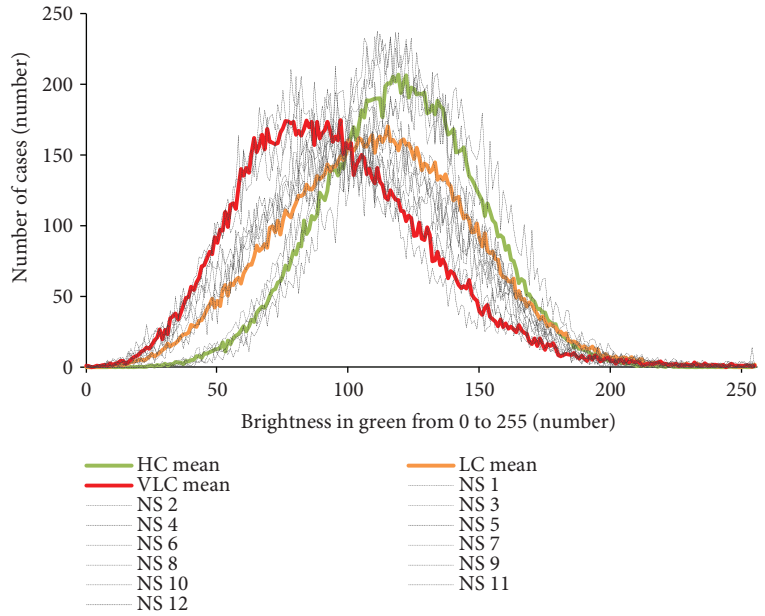

Figure 9: Histogram of the different cases.

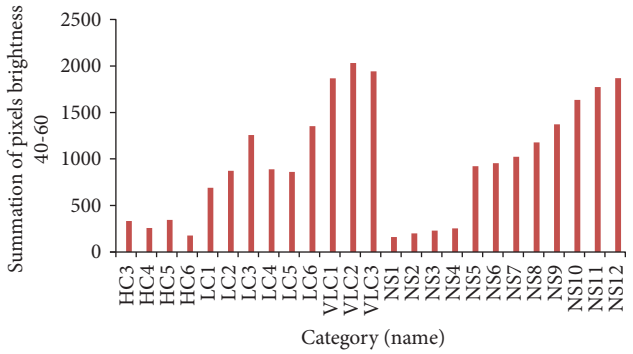

Figure 10: Summation of pixels with values of brightness between 40 and 60.

(WP_{drone}) depends on the flight height (FH) and on the focal aperture of the camera (FA) (see (3)). In our examples, the WP_{SAW} is 0.5 m and the WP_{DRON} is 6.6 m. The area contained in each picture gathered with the drone is 4.95×6.6 m. The FH must be set according to the required resolution in the pictures, which, in our case, was 15 m. The values of P, for each garden, are shown in Table 3. The P value for the drone is much lower than the P value for the SAW because they have different WP.

$$P = \frac{SS}{WP}, \tag{1}$$

$$WP_{SAW} = WI_{SAW}, \tag{2}$$

$$WP_{drone} = \tan\left(\frac{FA}{2}\right) \times FH \times 2. \tag{3}$$

Once the number of turns is calculated, the next indicator is to calculate the total distance travelled to cover the field. In order to simplify the simulation, the travelled distance (TD) is calculated as the distance travelled in each turn (the number of turns along the longer side (LS)) plus the distance travelled to change from one turn to another (the number of turns minus 1 and multiplied by the width of each turn) (4). The TD for each garden can be seen in Table 3. The TD is lower when using the drone as opposed to using a SAW.

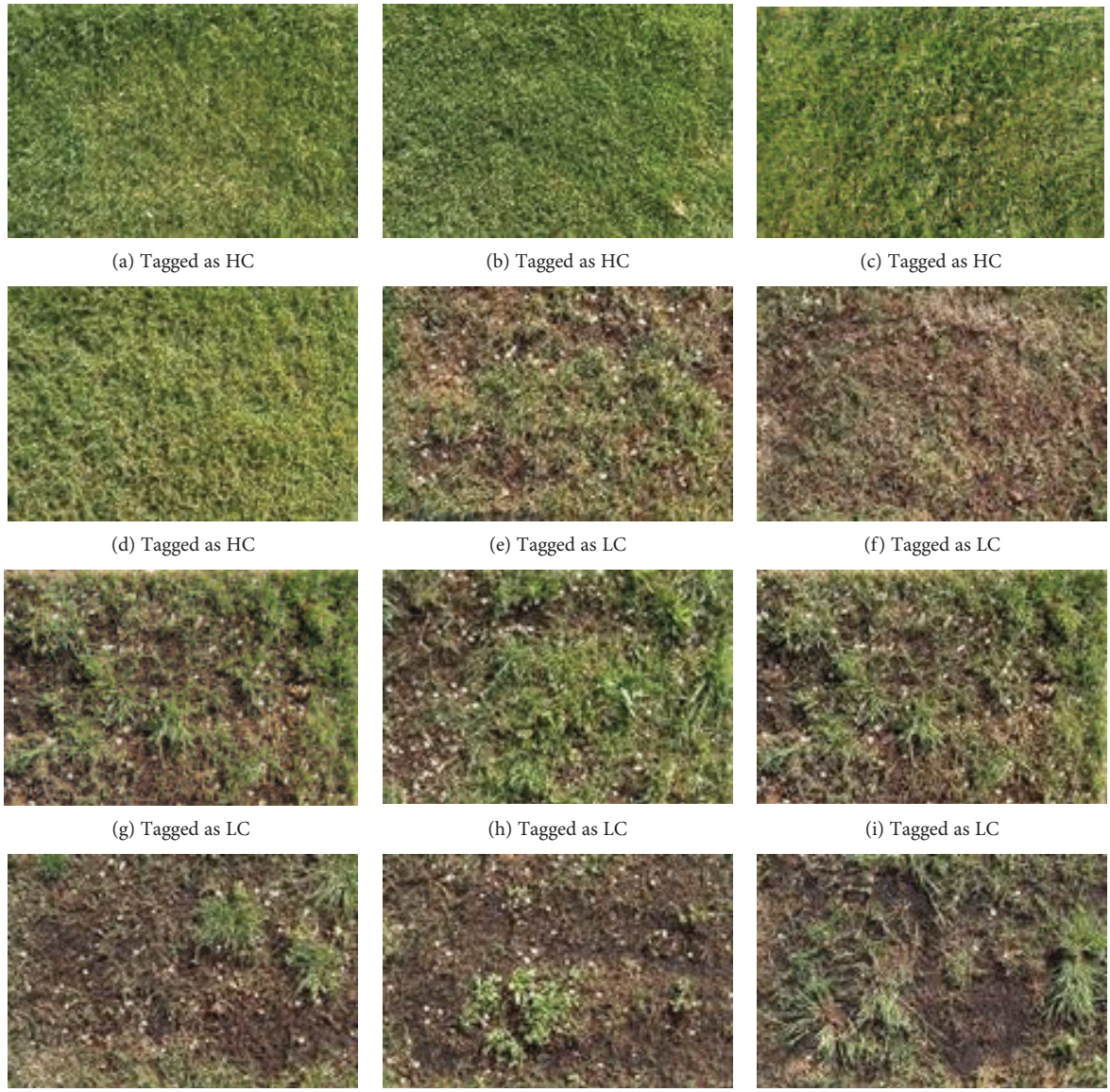

(a) Tagged as HC (b) Tagged as HC (c) Tagged as HC

(d) Tagged as HC (e) Tagged as LC (f) Tagged as LC

(g) Tagged as LC (h) Tagged as LC (i) Tagged as LC

(j) Tagged as VLC (k) Tagged as VLC (l) Tagged as VLC

Figure 11: Pictures used and their classification.

The TD with the drone is lower than a tenth part than the TD with a SAW.

$$\mathrm{WP}_{\mathrm{drone}} = \tan\left(\frac{\mathrm{FA}}{2}\right) \times \mathrm{FH} \times 2. \quad (4)$$

To complete the comparison, we need to calculate the time consumed (TC) to collect the data from each garden. The time consumed (5) is calculated as the travelled distance at the mean velocity (MV) plus the lost time (LT) in the deceleration and acceleration at the end and the beginning of each turn, multiplied by the number of turns.

There are some considerations that must be taken into account to select the mean velocity. The time that takes the SAW to gather and process each recorded data (TGD) and the area covered in each record (CA) must be considered to calculate the mean velocity of the SAW ($\mathrm{MV}_{\mathrm{SAW}}$) (6). To calculate the mean velocity of the drone ($\mathrm{MV}_{\mathrm{DRONE}}$) (7), we should consider the pictures per second (PPS) that the camera should take and the distance of the shortest side of each picture (SSP). The shortest side of the picture is defined as

Table 3: The P and TD with the drone and with the SAW.

Garden number	Size (m^2)	P (number)		TD (m)	
		Drone	SAW	Drone	SAW
1	180	1	14	27	360
2	900	5	60	136	1800
3	4600	10	136	697	9200
4	7000	13	186	1061	14,000
5	162,000	61	800	24,545	324,000

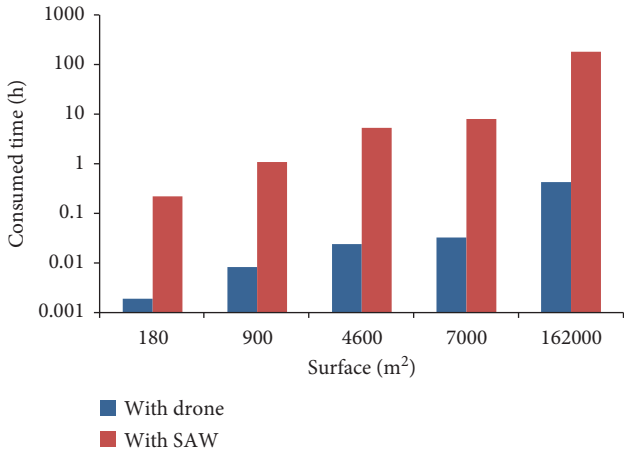

Figure 12: The TC for different gardens with SAW and drone.

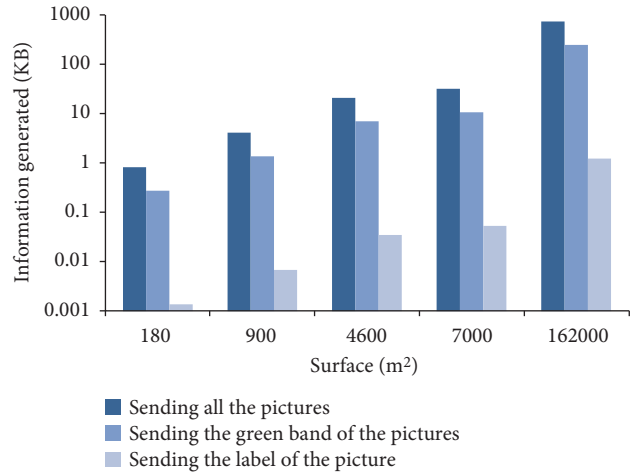

Figure 13: Volume of information generated of each garden and different formats of sent data.

the number of pixels of the shortest side of the picture (NP_{SSP}) multiplied by the width of each turn divided between the number of pixels of the longest side of the picture (NP_{LSP}) (see 8). The PPS must be set by the user according to the camera features. The consumed time for each garden is shown in Figure 12. It is possible to see that the TCs with the SAW for the gardens are much higher than the TCs with the drone. In the biggest garden, the TC for the SAW is up to 180 h, while for the drone is 25 min and 30 sec. The SAW is only useful for small gardens like garden 1 and garden 2 with a TC of 0.22 h and 1.08 h, respectively. For gardens with more than 1000 m^2, the SAW is not advisable due to the TC. The mean flying time of the employed drone is 30 minutes; the largest space that can be monitored by a single drone depends on the shape of the area and the number of turns needed. To give an example, a fully charged drone can cover an area of 200,000 m^2 with one side of 400 m and the other of 500 m.

$$TC = TD \times MV + LT \times P, \tag{5}$$

$$MV_{SAW} = \frac{CA}{TGD}, \tag{6}$$

$$MV_{drone} = PPS \times SSP, \tag{7}$$

$$SSP = \frac{NP_{SSP} \times WP_{drone}}{s}. \tag{8}$$

From this point, we will only continue with the simulation for the case of using a drone. Finally, the number of pictures (TP) can be calculated as the number of pictures per second multiplied by the total distance and divided into the mean velocity (see 9). The TP in the selected gardens are 5, 27, 139, 212, and 4909 for gardens 1 to 5, respectively. To calculate the volume of information generated if we want to send all the pictures (VI_{PIC}), we should take into account the number of pictures and the weight (in bytes) of each picture (WPi) (see 10). However, if we want to send the green band of the picture (VIG_{PIC}), we will transmit the matrix with the values of the green band of the picture, that is, the volume of useful data will be the third part of the volume (11). Moreover, it is possible to send only the label classification of each picture (VIC_{PIC}). That is, we will only consider the number of pictures and the weight of each category (W*C*) (see 12). Figure 13 shows the comparison between the VI_{PIC}, VIG_{PIC}, and VIC_{PIC} in each garden. As expected, the transmission of the VIC_{PIC} means lighter transmission. Sending the VIG_{PIC} leads to a reduction of two-thirds or 66.7% of the total volume of data compared to sending the VI_{PIC}. Sending the VIC_{PIC} supposes a reduction of 99.8% of the data volume compared to sending the VI_{PIC}. So, taking into account our results, it is demonstrated that the best option for data transmission is to only send the label of the plot characteristics together with its plot identification or position. Finally, this label is locally calculated by our system and stored in the SD card in order to be wirelessly transmitted to the landing base. Thus, the only information transmitted from the drone to the base station is one label per gathered picture. By doing this, we are reducing the energy consumption as we do not keep the wireless connection continuously enabled. In order to know the position of each picture, we have included in the database the route of each drone. Then, it is possible to relate the label of each picture with the position of the drone according to the number of the picture. In this case, the GPS is not useful to identify the pictures due to the small distance between the drone positions.

$$TP = PPS \times \frac{TD}{MV}, \tag{9}$$

$$VI_{PIC} = TP \times WPi, \tag{10}$$

$$VI_{GPIC} = TP \times \frac{WPi}{3}, \tag{11}$$

$$VIC_{PIC} = TP \times WC. \tag{12}$$

5.3. Discussion and Comparison with Existing Systems. In this section, we are going to analyze the gaps in our system, and we will explain why our alternative is better than the existing ones.

Table 4: Summary of different techniques.

	Smart sprinkler	Satellite sensing	Airplane sensing	SAW	Our system
Method of measurement	Uses meteorological sensors and moisture sensor for detecting the needs of irrigation	Analyzes the different electromagnetic bands of an area captured by satellites (NDVI, NIR, etc.)	Analyzes the different electromagnetic bands of an area captured by camera in an airplane (NDVI, NIR, etc.)	Uses a CMOS sensor placed in the SAW to take a picture and analyzes your histogram	Uses a CMOS sensor placed in a drone to take a picture and analyzes the histogram to classify the degree of coverage. Moisture sensors will detect the hydraulic needs
Results obtained	Evapotranspiration and moisture in the soil	Value of the electromagnetic waves with which parameters such as the NIR and NVDI are calculated	Value of the electromagnetic waves. Parameters such as the NIR and NVDI are calculated	Histogram of garden colors	Histogram of the green color, the degree of coverage, and the level of moisture
Spatial precision	Depends on the number of sensors	1.24 meters	0.2 meters	Depends on the SAW speed	4.7 cm
Detects the need of replanting	No	Yes	Yes	Yes	Yes
Detects irrigation needs	Yes	Yes	Yes	Yes	Yes
Can it be used on windy days?	Yes	Yes	Yes	Yes	No
The covered sky can affect the measurement	No	Yes	Yes	Yes	Yes
Can it be used days?	Yes	No	No	Yes	Yes

Drone-based systems have three important issues: (I) drones cannot fly in windy conditions; (II) some countries have a more restrictive legislation in the use of drones; and (III) there is a change of environment illumination.

Regarding the first issue, the number of windy days is usually small compared to that of sunny days, although this fact depends on the geographical region. In addition, the changes in the grass are not usually so abrupt, and therefore the fact of not performing the daily monitoring is not significant. In relation to the second problem, legislation regarding the use of drones has been very restrictive because most countries did not have previous legislation and they wanted to avoid problems by limiting the use of drones. However, they are currently adapting new laws to the evolution of drones. Finally, the illumination can have negative effects on the classification of grass. The illumination can change because of (I) the sky covered with clouds; (II) the shadows of buildings, trees, and so on; (III) the time of day when the monitoring tasks are performed; and (IV) the season of year when the monitoring tasks are performed [23]. To reduce the problem with shadows, we will fly the drone in a sunny noon to reduce the size of the shadows, and in future works, we would like to include a lux meter in the drone to include this parameter in the classification algorithm as a correction factor.

Finally, we compared our system with other systems (see Table 4). The needs of irrigation can be monitored with remote sensing (satellite or airplane [24]), SAWs, smart sprinkler (WSN with weather information for calculating the evapotranspiration), and our system. Some existing solutions include sensors to detect electromagnetic radiation to determine the coverage of the vegetation. As we saw in Section 2, the NDVI, NIR, and other indicators related to the infrared can be used for monitoring the vegetation and are very common in remote sensing. In this paper, we demonstrated that the use of visible light waves can be used without the need of an infrared camera.

All systems that use electromagnetic sensors will be affected by the shadows and changes of environmental light. In the case of satellite sensing, the clouds can cover the image, and therefore it cannot be used to monitor the urban lawns. This does not happen with airplanes and drones because they fly below the clouds. Finally, remote sensing cannot be used for daily monitoring due to the low temporal resolution time, and we cannot have a schedule to take pictures on a daily basis for an urban garden. Due to these facts, we only have the option of SAWs or drones for monitoring the grass. As we have previously seen, the SAW requires a lot of time to cover a large surface, and it is not recommended for urban lawns greater than $1000\,m^2$.

To monitor the irrigation needs, we can use the smart sprinkler (the use of remote sensing for managing irrigation is not very common). The smart sprinklers are programmed according to the moisture of the soil and the calculation of the evapotranspiration of the plants by means of the meteorological data. We decide to use moisture sensors because they are cheaper than smart sprinklers. Finally, Table 4 shows a summary of this discussion.

6. Conclusions

In this paper, the use of a drone equipped with an Arduino module and a camera for urban lawn monitoring has been evaluated. Prior to evaluating our proposal, we have used the proposed methodology to classify the grass quality based on RGB sensors explained in our previous work. The algorithm proposed in the previous paper [9] obtained the 100% of hits. Besides, we have evaluated the performance of employing a drone or a SAW to cover gardens of different sizes. The results show that for gardens bigger than $1000\,m^2$, the use of SAW is not recommended. Finally, we compare the possibilities of sending the entire picture to be processed in a remote server, the green band of the picture, or just the category of each picture. By sending only the category of each picture instead of sending the entire picture, we obtain a reduction in the volume of information of 99.8%. The total cost of our system is €30 (not including the price of the drone). The same system could be installed in cheaper drones with lower flight autonomy but with similar results.

This proposal is part of a bigger study where the images will be locally processed by drones, and they will only send the tag for a specific area. Thus, this paper has presented the design, implementation, and verification of the drone operation and how it collects pictures. After collecting the images, they will be processed to analyze the color composition, and finally our designed algorithm will classify them. As a future work, further studies will integrate this function in the drone in order to locally process them. It is also planned to add moisture soil sensors to control the irrigation regime. The moisture sensors will be connected to a wireless node. The wireless node will be in charge of sending the data gathered to the base station. With the moisture soil sensors, it is possible to monitor the remaining water in the soil, and with the CMOS sensor, it is possible to identify the grass coverage using the green histograms of the obtained pictures. Moreover, it will be interesting to test the possibilities of detecting and classifying different plant diseases. In addition, we pretend to extend this work including the analysis of pictures of other plant species. Finally and to solve the problems related to different light conditions, we will include a light sensor in the drone and perform several tests under different conditions in order to have different ranges for different light conditions.

Data Availability

The datasets generated during and/or analyzed during the current study are available from the corresponding author on reasonable request.

Conflicts of Interest

The authors declare that they have no conflicts of interest.

Acknowledgments

This work has been partially supported by the "Conselleria de Educación, Investigación, Cultura y Deporte," through

the "Subvenciones para la contratación de personal investigador de carácter (Convocatoria 2017)" Grant no. ACIF/2017/069. Finally, the research leading to these results has received funding from "la Caixa" Foundation and Triptolemos Foundation.

References

[1] NASA, "The importance of freshwater," 2017, December 2017, https://pmm.nasa.gov/waterfalls/Science/freshwater.

[2] FAO, Food and Agriculture Organization of the United Nations, "Towards a water critical perspectives for policy-makers," 2015, December 2017, http://www.fao.org/nr/water/docs/FAO_WWC_white_paper_web.pdf.

[3] K. Xiao, D. Xiao, and X. Luo, "Smart water-saving irrigation system in precision agriculture based on wireless sensor network," *Transactions of the Chinese society of Agricultural Engineering*, vol. 26, no. 11, pp. 170–175, 2010.

[4] R. Bongiovanni and J. Lowenberg-Deboer, "Precision agriculture and sustainability," *Precision Agriculture*, vol. 5, no. 4, pp. 359–387, 2004.

[5] A. Shalaby and R. Tateishi, "Remote sensing and GIS for mapping and monitoring land cover and land-use changes in the Northwestern coastal zone of Egypt," *Applied Geography*, vol. 27, no. 1, pp. 28–41, 2007.

[6] Imaging, Satellite, "Satellite Sensor," 2017, Decemeber 2017, http://www.satimagingcorp.com/satellite-Sensors/geoeye-2/.

[7] D. J. Mulla, "Twenty five years of remote sensing in precision agriculture: key advances and remaining knowledge gaps," *Biosystems Engineering*, vol. 114, no. 4, pp. 358–371, 2013.

[8] C. Cambra, S. Sendra, J. Lloret, and L. Parra, "Ad hoc network for emergency rescue system based on unmanned aerial vehicles," *Network Protocols and Algorithms*, vol. 7, no. 4, 2016.

[9] J. Marín, J. Rocher, L. Parra, S. Sendra, J. Lloret, and P. V. Mauri, "Autonomous WSN for lawns monitoring in smart cities," in *2017 IEEE/ACS 14th International Conference on Computer Systems and Applications (AICCSA)*, Hammamet, Tunisia, November 2017.

[10] L. Parra, S. Sendra, J. Lloret, and J. J. Rodrigues, "Low cost wireless sensor network for salinity monitoring in mangrove forests," in *IEEE SENSORS 2014 Proceedings*, Valencia, Spain, November 2014.

[11] A. K. Tripathy, A. Vichare, R. R. Pereira, V. D. Pereira, and J. A. Rodrigues, "Open source hardware based automated gardening system using low-cost soil moisture sensor," in *2015 International Conference on Technologies for Sustainable Development (ICTSD)*, pp. 4-5, Mumbai, India, February 2015.

[12] A. Macedo-Cruz, G. Pajares, M. Santos, and I. Villegas-Romero, "Digital image sensor-based assessment of the status of oat (Avena sativa L.) crops after frost damage," *Sensors*, vol. 11, no. 6, pp. 6015–6036, 2011.

[13] J. Lloret, I. Bosch, S. Sendra, and A. Serrano, "A wireless sensor network for vineyard monitoring that uses image processing," *Sensors*, vol. 11, no. 6, pp. 6165–6196, 2011.

[14] A. Matese, P. Toscano, S. di Gennaro et al., "Intercomparison of UAV, aircraft and satellite remote sensing platforms for precision viticulture," *Remote Sensing*, vol. 7, no. 3, pp. 2971–2990, 2015.

[15] L. García Torres, J. M. Peña-Barragán, F. López-Granados, M. Jurado-Expósito, and R. Fernández-Escobar, "Automatic assessment of agro-environmental indicators from remotely sensed images of tree orchards and its evaluation using olive plantations," *Computers and Electronics in Agriculture*, vol. 61, no. 2, pp. 179–191, 2008.

[16] B. Xu, X. C. Yang, W. G. Tao et al., "Modis-based remote sensing monitoring of grass production in China," *International Journal of Remote Sensing*, vol. 29, no. 17-18, pp. 5313–5327, 2008.

[17] C. Yang, "A high-resolution airborne four-camera imaging system for agricultural remote sensing," *Computers and Electronics in Agriculture*, vol. 88, pp. 13–24, 2012.

[18] O. Mutanga and A. K. Skidmore, "Integrating imaging spectroscopy and neural networks to map grass quality in the Kruger National Park, South Africa," *Remote Sensing of Environment*, vol. 90, no. 1, pp. 104–115, 2004.

[19] S. Candiago, F. Remondino, M. De Giglio, M. Dubbini, and M. Gattelli, "Evaluating multispectral images and vegetation indices for precision farming applications from UAV images," *Remote Sensing*, vol. 7, no. 4, pp. 4026–4047, 2015.

[20] C. Cambra, J. R. Díaz, and J. Lloret, "Deployment and performance study of an ad hoc network protocol for intelligent video sensing in precision agriculture," in *In International Conference on Ad-Hoc Networks and Wireless*, pp. 165–175, Springer, Benidorm, Spain, 2014.

[21] V. S. Kumar, I. Gogul, M. D. Raj, S. K. Pragadesh, and J. S. Sebastin, "Smart autonomous gardening rover with plant recognition using neural networks," *Procedia Computer Science*, vol. 93, pp. 975–981, 2016.

[22] "Dronedeploy Application," 2017, December 2017, https://www.dronedeploy.com/agriculture.html.

[23] J. L. Morgan, S. E. Gergel, and N. C. Coops, "Aerial photography: a rapidly evolving tool for ecological management," *Bioscience*, vol. 60, no. 1, pp. 47–59, 2010.

[24] C. Toureiro, R. Serralheiro, S. Shahidian, and A. Sousa, "Irrigation management with remote sensing: evaluating irrigation requirement for maize under Mediterranean climate condition," *Agricultural Water Management*, vol. 184, pp. 211–220, 2017.